

See discussions, stats, and author profiles for this publication at: <https://www.researchgate.net/publication/230631739>

ChemInform Abstract: Aromatic Amide Foldamers: Structures, Properties, and Functions

ARTICLE *in* CHEMICAL REVIEWS · AUGUST 2012

Impact Factor: 46.57 · DOI: 10.1021/cr300116k · Source: PubMed

CITATIONS

152

READS

134

4 AUTHORS:



Dan-Wei Zhang

Fudan University

70 PUBLICATIONS 685 CITATIONS

[SEE PROFILE](#)



Xin Zhao

Shanghai Jiao Tong University

86 PUBLICATIONS 1,665 CITATIONS

[SEE PROFILE](#)



Jun-Li Hou

Fudan University

34 PUBLICATIONS 1,728 CITATIONS

[SEE PROFILE](#)



Li Zhan Ting

Fudan University

190 PUBLICATIONS 4,535 CITATIONS

[SEE PROFILE](#)

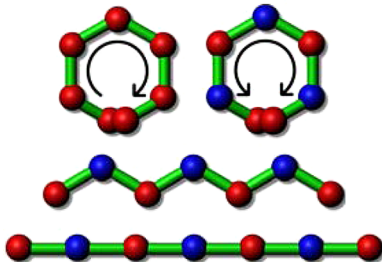
Aromatic Amide Foldamers: Structures, Properties, and Functions

Dan-Wei Zhang,[†] Xin Zhao,[‡] Jun-Li Hou,[†] and Zhan-Ting Li*,[†]

[†]Department of Chemistry, Fudan University, 220 Handan Road, Shanghai 200433, China

[‡]Shanghai Institute of Organic Chemistry, Chinese Academy of Sciences, 345 Lingling Road, Shanghai 200032, China

Aromatic amide foldamers



CONTENTS

1. Introduction	5271
2. Intramolecular Hydrogen-Bonding Patterns	5272
3. Factors That Affect the Stability of the Hydrogen-Bonding Patterns	5274
4. General Synthetic Considerations	5276
5. Characterization of the Secondary Structures	5276
6. Extended Secondary Structures	5277
6.1. Aromatic Amide Oligomers	5277
6.2. Aromatic–Aliphatic Amide Oligomers	5280
6.3. Benzoylurea Oligomers	5281
6.4. Aromatic Hydrazide Polymers	5281
6.5. Aromatic–Aliphatic Hydrazide Oligomers	5282
6.6. Arylene Oligomers and Polymers	5282
6.7. <i>p</i> -Phenylenethynylene Oligomers	5282
7. Folded or Helical Secondary Structures	5283
7.1. Oligomeric Amides with Benzene Spacers	5283
7.2. Oligomeric Amides with Heterocycle Spacers	5286
7.3. Oligomeric Amides with Mixed Aromatic Spacers	5287
7.4. Oligomeric Amide–Sulfonamide Hybrids	5289
7.5. Oligomeric Imides with Pyridine Spacers	5290
7.6. Oligomeric Hydrazides with Benzene Spacers	5290
7.7. Poly- and Oligourea Foldamers	5290
7.8. <i>m</i> -Phenylenethynylene Oligomers	5291
8. Branched Architectures	5291
9. Folded Dendrimers	5292
10. Binding-Induced Folding	5293
11. Folding-Promoted Reactions	5294
11.1. Macrocyclization	5294
11.2. Pyridine Oxidation	5299
11.3. Quinoline Chlorination and Bromination	5300
11.4. Anisole Hydrolysis	5300
12. Molecular Recognition	5300
12.1. Amide Foldamer Receptors	5300
12.2. Hydrazide Foldamer Receptors	5303
12.3. Macrocyclic Receptors	5303
12.4. Biological Functions	5303
13. Self-Assembly	5305
13.1. Double, Triple, and Quadruple Helices	5305
13.2. [2]Catenanes and [2]Rotaxanes	5307
13.3. Organogels, Vesicles, and Liquid Crystals	5308
14. Tuning Intramolecular Donor–Acceptor Interactions	5309
15. Tuning Dynamic Property of Copolymers	5310
16. Conclusions and Prospects	5310
Author Information	5311
Corresponding Author	5311
Notes	5311
Biographies	5311
Acknowledgments	5312
List of Abbreviations	5312
References	5312

1. INTRODUCTION

The past several decades have witnessed great progress in the understanding of the high-order structure of biomacromolecules. Currently, it is well-recognized that folding of proteins is the base for their higher-order tertiary and quaternary structures and, thus, their remarkable functions, such as molecular recognition, transport, electron transfer, and catalysis. As the database of the protein sequences and structures grows, in the past two decades, interest in creating artificial compact structures has also grown rapidly. Particularly, oligomers consisting of discrete unnatural aliphatic amino acids have received great attention.^{1–7} This is not unexpected, considering that natural α -amino acid-based peptides and proteins utilize hydrogen bonding, as well as hydrophobicity, to stabilize their compact structures. In organic solvents, hydrogen bonding plays a more important role for stabilizing the artificial systems. Both experimental and theoretical studies have revealed that unnatural amide sequences, specifically those consisting of β -amino acid and hybridized α -/ β -amino acid residues, can form helices, turns, and sheets.^{1–7} Other noncovalent forces, including hydrophobicity for oligomeric arylacetylenes,^{8,9} naphthalene-incorporated ethylene glycols,¹⁰ and cholates,¹¹ electrostatic (dipole–dipole) repulsion for oligomeric heteroaromatic strands,¹² and donor–acceptor interaction for 1,5-dialkoxy naphthalene-incorporated oligoglycols and naphthalene diimide-incorporated peptide derivatives,^{13–16} have also been extensively utilized. The subject along this line has been recognized as the field of foldamers.^{2a} A *Chemical Reviews* article by Moore and co-workers provided a

Received: March 19, 2012

Published: August 7, 2012

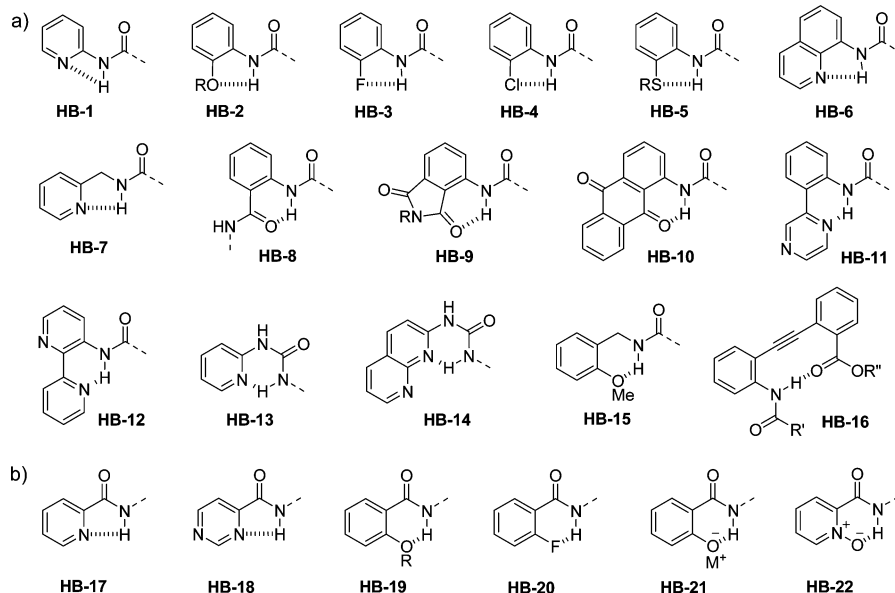


Figure 1. Representative intramolecular hydrogen-bonding patterns for the construction of aromatic amide foldamers. (a) The aromatic unit is attached to the amide nitrogen atom. (b) The aromatic unit is attached to the carbonyl carbon atom.

comprehensive background in this field and summarized the progress before 2001,¹⁷ and a book, edited by Hecht and Huc, accumulated reviews of the related literature until 2005.¹⁸

This review covers the family of foldamers that comprise aromatic amide segments and are stabilized mainly by intramolecular hydrogen bonding. The first examples of aromatic amide-based foldamers were reported in 1994 by Hamilton and co-workers.¹⁹ In their seminal papers,^{19,20} two series of compact structures were described. The first series was based on 2-substituted anthranilamide oligomers, which exhibited an extended sheet conformation stabilized by six-membered N–H...O=C hydrogen bonding between adjacent amides. The backbones of the second series were composed of a pyridine-2,6-dicarboxamide N-oxide or pyridine-2,6-dicarboxamide spacer connected with two anthranilamide subunits, which were induced by six-membered N–H...O⁻–N⁺(Py) and five-membered N–H...N(Py) hydrogen bonding to adopt a folded or helical conformation. Since 2000, a large number of heterocyclic and benzene-derived monomeric precursors have been designed and developed.^{21–27} Because of the inherent rigidity and planarity of aromatic amide segments, this family of foldamers shows a high preference for forming predictably folded structures. Compared with other kinds of aromatic foldamers such as those based on *m*-phenylene ethynylene oligomers,^{8,9,17} aromatic amide foldamers may also fold to form cavities of varying sizes. In addition, depending on the nature of the monomeric segments, the backbones can give rise to many different conformations such as extended or straight,^{28,29} zigzag,³⁰ and V-styled structures,³¹ and a combination of different kinds of segments into one sequence may produce many more possibilities, if they are long enough. Although different from natural α -amino acids, which, except glycine, all bear a chiral carbon, aromatic monomeric segments contain no chiral centers; chiral folded or helical structures can be readily constructed by simply introducing one or more chiral groups at the ends or in the middle of the backbones.³² Therefore, in the past decade, aromatic amide foldamers have found extensive applications in many different areas, including, among others, molecular design for targeting biomacromolecules and cell

membranes,^{28,33,34} molecular recognition and self-assembly,^{24,35} tuning the functionalities of molecular and macro-molecular systems,^{36–39} and promoting macrocyclization.^{40–47}

A number of reviews dealing with aromatic amide foldamers have been published. Early papers described original efforts in molecular design and the development of hydrogen-bonding patterns.^{48,49} Several recent papers mainly summarized their applications in specific areas, such as supramolecular self-assembly,^{50–52} macrocycle synthesis,⁵³ and peptidomimetics and chemical biology.^{54,55} This review provides a comprehensive survey of this family of aromatic foldamers. We first discuss the design principles, intramolecular hydrogen-bonding patterns, monomer structures, general synthetic strategies, and structural characterizations and then describe the important structures and their properties and/or functions. To provide a complete overview of the topic, partially intramolecularly hydrogen-bonded oligobenzamides, and hydrogen-bonded compact structures generated by aromatic urea, hydrazide, and conjugated oligomers, as well as aromatic/aliphatic amide hybrids,⁵⁶ except those with limited aromatic amide subunits,⁵⁷ are also included.

2. INTRAMOLECULAR HYDROGEN-BONDING PATTERNS

Because of its partial double bond nature, the rotation around the amide C–N bond is remarkably restricted. The rotational barrier is estimated to be 65–90 kJ/mol, depending on connected groups and the environment.⁵⁸ In principle, an amide unit may exist as two rotamers. However, the trans form is substantially favored due to an energy discrimination of ~8 kJ/mol over the cis form.⁵⁸ For aromatic amide oligomers, if the ortho-positions of the amide unit have no substituents, the (Ar)C–CO(NHAr) and (Ar)C–NH(COAr) bonds will rotate freely, leading to two partially coplanar conformations of comparable stability. Thus, for the formation of any stable secondary structure with these segments, the key is to restrict this kind of rotation. Intramolecular hydrogen bonding provides the most simple, efficient, and reliable approach.

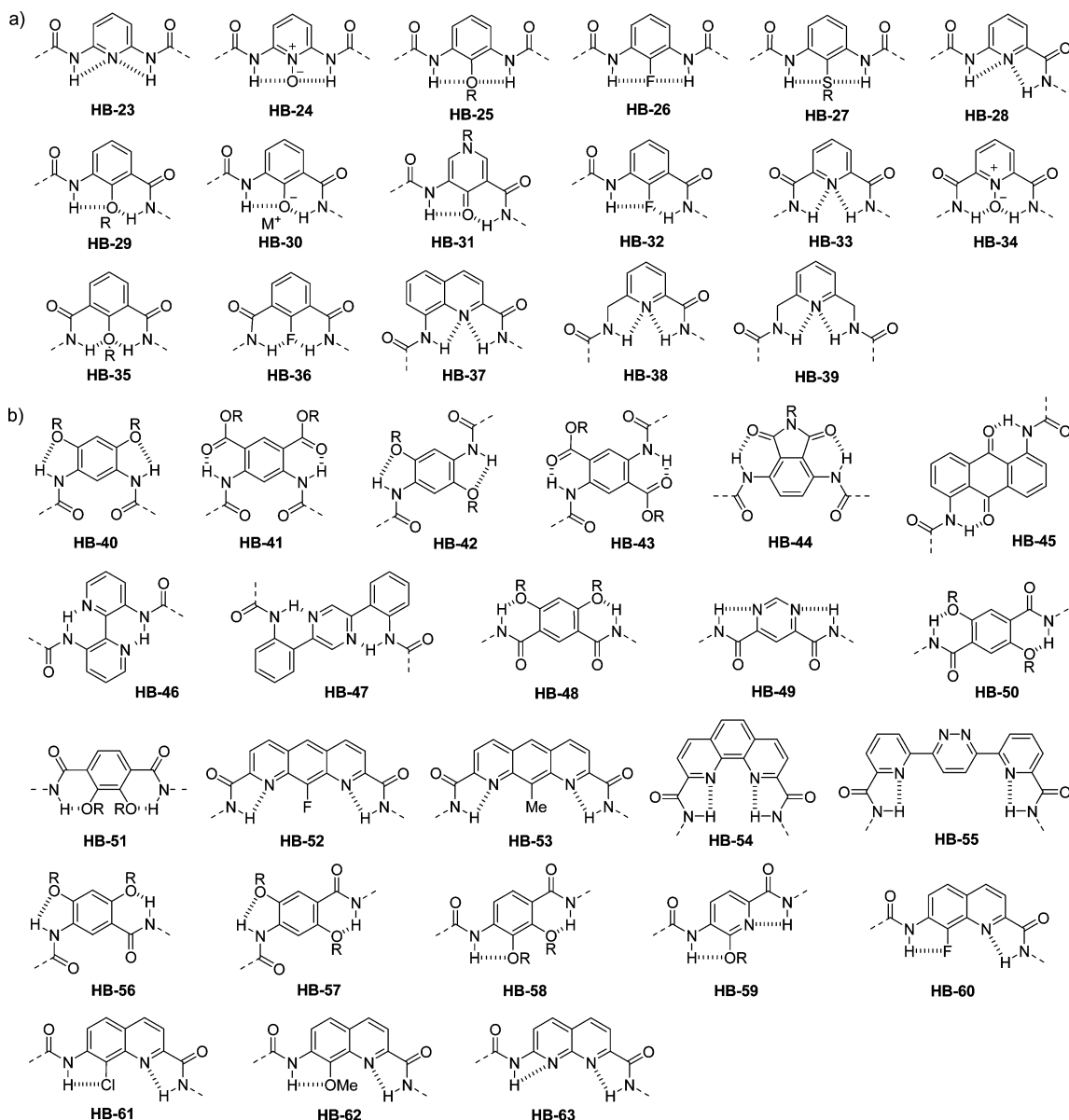


Figure 2. Aromatic segments that form two hydrogen bonds for the construction of aromatic amide foldamers: (a) Bifurcated three-center patterns in which two amide protons are hydrogen-bonded to one acceptor. (b) Two hydrogen bonds are formed separately.

Hydrogen bonding has recently been defined by an IUPAC task group as “*an attractive interaction between a hydrogen atom from a molecule or a molecular fragment X–H in which X is more electronegative than H, and an atom or a group of atoms in the same or a different molecule, in which there is evidence of bond formation.*”⁵⁹ For amides, in most cases, the stability of the hydrogen bonding formed by their hydrogen atoms increases with the increase of the electronegativity of the acceptors.⁶⁰ This is exactly the case for the oxygen and nitrogen acceptors, and intramolecular hydrogen bonds formed between them and aromatic amide hydrogen atoms are usually strong and have been widely used for the construction of compact structures. In contrast, halogen and sulfur atoms in neutral organic molecules are relatively weak hydrogen-bonding acceptors.^{61,62} As for fluorine, although it possesses the highest electronegativity, over the years it was accepted that fluorine “hardly ever accepts hydrogen bonds”,^{62b} presumably due to its low polarizability and tightly contracted lone pairs. Nevertheless, the intramolecular hydrogen-bonding patterns formed between aromatic amides

and fluorine, or even chlorine and sulfur atoms, have been confirmed and have found applications in the construction of foldamers.^{24b,34,63}

Figure 1 summarizes the representative intramolecular hydrogen-bonding patterns that have been utilized for the construction of aromatic amide foldamers. The first series are those with the hydrogen bonding being formed between the amide hydrogen atom and acceptors in or on the aromatic unit attached to the amide nitrogen atom. *N*-(2-Pyridyl)amides and their quinoline analogues can form four-membered hydrogen-bonding pattern **HB-1**.^{64,65} In the presence of strong acid, the pyridine nitrogen atom can be protonated to change into a hydrogen-bonding donor for the adjacent carbonyl oxygen.⁶⁶ Five-membered hydrogen-bonding patterns **HB-2–7** are among the main choices in this family for the development of folded structures. The six-membered pattern **HB-8** with the carbonyl oxygen atom as acceptor had been used to build one of the first reported kinds of aromatic amide-based extended structures.^{19,20} In a similar way, **HB-9** and **HB-10** can also be

formed with phthalimide or anthraquinone carbonyl oxygen atom as acceptor.^{67,68} Owing to the rigidity of the backbones, these hydrogen-bonding patterns should be more stable than **HB-8**. The aromatic units may also be biaryls. Two six-membered patterns of this kind, **HB-11** and **HB-12**, have been reported.⁶⁹ 1-(Pyridin-2-yl) and 1-(1,8-naphthyridin-2-yl) urea derivatives can form six-membered patterns **HB-13** and **HB-14**.⁷⁰ However, the latter system can also adopt an extended conformation, which is stabilized by the formation of a homodimer through four intermolecular hydrogen bonds.⁷¹ The amides of 2-(aminomethyl)-substituted pyridine and anisole can form five- and six-membered hydrogen-bonding patterns **HB-7** and **HB-15**,^{72,73} respectively, which have been applied to build helical and extended structures. The diamides of benzene-1,2-diamine and phthalic acid might form intramolecular seven-membered hydrogen bonding. However, this pattern has not been observed in the crystal structures of several related compounds.⁷⁴ Owing to a large steric hindrance, the two adjacent amide subunits are rotated out of planarity with the aromatic ring, which favors the formation of intermolecular hydrogen bonding. No eight- or nine-membered hydrogen-bonding patterns formed by aromatic amides have been reported, even though stable nine-membered hydrogen bonding can be formed by aliphatic diamides.⁷⁵ However, 10-membered hydrogen-bonding pattern **HB-16** can be formed by 1,2-diphenylethyne amide derivatives.^{76–79} For the second series with the hydrogen bonding being formed between the amide proton and acceptors in or on the aromatic ring attached to the amide carbon atom (Figure 1), **HB-17** and **HB-18** are the five-membered patterns that have found wide applications in developing helical and zigzag structures.^{21,34} The pyridine nitrogen can also be protonated with strong acid and in this way forms five-membered hydrogen bonding with the adjacent carbonyl oxygen.⁶⁶ **HB-19** and **HB-20** are among the most widely used six-membered patterns.^{50,53,54} For one case, phenoxide salts form similar six-membered hydrogen-bonding pattern **HB-21**, which induces the related ionic amide oligomers to generate folded structures.⁸⁰ The six-membered hydrogen bonding of pyridine oxide, **HB-22**,^{19,20,81} can force the amide to generate a configuration similar to that of **HB-17**.

For the formation of a defined secondary structure, the rotation of all the single bonds of the backbones should be restricted. To realize this, all the linking aromatic segments in the backbones should form two hydrogen bonds, which requires that the hydrogen atoms of the amide units in the backbones are engaged in bifurcated hydrogen bonding.⁸² For the aromatic segments, they can be loosely classified into two groups: ones forming bifurcated three-center hydrogen bonding with one heteroatom as acceptor and others which form two separate hydrogen bonds with two acceptors in or on the ring. Figure 2 lists these two classes of aromatic segments that have been utilized for the construction of aromatic amide foldamers. Most of these hydrogen-bonding patterns can be considered as a rational combination of the single hydrogen bonds shown in Figure 1. For the first class, that is, **HB-23–39** (Figure 2a), two amide hydrogen atoms are hydrogen-bonded to one acceptor. Patterns **HB-23–27**, **HB-33–36**, and **HB-39** possess two identical hydrogen bonds, and the compact structures formed by them are thus symmetric. Patterns **HB-28–32** and **HB-37,38** are composed of two different hydrogen bonds. Foldamers constructed from these segments resemble natural peptides that comprise a one-way sequence of amino acids. Pattern **HB-31** is the only one that is constructed based on the

1-alkylpyridin-4(1H)-one ring.⁸³ Without the alkyl group, the pyridin-4(1H)-one ring may tautomerize to 4-hydroxypyridine, leading to other hydroxyl-mediated hydrogen-bonding patterns.^{49,65} For the second class, that is, **HB-40–63** (Figure 2b), patterns **HB-40–55** are symmetric, which are constructed with aromatic diamine or dicarboxylic acid precursors, whereas patterns **HB-56–63** are unsymmetric and constructed from corresponding aromatic amino acid precursors. With so many building blocks available, different secondary structures may be constructed by a rational combination of them in one sequence in a coded way.

For most of the aromatic segments shown in Figure 2, the two amides define an angle smaller than 180°. These segments include meta-orientated benzene and pyridine-based systems as well as double (**HB-60**,⁸⁴ **HB-61**,^{26c} and **HB-62**,⁶³⁴⁷) and triple (**HB-52**,⁸⁴ **HB-53**,⁸⁵ **HB-54**,²⁵ and **HB-55**,⁸⁶) ring-derived larger systems. Oligomers produced from these segments form folded or helical conformations. In contrast, oligomers formed by the symmetric segments, such as **HB-45**,⁶⁸ **HB-46**,^{69b} **HB-47**,^{69a} and **HB-50**,^{29,69b} whose amides are orientated in opposite directions, generate extended conformations. Because of the unsymmetric nature of their aromatic units, the angle defined by the two amides of one-way segments **HB-58**,^{23b} and **HB-59**,²⁸ is just slightly smaller than 180°. Thus, shorter oligomers formed from them can still keep an extended conformation.^{23b,28} For the folded or helical structures, incorporation of the large heterocycle segments, such as **HB-52–55**, or the benzene segments with two amide subunits being orientated at para-positions like **HB-42**, **HB-43**, and **HB-57**, will enlarge their cavity, which is important for the encapsulation of large guests.

3. FACTORS THAT AFFECT THE STABILITY OF THE HYDROGEN-BONDING PATTERNS

The stability of the secondary structure of an aromatic amide foldamer heavily depends on the strength of the intramolecular hydrogen bonding formed by monomeric segments. The ability of the amide hydrogen atom in simultaneously hydrogen bonding to two electronegative atoms has been recognized for several decades.^{87,88} For aromatic amide oligomers consisting of the same segments, it may be expected that the capacities of their amide hydrogen atoms as hydrogen-bonding donors are comparable. Therefore, the strength of the intramolecular hydrogen bonding formed between these hydrogen atoms and acceptors at the ortho-positions of the connected aromatic rings should mainly depend on the nature of the acceptors and the geometry of the hydrogen bonding and the aromatic ring. As for amide derivatives of 2-aminopyridine and 2,6-diaminopyridine, their crystal structures, except those of a few cyclic molecules, display the formation of the four-membered N–H···N hydrogen bonding.^{89,90} In addition to the electrostatic attraction between the amide hydrogen atom and the electronegative pyridine nitrogen atom that stabilizes this anti conformation, the repulsive interaction between the carbonyl oxygen atom and the pyridine nitrogen atom in the syn conformation also contributes significantly (Figure 3).⁹⁰ This electrostatic repulsion forces the two electronegative atoms to be away from each other, and the conjugation between the amide and pyridine units pushes them to be coplanar, leading to the favored anti conformation. This repulsive interaction exists in the syn conformation of other similar heterocyclic amides (Figure 3) and conjugated aromatic oligomers.^{12,86,91}

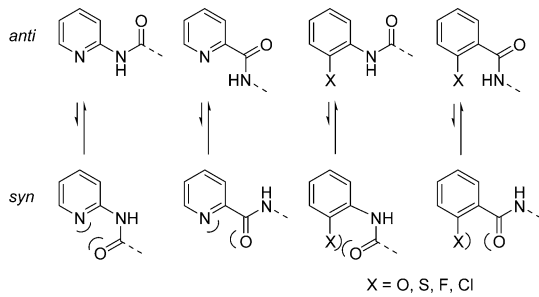


Figure 3. Two coplanar conformations of pyridine and benzene-based amide segments. The anti conformation is always more preferred over the cis one due to the electrostatic repulsion that exists in the syn conformation.

and, thus, is always a positive driving force for the formation of the required anti conformation.⁴⁹

The energy differences between the trans and syn conformations of compounds **1–6** have been evaluated using theoretical calculations (Figure 4).^{90,92} Using MOPAC at the

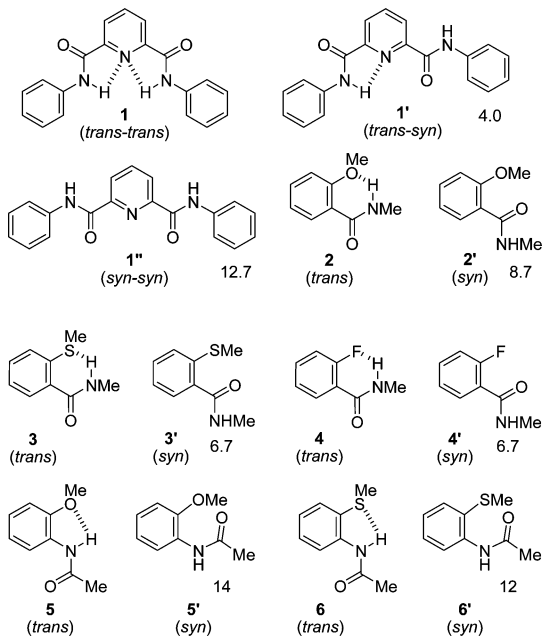
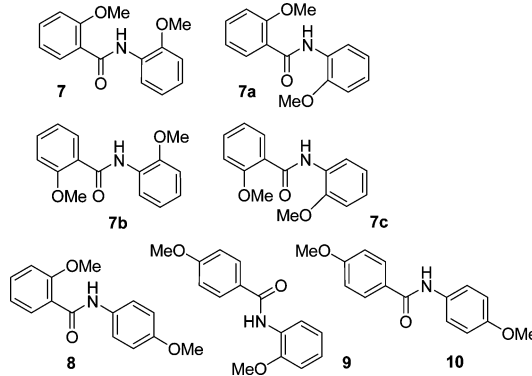


Figure 4. Structures of compounds **1**,⁹⁰ **2**,^{92b} **3**,^{92b} **4**,^{92d} **5**,^{92e} and **6**,^{92b,e} and their conformers (**1'–6'**). The values denote the torsion barriers (kcal/mol) of the less-favorable conformers relative to the favorable conformers.

AM1 level, the heats of formation for *trans-trans*-**1** and its two conformers *trans-syn*-**1'** and *syn-syn*-**1''** were calculated.⁹⁰ The *trans-trans* conformer was found to be more stable than the *trans-syn* and *syn-syn* ones by around 4.0 and 12.7 kcal/mol (Figure 4), which was in agreement with earlier theoretical calculations for a pyridine-2,6-dicarboxamide-derived cyclophane.^{92a} The torsion potential energies of *trans*-**2–6** to *syn*-**2'–6'** have also been obtained using quantum chemistry methods at various levels (Figure 4), which indicated that the syn conformation of all these compounds is significantly less favorable than the trans one. The following two factors were also proposed to rationalize the result: the syn system produces a high repulsion between the acceptor heteroatom and the C=O group and loses the stabilizing hydrogen bonding that exists in the trans conformer (Figure 4).^{92b}

It has also been evidenced that intramolecular five- or six-membered hydrogen bonding is more stable than other forms of hydrogen bonding.⁹³ Thus, for the construction of aromatic amide foldamers, the N–H···N and N–H···O hydrogen bonding of this type have received the widest applications. In crystal structures, except a few cases which all involved benzamide derivatives, most rationally designed molecules exhibited the expected five- and six-membered hydrogen bonding.⁹⁴ Anthranilamides may also form intramolecular seven-membered N–H···O=C hydrogen bonding, which, however, has not been observed in crystal structures,⁷⁴ reflecting the instability of this hydrogen-bonding pattern. The two hydrogen bonds in the three-centered hydrogen-bonding patterns may reinforce mutually.^{94b,c} This cooperativity was supported by detailed ab initio calculations on compounds **7–10** and conformational isomers of **7**, **7a–c**.^{94b} Compared with that of control compounds, the stretching frequency of the N–H bond of **8** and **9**, which forms a two-center hydrogen bond, underwent a red-shift, the bending frequency displayed a blue-shift, and the bond length increased generally. The calculated chemical shifts of their NH signals were also shifted to the lower field. For three-centered hydrogen-bonded compound **7**, all these changes were enlarged considerably, indicating a positive cooperativity existed between its two two-centered hydrogen bonds. It is reasonable to propose that the amide hydrogen atom in the three-centered pattern is spatially “saturated”. Thus, its tendency for the formation of intermolecular N–H···O=C hydrogen bonding and the competition of the solvent molecules are both substantially suppressed, which may be responsible for this cooperativity.



The competitive intermolecular N–H···O=C hydrogen bonding of the amide unit is always a negative interaction for the formation of intramolecular hydrogen bonding, because it causes the amide unit to rotate out of planarity with the connected aromatic rings. This intermolecular hydrogen bonding is the main driving force for the high-strength feature of commercial aromatic polyamides such as Kevlar and Nomex.⁹⁵ With local heterocycle nitrogen atoms or ether oxygen atoms as acceptors, the corresponding three-centered hydrogen-bonding patterns are usually stable enough to win the competition over this intermolecular interaction, and in most cases, the intermolecular N–H···O=C hydrogen bonding can be suppressed in the solid state. However, simple two-centered intramolecular hydrogen bonding usually coexists with intermolecular hydrogen bonding in crystal structures.^{94b,96}

Because azaheterocycles utilize their fused nitrogen atoms to serve as hydrogen-bonding acceptors, which minimizes the substituent-initiated spatial hindrance, foldamers based on

azaheterocycles exhibit an increased stacking tendency and may form double,^{21,97} triple,⁹⁸ or even quadruple helices.^{26a} The absence of substituents at the ortho-position of the amide units also makes it possible for them to form N–H···O=C hydrogen bonding across the strands within the helices but not across different helices.

When using fluorine atom as acceptor, both the five- and six-membered and three-centered F–H···N hydrogen-bonding patterns can be observed in crystal structures.^{24b,63a,99} However, the fluorine atom is considerably smaller than methoxyl, the smallest alkoxy group. Thus, the amide hydrogen atom engaged in the three-centered hydrogen-bonding pattern can further form intermolecular N–H···O=C hydrogen bonding.^{63a} In the crystal structures of several aromatic amides that bear fluorine substituent at the ortho-position, intramolecular F–H···N hydrogen bonding is not observed due to a large torsion of the amide unit from the benzene ring as a result of steric hindrance or strong intermolecular N–H···O=C hydrogen bonding.¹⁰⁰ These observations are consistent with the fact that the fluorine atom as hydrogen-bonding acceptor is not as strong as oxygen or nitrogen. However, both ¹H NMR and IR experiments supported that five- and six-membered F–H···N hydrogen bonding existed in solution for all investigated compounds.^{24b}

Owing to poor solubility of aromatic amide backbones, side-chains are frequently attached to the designed backbones to tune their solubility. Nonpolar alkyl chains improve solubility in less-polar organic solvents, while oligomeric ethylene glycols or ionic side-chains can provide solubility in polar organic or aqueous media. Derivatives bearing long side-chains are difficult to crystallize. Thus, for the growth of single crystals for X-ray diffraction analysis, short side-chains are usually chosen and the isobutyl group has been found to be good for balancing solubility and crystallinity.²² For the assembly of ordered supramolecular structures from foldamer derivatives, amphiphilic amide side-chains have also been developed.^{35d} Side-chains are usually not engaged in intramolecular hydrogen bonding. Thus, in solution they do not impose a large influence on the compact conformation of the backbones. However, in crystal structures, the side-chains may affect the stacking behavior via imposing steric hindrance or forming intermolecular von der Waals interaction, leading to the disruption of intramolecular hydrogen bonding.^{63c} For extended and most of the folded or helical systems, the stacking of long backbones enhances intramolecular hydrogen bonding by increasing the coplanarity of adjacent aromatic segments.

In solution, intermolecular N–H···O=C hydrogen bonding is highly dependent on the concentration of the samples as well as the solvent polarity. In contrast, the change of the concentration has a little influence on intramolecular hydrogen bonding, if there exists no important stacking of the backbones. Increasing solvent polarity usually enhances intermolecular stacking interaction. However, reducing concentration can substantially weaken it, even to a negligible extent. Increasing solvent polarity also weakens intramolecular hydrogen bonding. Molecular dynamics simulations showed that, in the gas phase, compounds **2** and **4** are primarily in the hydrogen-bonded conformation, and for compound **3**, 28.8% of all conformations are intramolecularly hydrogen-bonded.^{92e} In polar methanol, the number of other flexible conformations increases for all three molecules. In aqueous solution, the percentage of intramolecularly hydrogen-bonded conformations is reduced to 51.7% for **2**, 43.0% for **4**, and 3.7% for **3**. For azaheterocycle

foldamers, the fused nitrogen atom may be acidified by strong acid to become a hydrogen-bonding donor,¹⁰¹ which represents a general strategy for controlling conformational transitions of the backbones.¹⁰²

4. GENERAL SYNTHETIC CONSIDERATIONS

Thanks to the progress in peptide synthetic chemistry,^{103,104} the synthesis of aromatic amide foldamers is relatively straightforward. Most of the synthesis involves the formation of the amide bonds in solution phase, while the solid-phase strategy has just received limited attention.¹⁰⁵ If possible, carboxylic acids are usually converted into acid chlorides by treating the acids with thionyl chloride or oxalyl dichloride for subsequent coupling with amines. The acids may also be converted to activated esters before coupling with amines. Direct coupling of acid and amine precursors in the presence of coupling reagents is also widely adopted. For multistep synthesis, the carboxylic acids are usually protected as methyl or ethyl esters, which can be easily saponified with alkali hydroxide, whereas the amines can be obtained from deprotection of the corresponding carbamates (Boc, Cbz, and Fmoc) or from the reduction of a nitro group.¹⁰⁶ Acid precursors that bear acid-labile protecting-groups may also be activated by Ghosez reagent,¹⁰⁷ that is, tetramethyl- α -chloroaniline, to avoid the formation of hydrochloride during the reactions.¹⁰⁸ The synthesis of long oligomers is usually performed through a convergent strategy to minimize the number of reaction steps. This strategy involves the formation of two peptide bonds from the reaction of a diamine and a monoacid (1:2) or a monoamine and a diacid (2:1). In this way, oligomers of high molecular weights can be prepared after a limited number of steps.

When oligomeric building blocks are long enough to form a helical conformation, the coupling process will become slow and inefficient, which is usually attributed to intramolecular stacking of the precursors or intermediates in the helical conformation. Longer reaction times and higher temperature may improve the yields. Using polar solvents may also help because they destabilize the intramolecular hydrogen bonding and increase the flexibility of the backbones. To restrain the formation of the helical conformation during synthesis, the acid-labile 2,4-dimethoxybenzyl group has been attached to the amino group in the precursors.^{109,110} The amides obtained thereby bear no hydrogen atoms, and thus the resulting oligomers do not form a helical conformation to impose steric hindrance for further coupling. By using this approach, a 15-mer aromatic amide oligomer has been prepared.¹¹⁰

5. CHARACTERIZATION OF THE SECONDARY STRUCTURES

Compared to aliphatic amide counterparts, aromatic amide foldamers possess relatively stable and defined conformations and are therefore easy to characterize. X-ray diffraction is the major tool for the structural characterization in the solid state. Crystal structures of a large number of model molecules and short oligomers have been reported. Crystal structures of many long, complicated heterocycle-based helices are also available. For benzene-based systems, long backbones are usually difficult to crystallize. However, the structural parameters of their basic building blocks are well-defined. For long oligomers consisting of repeated segments, the compact structure of the whole backbone can be regarded as a combination of all locally

defined conformations. Using the parameters collected from the basic motifs as structural constraints, molecular structural modeling could predict the secondary structures of long benzene-based foldamers.

¹H NMR spectroscopy is the most important technique for the characterization of the compact conformations in solution. Discrete two-dimensional techniques have been used to assign signals in the low-field region. Typically, compared with those of the controls, the signals of hydrogen-bonded amide hydrogen atoms exhibit a remarkable downfield shifting, which is an indicator of the formation of intramolecular hydrogen bonding. Intramolecular nuclear Overhauser effect (NOE) contacts are regarded as evidence for local compact conformations,^{11a} whereas the end-to-end NOE contacts have been used to support the formation of the helical structures. Hydrogen/deuterium-exchange experiments can also be performed to evaluate the stability of the hydrogen bonding.^{11b,c}

IR spectroscopy may also be useful for the characterization of intramolecular hydrogen bonding.^{11d} The stretching frequency of hydrogen bonding-free amide N–H bonds usually appears in the region of 3400–3500 cm⁻¹.^{11d} When the amide hydrogen atoms are hydrogen-bonded, they will undergo a red-shifting, regardless of whether it is in solution or solid state. If the molecules bear no hydroxyl groups, the IR spectrum can be thus used as evidence for the formation of intramolecular hydrogen bonding by aromatic amides, if the absorption frequencies are independent of concentration changes.

In solution, intramolecular hydrogen bonding enhances the coplanarity of the aromatic backbones. This may cause their long-wavelength absorption bands in UV-vis spectra to shift bathochromically.^{28,29,69a,77,78a} For a series of short oligomers, the shifting may be enlarged with the elongation of the backbones because longer rigid molecules have enhanced amide bond delocalization and δ -conjugation as a result of the coplanarity of the repeating segments.

6. EXTENDED SECONDARY STRUCTURES

6.1. Aromatic Amide Oligomers

β -Sheet is one of the most common secondary structures in polypeptides. Mimicking this important structural motif may lead to the construction of well-defined artificial architectures that exhibit functions in discrete areas. Aromatic amide oligomers can adopt similar extended conformations when the amide units connecting the aromatic rings in the backbones are directed by intramolecular hydrogen bonding to adopt divergent orientations.

Hamilton and co-workers reported the synthesis of anthranilamide oligomers **11a,b** and **12a,b**.²⁰ Initial synthetic attempts for these molecules involved carboxyl activation of **13** followed by reaction with aniline derivatives. However, instead of forming anilide products, the reactions gave rise to azlactone **14** through intramolecular cyclization of the benzamide oxygen onto the adjacent carboxylic group.^{11d} A more successful approach involved masking the amide as a nitro group.¹⁰⁶ After the amide bond was generated, the nitro group in the product was reduced to the required amine for further coupling reactions. By using this strategy, all the oligomers could be prepared in good yields. X-ray structure of compound **11a** showed the expected zigzag structure (Figure 5),²⁰ which was stabilized by two strong intramolecular hydrogen bonds between adjacent amide and/or ester groups. The molecule

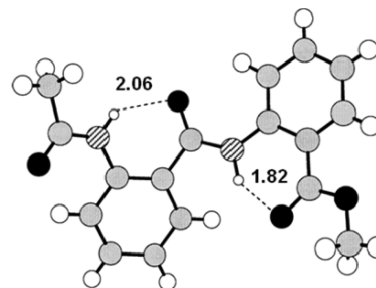
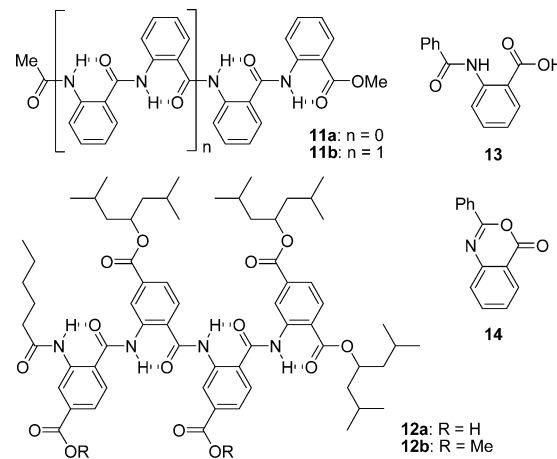


Figure 5. X-ray structure of anthranilamide **11a** in the extended conformation. Reproduced with permission from ref 20. Copyright 1996 American Chemical Society.

had an almost planar conformation with only a small deviation of the amide units from the connected benzene rings. The X-ray structures of compounds **11b** and **12a,b** are not available. Their extended conformations were evidenced by systematic ¹H NMR experiments.



The formation of the rigid zigzag conformations of the above compounds also reflects the inherent planarity of the amide units and their preference in adopting the trans configuration.⁵⁸ Li and co-workers described the construction of another kind of zigzag extended structures from anthranilamide oligomers **15a–d**.³⁰ These oligomers were conveniently prepared from the reactions of related amine and carboxylic acid precursors in the presence of a coupling reagent such as DCC. Crystal structures of **15a** and **15b** were obtained, both of which exhibited all the expected three-centered hydrogen bonds (Figure 6), which forced the backbones to adopt a nearly planar, zigzag conformation. Because the longer 7-mer **15c** and 9-mer **15d** possess the identical structural subunit, both molecules and the even longer analogues should exist in similar extended conformations. A space-filling model of planar **15d**, with a length of 4.60 nm, showed a slightly curved conformation (Figure 7). The para-positions of the methoxyl groups of the benzamide and isophthalamide rings can be appended with different functional groups. The corresponding derivatives have found wide applications in supramolecular chemistry.^{50b}

DeGrado and co-workers reported that the aromatic backbone of **16a** also formed a compact conformation.^{55,114} The crystal structure showed that the two sulfur atoms both formed a five-membered N–H···S hydrogen bond, and the two pairs of three-centered hydrogen bonds controlled the planar conformation (Figure 8). Similar three-centered hydrogen

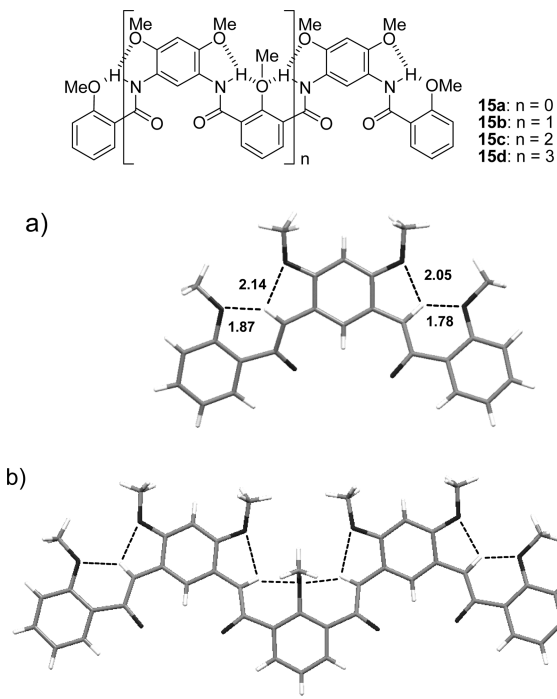


Figure 6. Crystal structures of 3-mer **15a** (a) and 5-mer **15b** (b).³⁰ Both molecules adopt preorganized conformations that are stabilized by the strong three-centered hydrogen bonding.

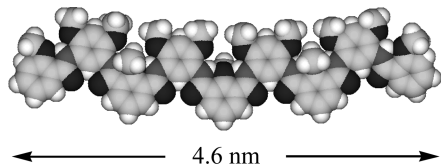


Figure 7. CPK model of 9-mer **15d**, showing a slightly curved shape. Reproduced with permission from ref 30. Copyright 2004 American Chemical Society.

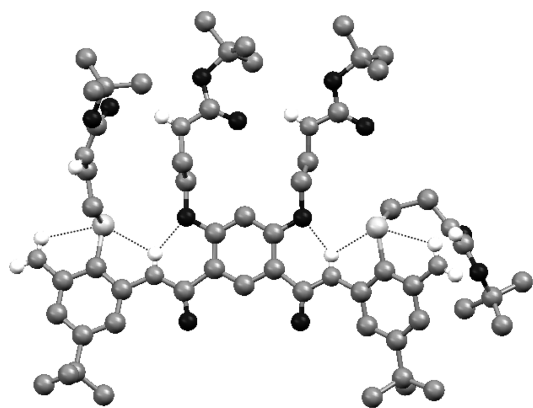
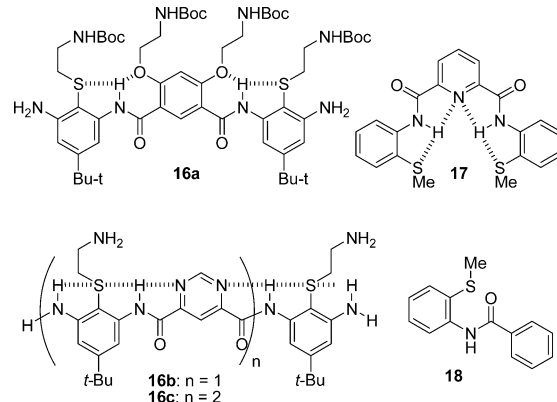


Figure 8. Crystal structure of compound **16a**,¹¹⁴ showing the formation of two pairs of N–H···S and N–H···O hydrogen bonds.

bonding was also formed in the crystal structure of compound **17**.¹¹⁵ In contrast, similar five-membered hydrogen bonding was not observed in the crystal structure of compound **18**,^{63c} the amide unit of which was twisted greatly from the methylthio-substituted benzene ring to form intermolecular N–H···O=C hydrogen bonding. This result appears to suggest

that the two kinds of different hydrogen bonds in **16a** and **17** reinforced mutually.^{94b} The Tew group further reported the synthesis of **16b** and **16c** by replacing the benzene ring in **16a** with a pyrimidine ring.³⁴ The two nitrogen atoms in the pyrimidine ring acted as hydrogen-bonding acceptors, making the scaffold more rigid. X-ray crystal structure of the Boc derivative of **16b** showed that the backbone formed the proposed compact conformation, which was also stabilized by the three-centered hydrogen-bonding motif.



Hamilton and co-workers reported that methyl-5-amino-6-alkoxypicolinate could be used to prepare pyridine trimers **19a**–**f**.²⁸ The three-centered hydrogen bonding in these molecules was confirmed in both CDCl₃ and dimethyl sulfoxide (DMSO)-d₆ by ¹H NMR technique and theoretical modeling. The crystal structure of nitro derivative **19f** further showed that the triamide backbone was planar and all the isopropyl side-chains were projected from one side of the backbone (Figure 9). Again, the backbone was slightly curved due to the

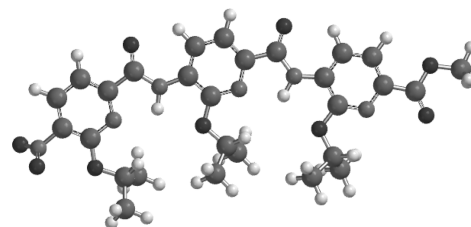
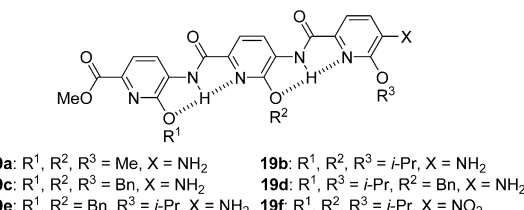


Figure 9. Crystal structure of compound **19f**. Reproduced with permission from ref 28. Copyright 2003 Wiley–VCH.

induction of the three-centered hydrogen bonding as well as the shrinking of the N–C bond relative to the C–C bond in the pyridine ring.



19a: R¹, R², R³ = Me, X = NH₂ **19b:** R¹, R², R³ = i-Pr, X = NH₂
19c: R¹, R², R³ = Bn, X = NH₂ **19d:** R¹, R³ = i-Pr, R² = Bn, X = NH₂
19e: R¹, R² = Bn, R³ = i-Pr, X = NH₂ **19f:** R¹, R², R³ = i-Pr, X = NO₂

Li and co-workers described the preparation of another type of extended, straight secondary structure, that is, oligomers **20a**–**d**, from suitably modified *p*-phenylenediamines and *p*-phthalic acids.²⁹ For the synthesis of 7-mer **20d**, the last step involved the reaction of 2,5-bis(hexyloxy)terephthaloyl dichloride with 2 equiv of the corresponding 3-mer amine

precursor. Direct coupling of 2,5-bis(hexyloxy)terephthalic acid with the amine in the presence of typical coupling reagents failed to afford the product due to low reactivity of the amine precursor. The crystal structures of 3-mer **20a** and **20b** and model compound **21** showed that all the amide protons were engaged in the designed six-membered (three-center) hydrogen bonding (Figure 10). The crystal structures of **20c** and **20d**

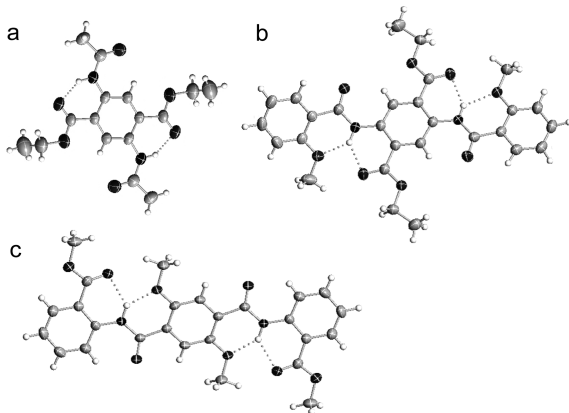
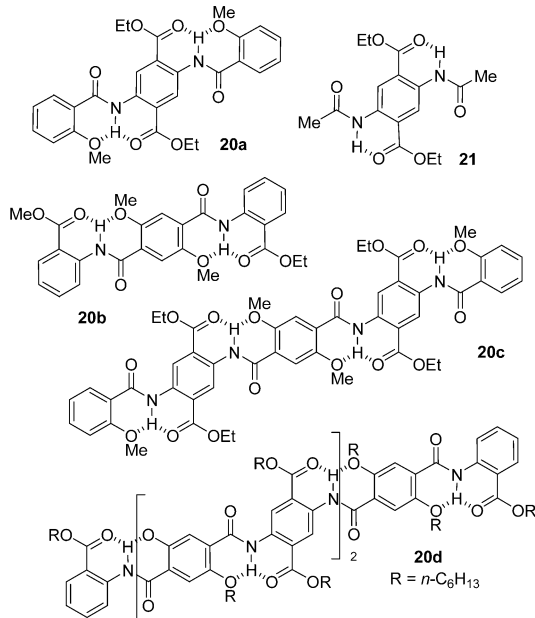


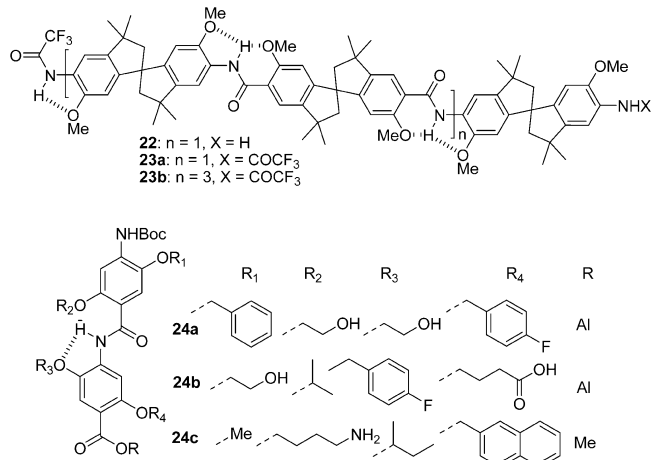
Figure 10. Crystal structures of compounds **21** (a), **20a** (b), and **20b** (c), highlighting the extended, straight conformation. Reproduced with permission from ref 29. Copyright 2004 American Chemical Society.

were not reported. Their extended conformations were characterized using ^1H NMR, IR, and UV-vis spectroscopy. The ester groups can also be replaced with alkoxy groups to form five-membered intramolecular hydrogen bonding.³¹ The corresponding diamine intermediates are more reactive for the formation of amide bonds.



The aromatic spacers of both diacid and diamine monomers have been modified for the construction of new secondary structures.¹¹⁶ For example, Sanjayan and co-workers reported the synthesis of oligomers **22** and **23a,b** using rigid spirobi(Indane) units as the linkers.^{116a} The stability of the three-centered hydrogen bonding of the amide groups is not affected by the spirocyclopentane moiety. Ab initio molecular orbital

(MO) calculations indicated that the longer oligomer **23b** had a propensity of forming an unusually large helical structure.



To mimic amphiphilic α -helices, Ahn and co-workers designed another kind of rigidified backbone **24a–c**, which was based on benzamide residues.¹¹⁷ The hydrogen-bonded aromatic scaffold placed four side-chain functional groups to positions found at the *i*, *i* + 2, *i* + 5, and *i* + 7 positions of a peptide helix. The crystal structure of **24a** confirmed that the amide hydrogen atom was engaged in the three-centered hydrogen-bonding pattern (Figure 11), which forced two of the

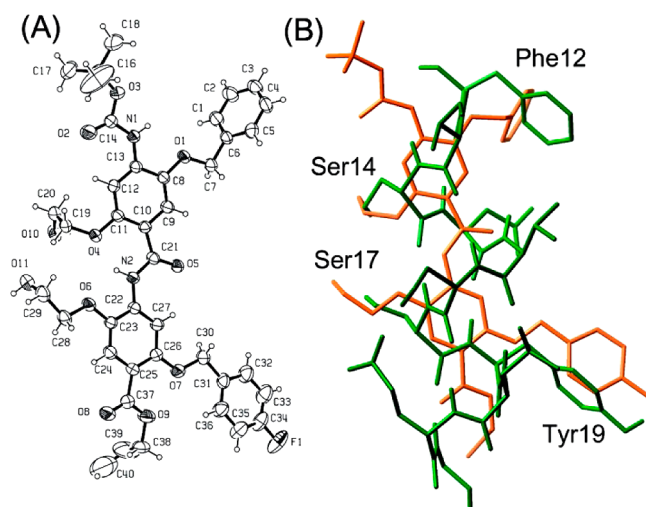
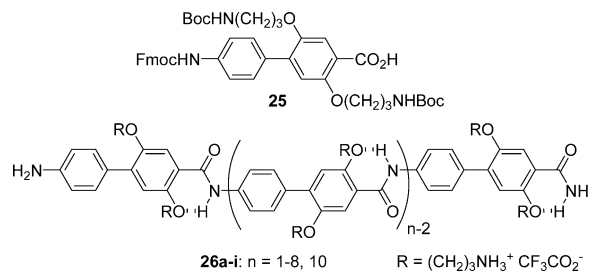


Figure 11. (A) X-ray crystal structure of α -helix mimetic **24a** and (B) superimposition of **24a** (orange) over the corresponding helical segment in GLP-1 (green). Reproduced with permission from ref 117. Copyright 2009 American Chemical Society.

four alkoxy groups to locate on the same side and another two on the opposite side. The structure well overlays on the corresponding α -helical peptide segment in GLP-1 (Figure 11B).¹¹⁸

For the above aromatic amide oligomers, the hydrogen atoms of the linking amides are all engaged in three-centered hydrogen bonding and thus induce the backbones to adopt the extended conformation of lowest energy. Removing one of the two bifurcated hydrogen bonds would allow for free rotation of the local (Ar)C–NH or (Ar)C–C(C=O) single bond. When every amide of an oligomer forms only one hydrogen bond, the backbone will possess multiple low-energy conformations in

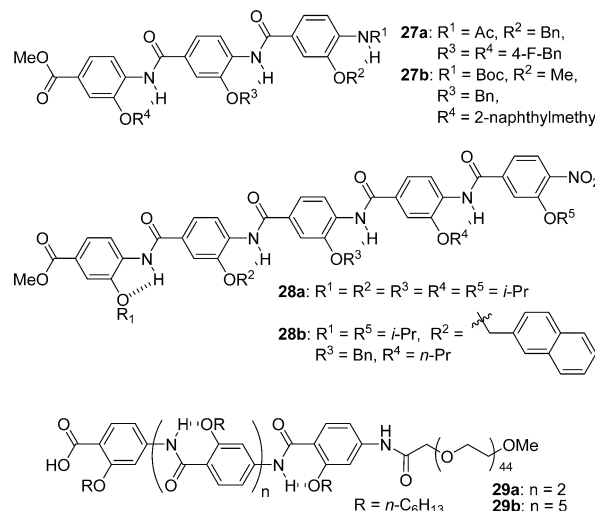
solution. Several kinds of such nonfully hydrogen-bonded aromatic amide oligomers have been developed. For example, Nowick and co-workers reported the synthesis of rodlike biphenyl-based amino acid **25**,¹¹⁹ which spans a distance of ~ 1 nm. Aminoalkyl chains were connected to the benzene rings to mimic the structure of lysine and also to increase solubility in water via protonation. The amide hydrogen atoms form intramolecular hydrogen bonding with adjacent ether oxygen atoms, imparting a local conformational rigidity to the molecule. The terminal amino group was protected as its Fmoc derivative for solid-phase synthesis. Oligomers **26a–i** have been prepared starting from **25** on Rink amide resin. Molecular modeling showed that 10-mer oligomer **26i** had a length of ~ 10 nm. The building block has been successfully used to construct new compact macrocycles.^{119b}



For the development of rigidified scaffolds for mimicking the face of α -helix, the groups of Ahn and Wilson had independently constructed five-membered hydrogen-bonding-mediated oligomers **27a,b** and **28a,b**.^{120a,b} The synthesis involved iterative reactions of aniline and benzoic acid derivatives. Basically, the ortho-positions of the amino units were attached with alkoxy groups to form five-membered hydrogen bonding to restrain the rotation of the N–C(Ar) single bond. The (Ar)C–C(=O) single bond is free to rotate in solution. Thus, the molecules should adopt different coplanar conformations of low energy in solution. However, in crystal structures, all the side-chains are oriented alternately on the opposite sides, which is consistent with the molecular modeling result. Very recently, Kulikov and Hamilton further modified the trimeric backbone by introducing many different side-chains.^{120c} Using a similar strategy, Seyler and Kilbinger synthesized the so-called monodisperse “hairy rod oligomers” **29a** and **29b**,¹²¹ which carry hexoxy side chains as well as a poly(ethylene glycol) chain at one end. Molecular modeling revealed that their ether oxygen atoms formed stable six-membered hydrogen bonding and the side-chains were oriented on the two sides alternately. The hexoxy side chains should play an important role in increasing the solubility of the oligomers by forming intramolecular hydrogen bonding, which could prevent the amide units from forming intermolecular hydrogen bonding. This interaction is the major reason for the notorious insolubility of benzamide oligomers. Both molecules stack strongly in polar solvents and form fibrous aggregates upon evaporation of the solvents.

6.2. Aromatic–Aliphatic Amide Oligomers

When one or more hydrogen-bonded aromatic segments are incorporated into a peptide strand, the resulting hybrid peptide sequence may be induced to form an extended conformation.¹²² In this context, Gong et al. synthesized compounds **30a,b** and **31**.^{122d} Two intramolecular six-membered hydrogen bonds were introduced to the aromatic segments to enhance the preorganization of the sequences. As a result, they formed



stable hetero- or homodimers that were stabilized by four intermolecular hydrogen bonds as evidenced by crystal structures of **30b** and **31** (Figure 12). The dimeric structures

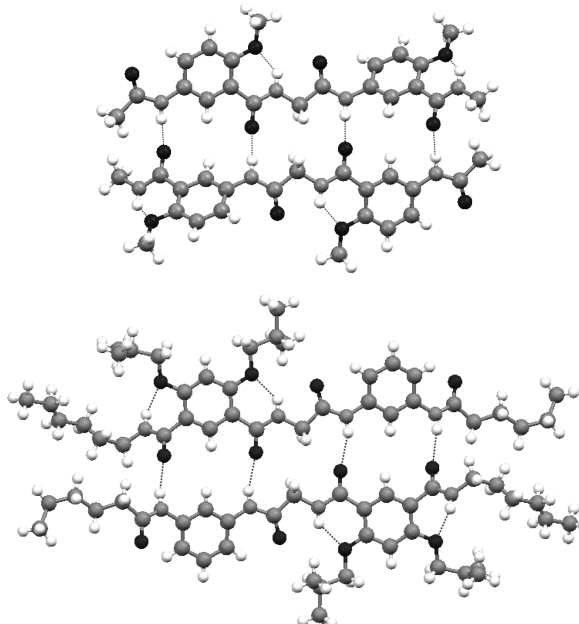
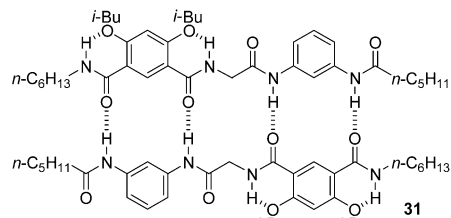
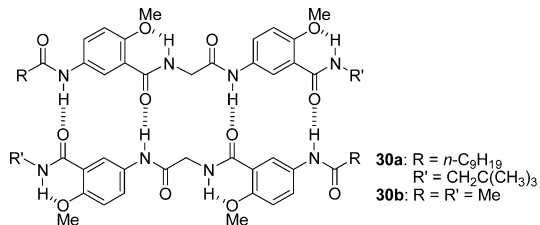


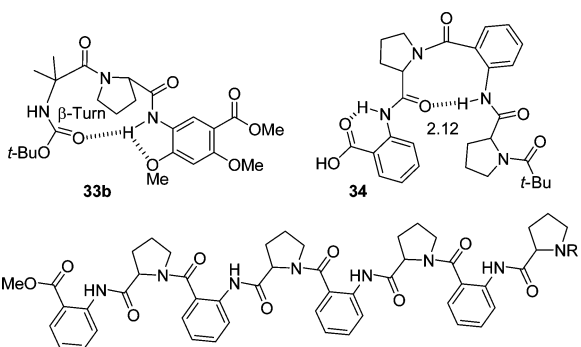
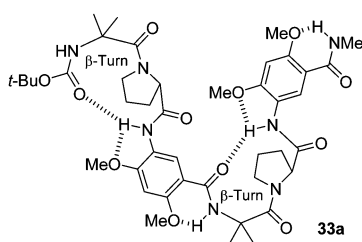
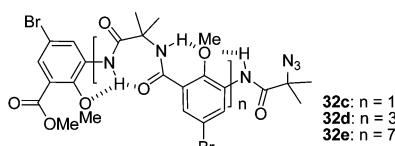
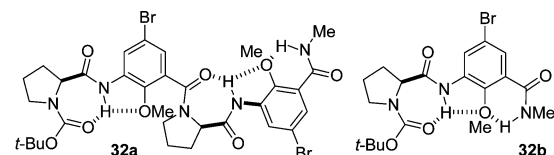
Figure 12. Crystal structures of compounds **30b** (top) and **31** (bottom),^{122d} highlighting the extended conformations stabilized by the dimeric structures.

further induced the monomers to adopt sheetlike extended conformations by enhancing their rigidity. In a similar manner, complementary monomers of six amides have been found to form more stable heterodimers via six intermolecular hydrogen bonds.^{122e} The benzene ring can also be replaced with a larger naphthalene ring to generate similar quadruply or sextuply hydrogen-bonded heterodimers.^{122f} When alkenyl group are tethered to the complementary monomers on the same side of a dimer, they may selectively undergo intermolecular metathesis to form new intramolecular duplexes.^{122g}

Sanjayan's group developed another general strategy for the construction of foldamers from hybrid sequences comprising conformationally constrained α -amino acid–aromatic amino acid segments.^{56b,123} For example, the group reported that oligomer **32a**, composed of two proline and two aromatic



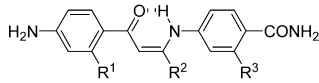
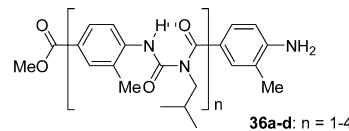
amino acid segments, adopted a periodic γ -turn conformation, which was stabilized by two pairs of three-centered hydrogen bonds.^{123a} The seven-membered hydrogen bonding of the proline subunit was evidenced by the crystal structure of model compound 32b. By replacing proline with α -aminoisobutyric acid subunit, the group also prepared another series of hybrid oligomers 32c–e,^{123b} which were also revealed to form extended architectures with similar three-centered hydrogen-bonding motifs.



Compound 33a, which consists of aromatic amino acid, proline, and α -aminoisobutyric acid subunits, was also prepared.^{123c} 2D ¹H NMR experiments showed that the two aromatic subunits both formed one 5- and one 6-membered hydrogen bond, whereas the two aliphatic segments formed a 10-membered hydrogen bond via a helical conformation. This unique structure was further confirmed by the crystal structure of model compound 33b. By forming this hydrogen-bonding pattern, longer oligomers or polymers should give rise to zigzag extended conformations. Oligomers 34 and 35a,b consisting of repeating L-proline-antranilic acid segments have also been prepared.^{123d} The crystal structure of 34 revealed that the anthranamide segment in the middle did not form the normal 6-membered hydrogen bond. Instead, it was engaged in a strong 9-membered hydrogen bond, which induced the backbone to adopt an interesting pseudo- β -turn conformation. The crystal structures of 35a and 35b are not available. However, 2D ¹H NMR spectra supported that their local residues also formed similar pseudo- β -turn conformations, while the whole backbones adopted a ripple-shaped secondary structure.

6.3. Benzoylurea Oligomers

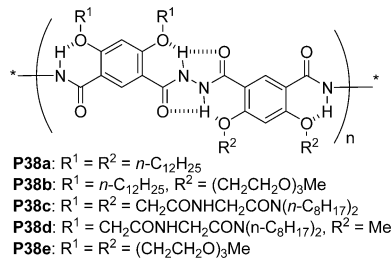
Rodriguez and Hamilton designed a kind of hydrogen-bonded benzoylurea oligomers, 36a–d,¹²⁴ for mimicking long α -helices that exist in transmembrane proteins, helix bundles, and some other higher-order structures.¹²⁵ The synthesis involved iterative coupling of rationally designed secondary amides with an isocyanate. Similar to the above para-substituted benzamide oligomers, the benzoylurea units in these scaffolds form stable six-membered hydrogen bonding, which was confirmed by the crystal structure of 36b as well as ¹H NMR experiments. However, the rotations of the C–C(Ar) and (Ar)C–N single bonds of these oligomers are not restricted in solution. The elongated helix mimetic 36d (*n* = 4) was shown to extend up to 3.7 nm, which corresponds to an α -helix with about 7 turns and 30 residues. The Hamilton group also reported the synthesis of enaminone derivatives 37 that bear different aliphatic side-chains. These oligomers were revealed to generate preorganized scaffolds due to the six-membered hydrogen bonding formed by the enaminone units.¹²⁶ The rigid structure was characterized by variable concentration and temperature ¹H NMR in both CDCl₃ and DMSO-*d*₆, as well as by X-ray analysis.



6.4. Aromatic Hydrazide Polymers

Li et al. reported the synthesis of polymers P38a–e from corresponding 4,6-dialkoxyisophthalic acid and 4,6-dialkoxyisophthalohydrazide precursors by using the Yamazaki polymerization conditions.^{38a} ¹H NMR indicated that these polymers also formed six-membered intramolecular hydrogen bonding in solution, which induced the backbones to adopt the zigzag, extended conformation. The planarity of the aromatic

hydrazides was also previously established in short oligomers.¹²⁷ Polymers P38c and P38d were found to gelate organic solvents due to enhanced stacking of their backbone.



6.5. Aromatic–Aliphatic Hydrazide Oligomers

2-Methoxybenzoic hydrazide is a useful template for the formation of duplex structures by forming two intermolecular hydrogen bonds.^{57a,127} Chen and co-workers have utilized this hydrogen-bonded aromatic segment to assemble a number of extended secondary structures by designing new aromatic–aliphatic hybrid strands (Figure 13).¹²⁸ Model compound 39a

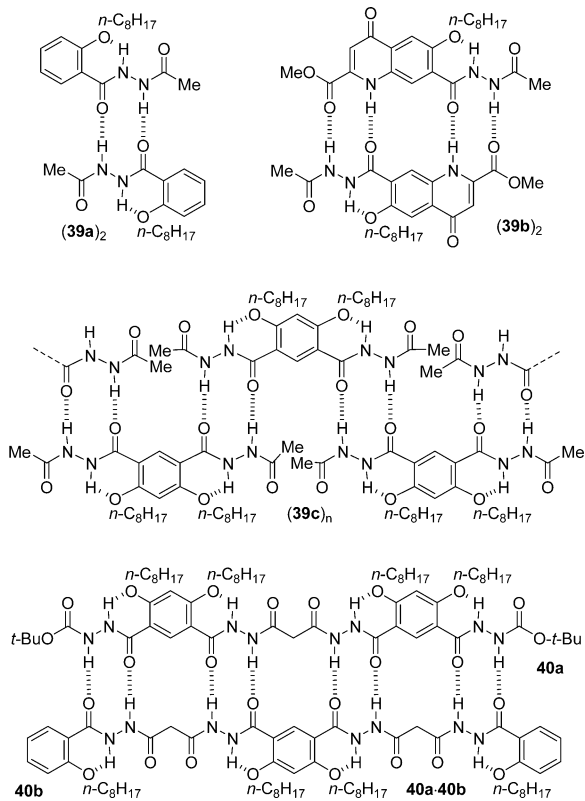


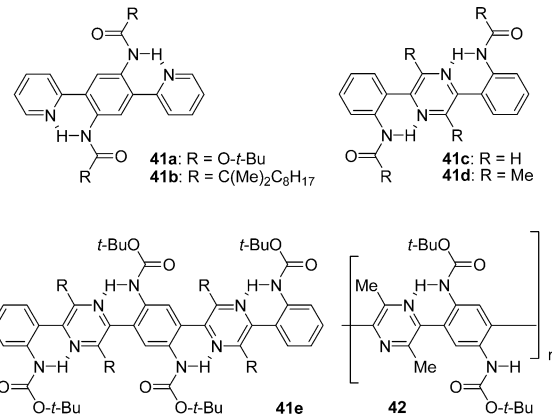
Figure 13. Structures of compounds 39a–c and 40a and 40b and their assembled dimeric structures.

formed a simple doubly hydrogen-bonded homodimer in both solution (chloroform) and the solid state,^{128b} where compound 39b produced a more stable, quadruply hydrogen-bonded homodimer, which was confirmed by ¹H NMR.^{128c} Compound 39c could not form self-complementarily a quadruply hydrogen-bonded dimer. Instead, it formed a zipper-like, doubly hydrogen-bonded array in the solid state by adopting a planar extended conformation.^{128b} As revealed in the duplexes reported by Gong,¹²² this extended conformation should also be stabilized by the formation of the dimeric structures. Chen

and co-workers further prepared longer compounds 40a and 40b.^{128d} ¹H NMR supported that the two compounds, respectively, formed sextuply hydrogen-bonded homodimers in chloroform, while their 1:1 mixture gave rise to more stable, octuply hydrogen-bonded heterodimer. Compound 40a and an analogue of 40b, which bears two peripheral naphthalene units, have been found to gelate chloroform.^{128e} However, their mixture did not display a similar capacity. Additional intermolecular hydrogen bonding existing in the single samples has been proposed to rationalize the difference by affording the polymeric array as observed for 39c.

6.6. Arylene Oligomers and Polymers

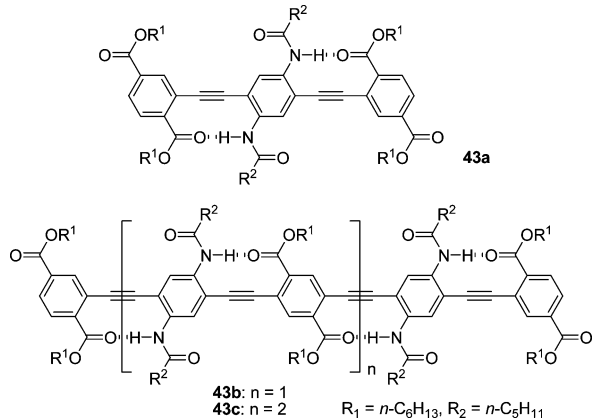
The hydrogen-bonded amide units in the above aromatic molecules are parts of the main backbones. The amides can also form stable intramolecular hydrogen bonding when they are intentionally designed as side-chains, or parts of them, of aromatic backbones. Meijer and co-workers have utilized such a kind of intramolecular hydrogen bonding to planarize oligoarenes 41a–e and polyarene 42.^{69a} Different from the above-described aromatic amide backbones, this series of rigidified architectures are composed of alternating 1,4-pyrimidine and benzene segments. The design was based on the finding that bipyridyl amide derivatives formed stable intramolecular six-membered N–H–N hydrogen bonding.¹²⁹ The increased coplanarity of the aromatic backbones of these oligomers and polymer can cause gradual red-shifting of their long-wavelength absorption band, which further increases with the elongation of backbones.



6.7. p-Phenylenethynylene Oligomers

Zhao and co-workers reported that the coplanarity of monodispersed oligo(*p*-phenylenethynylene)s 43a–c could be enhanced by the 10-membered intramolecular hydrogen bonding formed between the alternately appended amide and ester side-chains.⁷⁹ This intramolecular hydrogen-bonding motif was originally established by Kemp and Li.⁷⁶ Photochemical studies showed that these conjugated oligomers exhibited narrowed band gaps and extended conjugation lengths.

Wyrembak and Hamilton further extended the strategy for α -helix mimicry to the β -strand conformation.¹³⁰ Compounds 44a and 44b were thus designed and synthesized. For 44b, two intramolecular hydrogen bonds are formed between the carbonyl oxygen atoms of indolin-3-one and the amino hydrogen atoms of the neighboring indolin-3-one, which forces the three heterocyclic subunits to stay on one side of the aromatic backbone. As a result, the substituents on C2 of the



indolin-3-one align in a homofacial manner and thus mimic the distance between the *i*, *i* + 2, and *i* + 4 residues of an idealized peptide β -strand.¹³¹ The hydrogen-bonding was confirmed in solution by ¹H NMR and in the solid state by X-ray analysis (Figure 14). The crystal structure also showed that the hydrogen-bonding network of 44b induced the phenylacetylene bonds to bend slightly to give a curved structure.

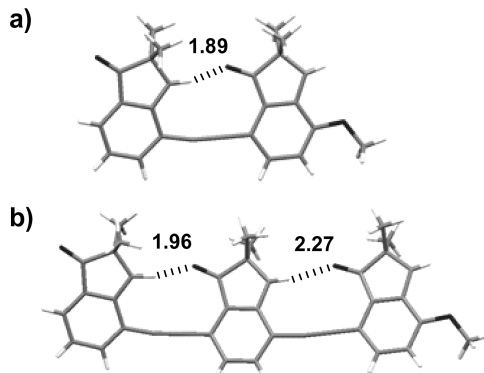
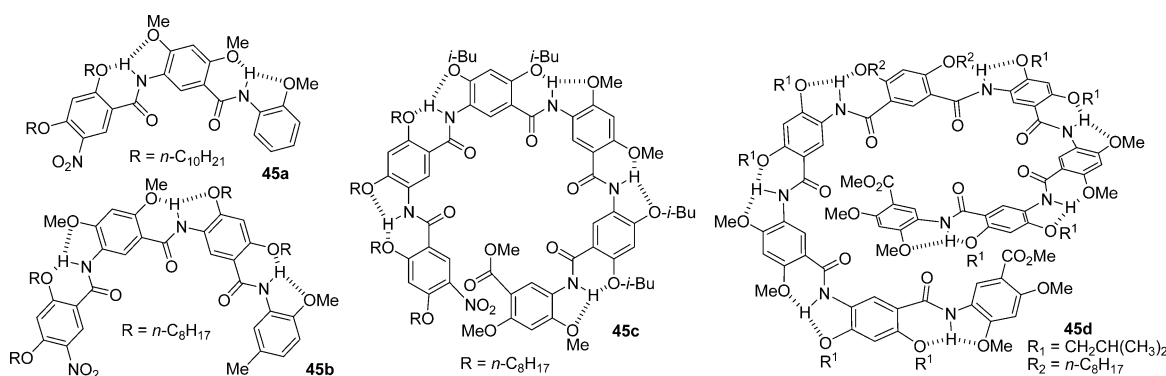
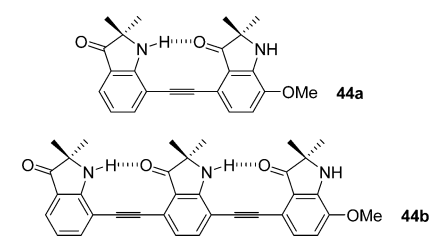


Figure 14. X-ray structures of compounds 44a (a) and 44b (b).¹³⁰



7. FOLDED OR HELICAL SECONDARY STRUCTURES

7.1. Oligomeric Amides with Benzene Spacers

Hydrogen-bonded amide oligomers built from 3-aminobenzoic acid derivatives have rigid, curved conformations. Gong and co-workers synthesized oligomers 45a–c from 5-amino-2,4-dialkoxybenzoic acid precursors.^{23a} The long aliphatic chains

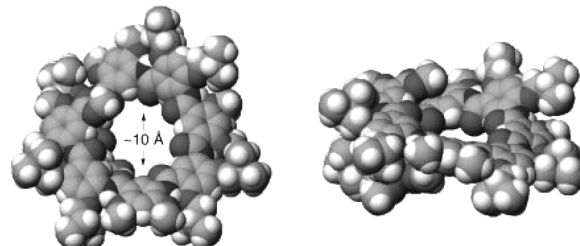


Figure 15. Crystal structure of oligomer 45d showing a helical conformation with a cavity of \sim 10 Å in diameter (left, top view; right, side view). Octyl groups are replaced with methyl groups for clarity. Reproduced with permission from ref 48a. Copyright 2001 Wiley–VCH.

were introduced to provide solubility in organic solvents. The successive three-centered hydrogen bonding induced the backbones to form a crescent shape. Because these were the first examples of this series of folded structures, systematic 2D ¹H NMR experiments were carried out to confirm their crescent shape. The crystal structure of 45a was obtained, which showed the formation of the two pairs of three-centered hydrogen bonds in the solid state. Driven by similar hydrogen-bonding patterns, symmetric 9-mer 45d with a 4,6-diethoxyisophthalimide linker in the middle of the backbone can fold to form a helical conformation.^{48a} Its crystal structure showed that six segments formed one turn, and the helical backbone produced a cavity of \sim 1 nm diameter (Figure 15). A longer 11-mer helix of the similar backbone was found to form a deeper helical cavity.^{23c}

By introducing a methoxyl group at the 2-position of 3-aminobenzoic acid derivatives to mediate the three-centered hydrogen-bonding pattern HB-29, Li and co-workers prepared oligomers 46a–c to create new folded structures.¹³² The three-centered hydrogen-bonding pattern was confirmed by the crystal structure of a 2-mer model molecule. Because all the methoxyl groups are oriented inwardly, the cavity formed by these foldamers is quite small. Zeng and co-workers further reported the synthesis of oligomers 47a,b and 48a,b.¹³³ The crystal structures of 47a and 48a indicated that this kind of oligomer formed one turn by five repeated segments (Figure

16), which was further supported in solution by 2D NOESY studies.^{27a} On the basis of this observation, Zeng and co-

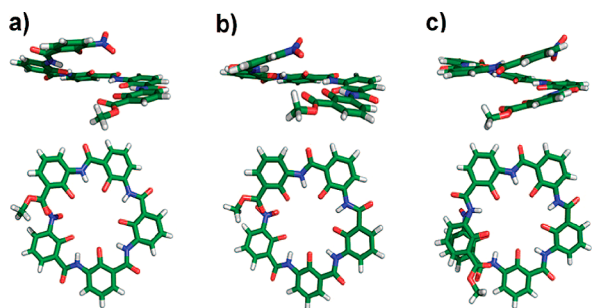
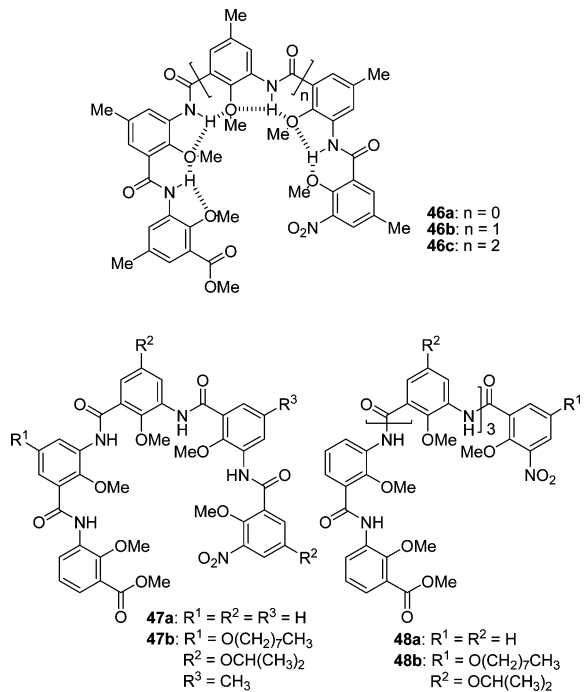


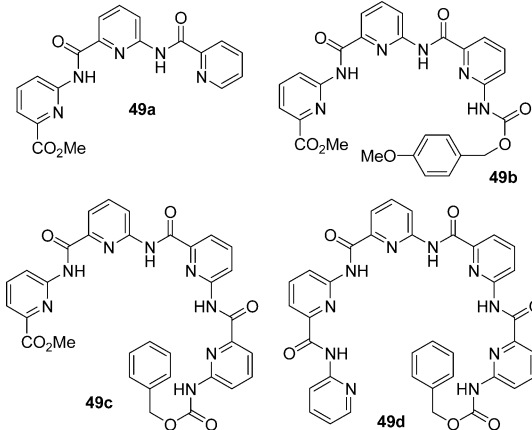
Figure 16. Side and top views of (a) the crystal structure of pentamer 47a, (b) ab initio calculated structure of 47a, and (c) the crystal structure of hexamer 48a. Interior methyl groups are omitted for clarity. Reproduced with permission from ref 133. Copyright 2009 American Chemical Society.

workers have constructed a number of structurally unique pentagon macrocycles.⁴⁵

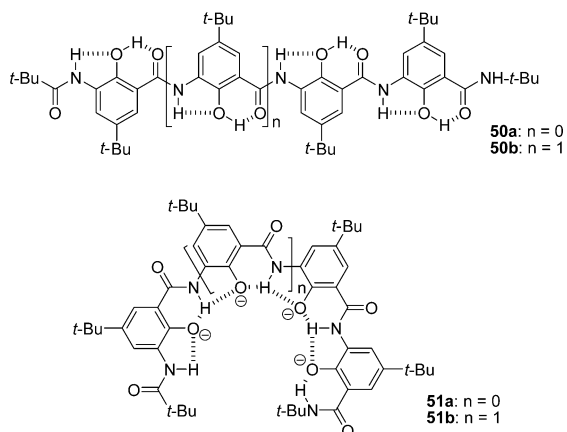


Zeng and co-workers established that oligomers 49a–d, prepared from 6-aminopicolinic acid, form similar compact conformations in crystal structures.^{27b} As expected, shorter 49a and 49b adopt a crescent conformation, whereas long tetramer 49c becomes helically shaped due to steric hindrance of the end ester and Cbz groups, and pentamer 49d is clearly a helix with the two end pyridine rings almost superimposed over each other. In 49d, each repeating unit in average corresponds to a ~84° turn, and 4.3 units furnish a helical turn.

Ueyama and co-workers described that phenolic oligoamides 50a,b formed extended conformations, with the hydroxyl oxygen and hydrogen atoms acting as hydrogen-bonding acceptors and donors, respectively.⁸⁰ Adding $\text{NEt}_4^+\text{OH}^-$ caused all the phenols to deprotonate to afford phenoxides 51a,b in DMSO. The backbones were thus changed to adopt folded conformations, which were stabilized by three-centered hydro-

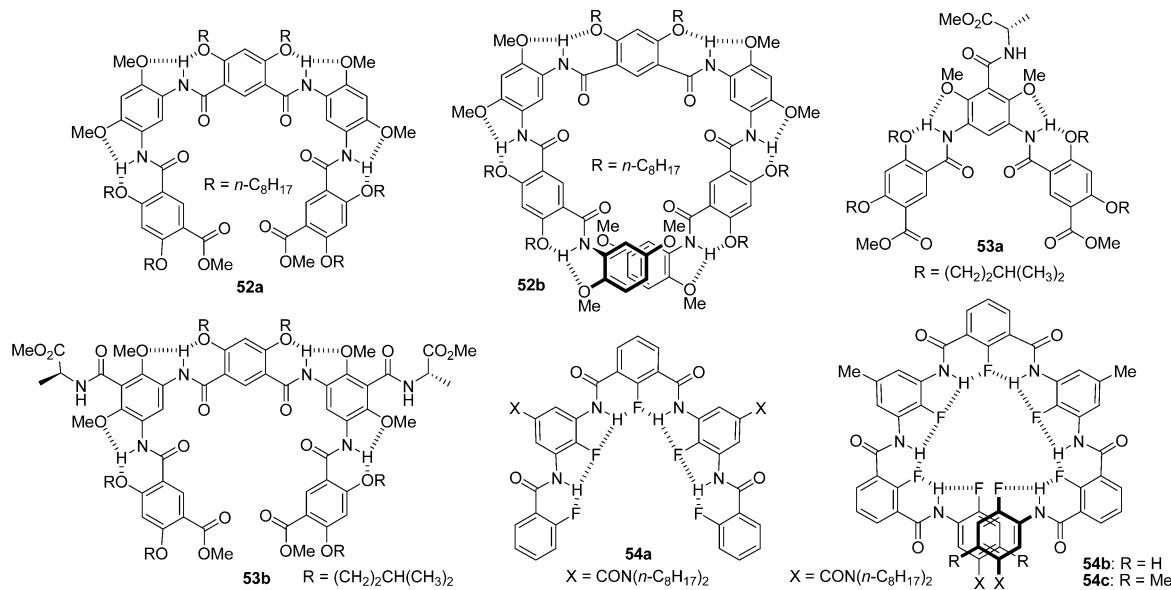


gen-bonding pattern HB-30. This conformational conversion was confirmed in solution by NOE studies and in the solid state by the crystal structures of a 2-mer model molecule.

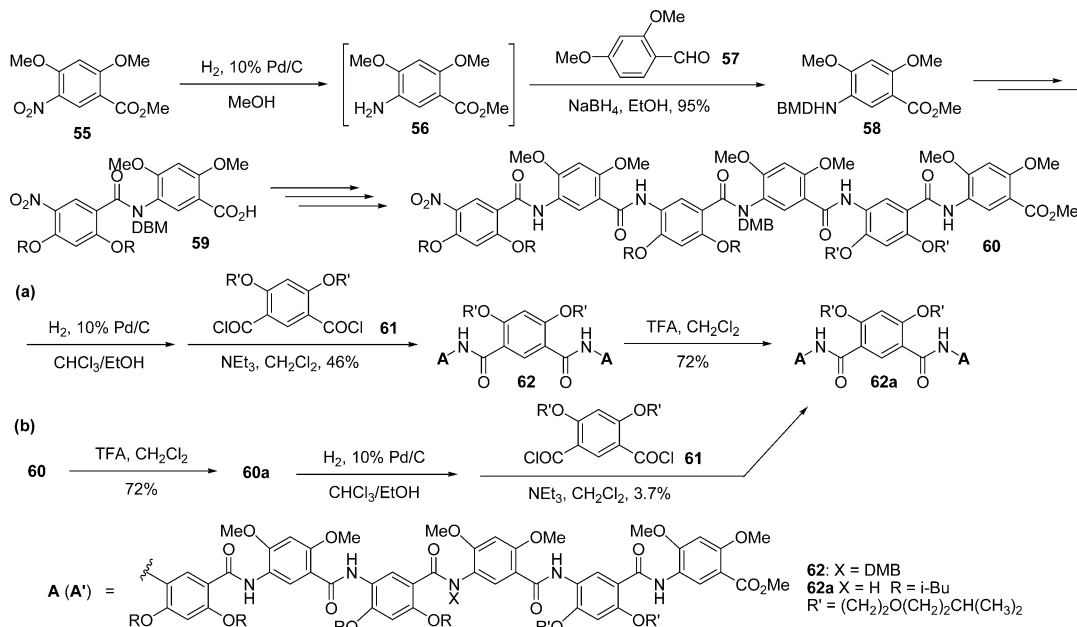


Benzene-1,3-diamine and isophthalic acid derivatives are also useful for the construction of folded structures. Gong and co-workers reported that the folding preorganization of uncyclized 6-mer oligomers formed by these residues remarkably promoted the formation of the corresponding macrocycles.^{41a} Li and co-workers synthesized oligomers 52a and 52b.¹³⁴ A molecular modeling study revealed that 5-mer 52a formed a crescent conformation, whereas 7-mer 52b was long enough to produce a helical conformation with the two peripheral benzene units stacking with each other. For 52b, all the C=O oxygen atoms point into the cavity, producing a polar cavity of ~0.8 nm diameter. Gong and co-workers found that introducing an amide group at the 5-position of the benzene-1,3-diamine residue did not disrupt the three-centered hydrogen bonding,^{41b} and related oligomers 53a and 53b still kept the folded conformation, which was supported by their crystal structures. Li et al. reported that fluorine could also act as a hydrogen-bonding acceptor to induce oligomers 54a–c to fold.^{24b} NOESY experiments indicated that the 7-mer oligomers were long enough to produce a helical conformation.

The above aromatic amide oligomers were prepared by iterative coupling of the related amine and acid or acid chloride precursors or intermediates. Using this strategy, oligomers that fold into crescents or helices of less than two turns can be prepared. However, longer oligomers are quite difficult to prepare due to steric hindrance produced by the helical conformation of long oligomeric precursors and/or intermediates. Gong and co-workers reported that more efficient



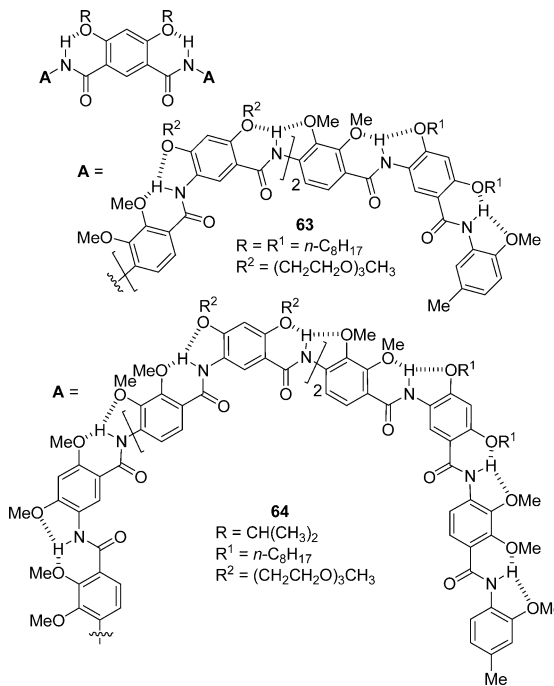
Scheme 1. Synthetic Routes for 13-Mer 62a



synthesis of long oligomers could be achieved by temporarily interrupting rigidified backbones by replacing the amide hydrogen with acid-labile 2,4-dimethoxybenzyl group (DMB).¹¹⁰ This group was introduced by treating the amines with 2,4-dimethoxybenzaldehyde followed by reducing the resulting imines to secondary amines. For the synthesis of 13-mer **62a** starting from **55**, two routes were designed for demonstrating the efficiency of the strategy (Scheme 1). In the first route, the 6-mer amine precursor was first obtained from **60** and coupled with diacid chloride **61** to afford 13-mer **62** in 48% yield. In the second route, the similar coupling reaction produced **62a** in only 3.7% yield, which was attributed to the helical conformation of the 6-mer amine precursor. The crystal structure of a DMB-modified pentamer intermediate showed that it adopted a twisted conformation and the termini were exposed completely.

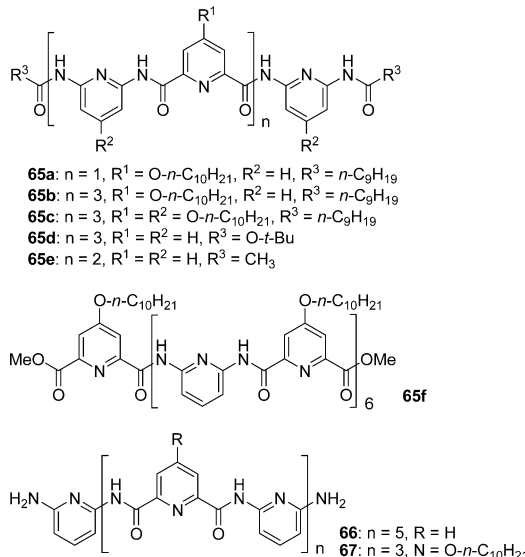
Meta-linked aromatic amide backbones adopt well-defined crescent or helical conformations. However, the size of the

benzene linkers limits the formation of enlarged folded backbones. Para-linked oligomers adopt straight or slightly curved conformations. Combining the two kinds of segments into one sequence would lead to curved backbones with tunable cavities. Gong et al. prepared 15-mer **63** and 21-mer **64**,^{23b} which contained six or ten 4-amino-2,3-dimethoxybenzamide residues. Crystal structures of two tetramers containing this residue confirmed that its two methoxyl groups both formed stable intramolecular hydrogen bonding. Molecular modeling showed that **63** was not long enough to make a full helical turn and thus existed as a crescent, while **64** made slightly more than one turn, with about 20 residues per turn, and a large interior cavity at least 3 nm across. Its NOESY spectrum revealed NOEs between the signals of the two terminal methyl groups and the two amides closest to the ends, proving the helical conformation.



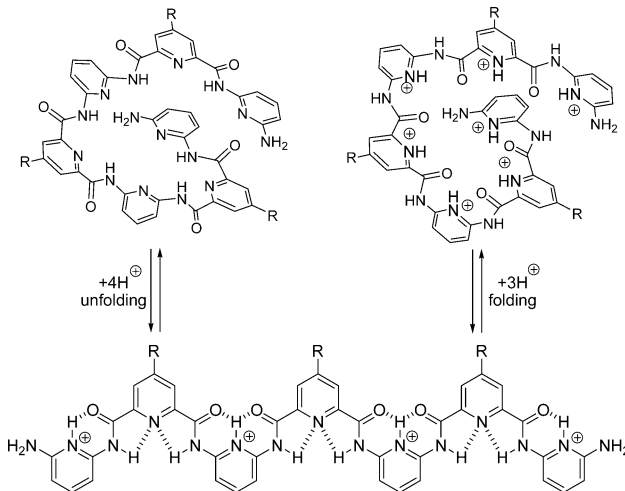
7.2. Oligomeric Amides with Heterocycle Spacers

Huc, Lehn, and co-workers designed oligomers **65a–d**, which consisted of alternating 2,6-diaminopyridine and 2,6-pyridinedicarbonyl segments.²¹ The crystal structure of 7-mer **65d**, recrystallized from the MeCN/DMSO solution, showed the formation of a single helix, and all the pyridine nitrogen atoms were hydrogen-bonded to the closed amide protons in the HB-23 and HB-33 patterns. The crystal structure also revealed that ~5 pyridine–amide units generated one turn, which is close to that of the backbones created from 6-aminopicolinamide.²⁷ In dilute solution, these oligomers also exist as single-folded strands. However, in concentrated solution, they form a double helix. Crystal structures of oligomers **65e** and **66** were also reported,¹³⁵ which also existed as single helices. To study the structure of this kind of foldamer in solution, 13-mer oligomer **65f** was prepared.^{111a} HMBC and HSQC experiments were pursued for assigning its signals in ¹H and ¹³C NMR spectra.



In the presence of an excess of TFA, the diaminopyridine units of 7-mer oligomer **67** can be selectively protonated. In the presence of an excess of stronger triflic acid, all the pyridine units are protonated.⁶⁶ These two processes cause the original helical conformation to shift to extended and then to another helical conformation (Scheme 2). 9-Mer oligomer **68**, which

Scheme 2. Acid-Induced Conformational Switching of 7-Mer Oligomer 67



bears a chiral 1-phenylethanamine at one end, was found to create a chirality bias for the whole helical structure in chloroform, and protonation caused the chiral helix to undergo conformational switching.¹³⁶ In the presence of chiral acids, the helix of **65b** can also exhibit weak chirality bias.¹³⁶ DFT calculation on shorter structures revealed that trimeric backbone is the smallest molecular fragment that can produce a chirality.^{32b}



Huc and co-workers also prepared oligomers **69a,b,e** from quinoline-derived δ -amino acid.²² The stable three-centered hydrogen bonding induces the backbones to form compact folded conformations. The crystal structure of **69e** revealed a helical conformation extending to more than three turns, and five segments formed two helical turns (Figure 17), which corresponds to the highest curvature reached by helical aromatic oligoamides. The solution structure of this kind of foldamer has been investigated using 2D NMR techniques.^{111a}

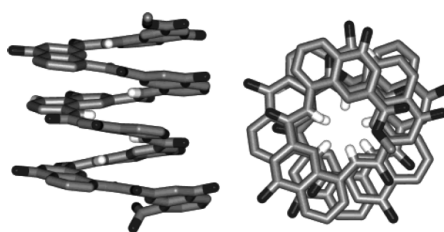
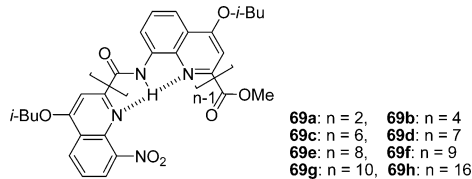
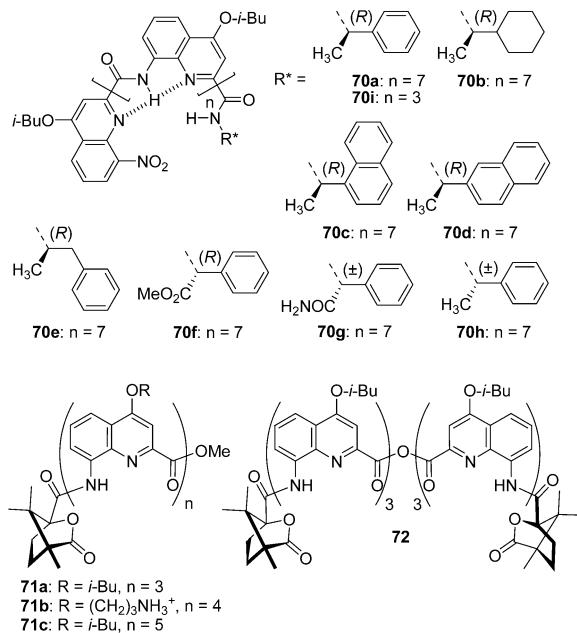


Figure 17. Side and top views of the crystal structure of 8-mer **69e**. Isobutyl chains are omitted for clarity. Reproduced with permission from ref 22a. Copyright 2003 American Chemical Society.

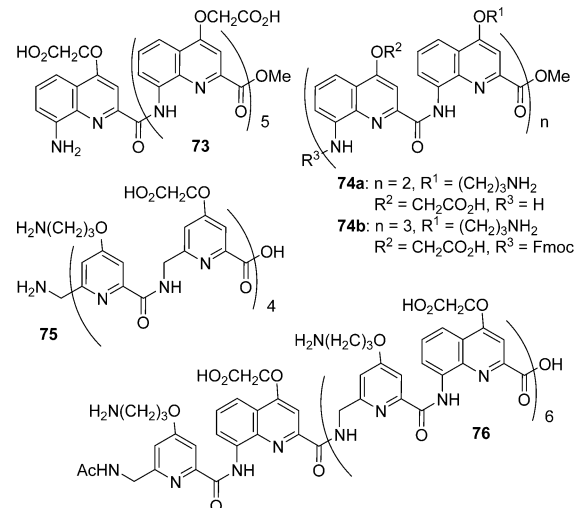
The right-handed (P) and left-handed (M) helical conformers of **69c–h** have also been studied. It was found that the two helix conformers underwent a slow exchange and could be separated using chiral high-performance liquid chromatography (HPLC).¹³⁷ However, even for the longest oligomer **69h**, slow racemization of the two conformers could not be suppressed completely. As a result, true kinetic inertness was not reached.



Huc and co-workers also prepared 8-mer oligomer **R-70a**, which bears a chiral *R*-phenethylamino group at the C terminus.¹³⁸ In solution, the ratio of *R*-P and *R*-M diastereoisomers was estimated to be 10:1, which corresponds to a diastereomeric excess of 82%. Both diastereomers also exist in crystals, and their ratio depends on the solvent used for recrystallization. For a more systematic investigation of chiral induction, oligomers **70b–h** were prepared and studied in solution by ¹H NMR and CD spectroscopy and in the solid state using X-ray crystallography.^{32a} The chiral inductions are all relatively weak (diastereomeric excess (de) < 83%), and diastereomeric helices coexist and interconvert in solution. However, oligomers **71a–c** and **72**, which bear one or two (1*S*)-(−)-camphanyl moieties at the *N*-terminus, were found to selectively form the right-handed helicity (de > 99%) in both protic and nonprotic solvents.¹³⁹ Oligomers **69a–h** and **70a–h** are not soluble in polar solvents. Attaching hydrophilic or cationic side-chains to the backbones provides solubility in aqueous media, and the helical structures are kept in the solid state.¹⁰⁸ ¹H NMR showed that, in methanol or water, an oligomer as short as a pentamer is able to fold into a stable helical conformation. For shorter oligomer **70i**, ab initio calculation and vibrational CD technique have been used to estimate the conformational energies and helical handedness preferences.¹⁴⁰



The above quinoline-based oligomers were all prepared from solution-phase coupling reactions. Solid-phase synthesis of water-soluble oligomers **73** and **74a,b** on bromomethyl Wang resin has been reported.^{105b} The method could be further utilized to prepare 8-mer oligomer **75** from 6-aminomethyl-2-pyridinecarboxylic acid derivative and 14-mer hybrid oligomer **76**.^{105b}



7.3. Oligomeric Amides with Mixed Aromatic Spacers

In 1994, Hamilton and co-workers reported the synthesis of oligomers **77a–c**.¹⁹ As the first examples of hydrogen-bonding-induced aromatic amide foldamers, their helical structures in solution were characterized by systematic ¹H NMR experiments and in the solid state by X-ray analysis (Figure 18),

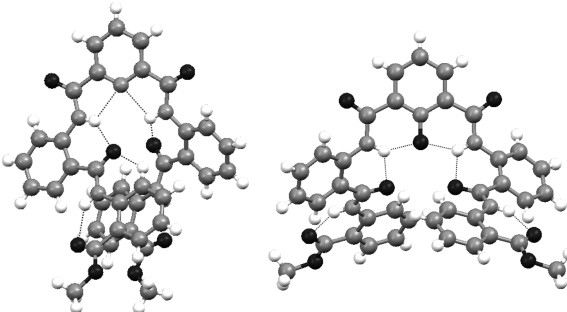


Figure 18. X-ray structures of oligomers **77a** (left) and **77c** (right).¹⁹

which showed the formation of all the designed intramolecular hydrogen bonds and that the backbones formed a helical conformation of more than one turn.^{19,20} Longer 9-mer oligomers **77d,e** were also prepared, which were found to form helices of two turns.¹⁴¹

Huc and co-workers also developed several series of oligomers consisting of discrete aromatic segments. Oligomers **78a,b** and **79** were prepared by linking quinoline amide helical segments to a 1,5-diaminoanthraquinone or 2,5-dimethoxyterephthalic acid spacer.⁶⁸ Their crystal structures revealed that the two helical quinoline oligomers were induced by two six-membered intramolecular hydrogen bonds to diverge from the central spacer and to have opposite helical handedness (Figure 19).

Oligomers **80a–c**, where two large quinoline segments are appended to a pyridine oligomer, were also prepared.¹⁴² X-ray

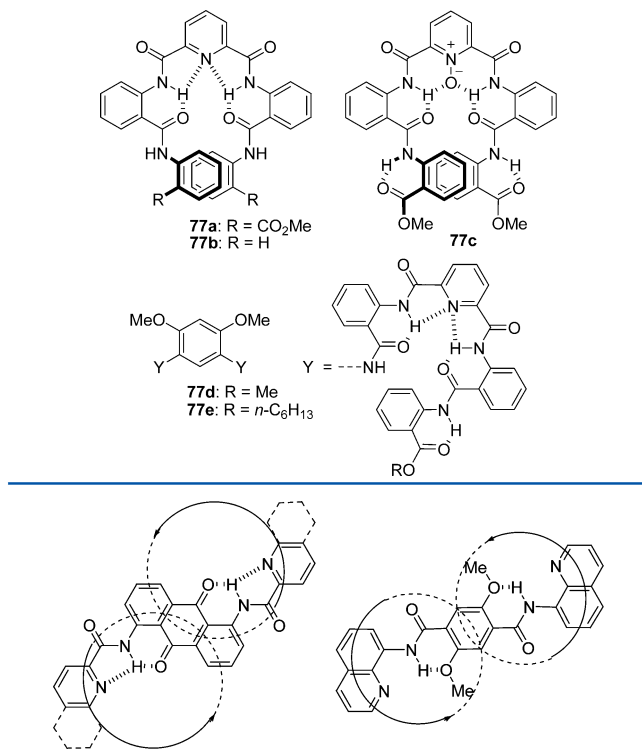
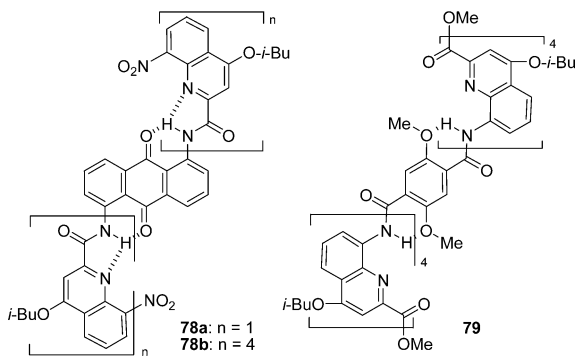
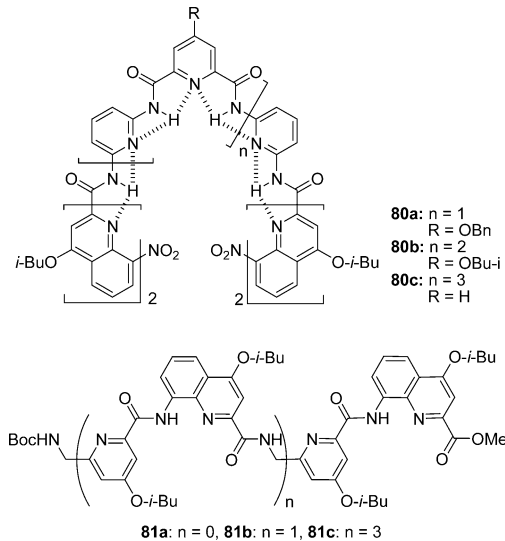


Figure 19. Schematic representation of the projection of the two helical quinoline segments of **78b** in the plane of the anthraquinone spacer (left) and of **79** in the plane of the terephthaloyl spacer (right). The arrows indicate the direction in which each oligomeric segment extends from the spacer.



analysis revealed that these molecules folded into a closed capsule. The two ends of the capsules were capped by the two shrinking peripheral quinoline units, and the closed cavity entrapped one or two water molecules. Oligomers **81a–c** contain alternating quinoline and methylpyridine residues.¹⁴³ Interestingly, the longer **81a** and **81c** form a herringbone helix in both solution and the solid state because their methylene moieties preferentially set the pyridine and amide units at a ~90° angle. To further exploit the possibility of forming helical structures by such a kind of hybrid backbone, the group further prepared oligomers with the sequence of $\text{Boc}-(\text{PQ}_4)_{2n}-\text{OMe}$ ($n = 1, 2, 4$), where **P** and **Q** denote the methylpyridine and quinoline segments, respectively.⁷² All these oligomers adopt helical conformations imposed by the **Q** monomers, and the overall helix stability increases with helix length. Remarkably, the 40-mer oligomer folds into a rodlike helix spanning over 16 turns with a length of 5.6 nm. The number of **P** units may be increased while keeping the helical conformation of the

backbones. However, the stability of the resulting helices tends to decrease due to fast inversion of the helix handedness.



Chen and co-workers prepared compounds **82a–e** from 1,10-phenanthroline diacid and *o*-phenylenediamine.²⁵ These oligomers can also form folded or helical conformations, which are stabilized by intramolecular hydrogen bonding and aromatic stacking interaction. Interestingly, the compact conformations are more favorable in polar methanol than in less polar chloroform and dichloromethane, suggesting that stacking interaction plays a key role for stabilizing the compact conformations. Crystal structures of **82b,d,e** showed that the adjacent amide units did not form intramolecular N–H···O=C hydrogen bonding. Intramolecular π–π stacking forced them to twist from the connected benzene rings. Oligomers **82d** and **82e** formed a helix of three and four turns, respectively (Figure 20). Because of the large curvature, these helices have nearly no

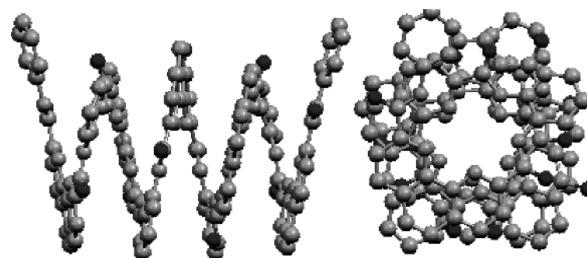
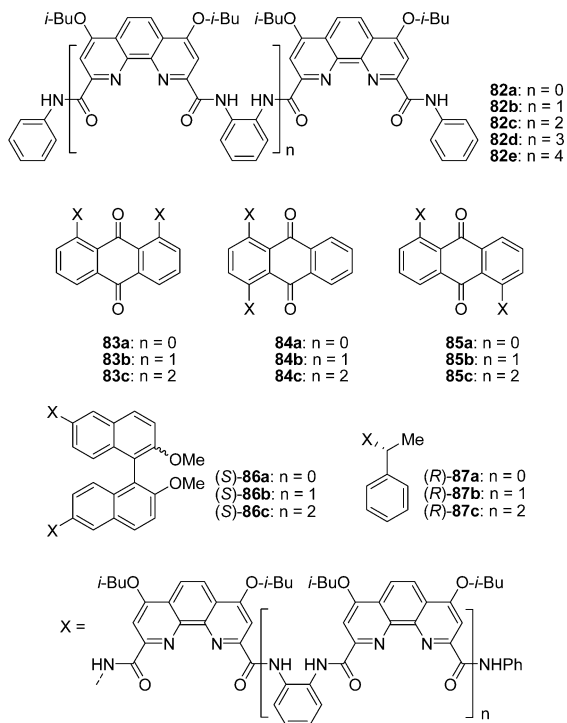


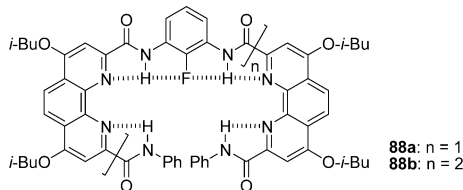
Figure 20. Side (left) and top (right) views of the crystal structure of oligomer **82e**. Included solvent molecules, hydrogen atoms, and isobutyl chains are omitted for clarity. Reproduced with permission from ref 25. Copyright 2006 American Chemical Society.

cavity. These alternating phenanthroline/benzene sequences have been attached to a diaminoanthraquinone linker to generate oligomers **83a–c**,^{144a} **84a–c**,^{144b} and **85a–c**.^{144b} All the attached sequences keep their helical conformations, while the suprasecondary structures of the whole backbones depend on their orientation on the anthraquinone linker. When the sequences are attached to a chiral BINOL or phenylethyl moiety, the helical structures of the corresponding oligomers **86a–c** and **87a–c** are induced to produce helicity bias, which can undergo acid- and base-controlled switching.

By replacing the 1,2-diaminobenzene unit with 2-fluoro-1,3-diaminobenzene, Chen and co-workers further prepared



oligomers **88a** and **88b**.^{145b} In both solution and the solid state, all the designed intramolecular hydrogen bonds were confirmed, which induced the backbones to form a helical conformation. These helical structures also have no cavity.



Parquette and co-workers synthesized oligomers **89a,b**, which comprise alternating pyridine-2,6-dicarboxamides and *meta*-(phenylazo)azobenzene units.^{146a} X-ray structures confirmed that **89a** adopted a two-turn helical conformation (P and M) in the solid state (Figure 21), even though benzene rings linking two azo units bear no amide units to form intramolecular N–H···O=C hydrogen bonding. ¹H NMR also showed that these oligomers formed a two- and four-turn helical conformation in solution. Irradiating the solution at 350 nm induced a *E* → *Z* isomerization of the azo linkages, which

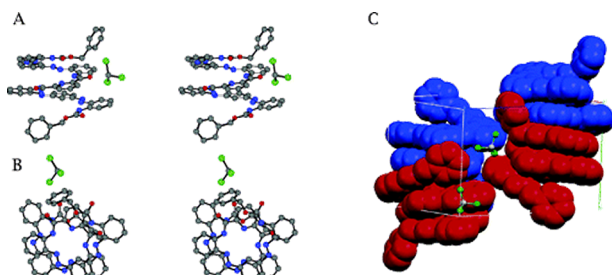
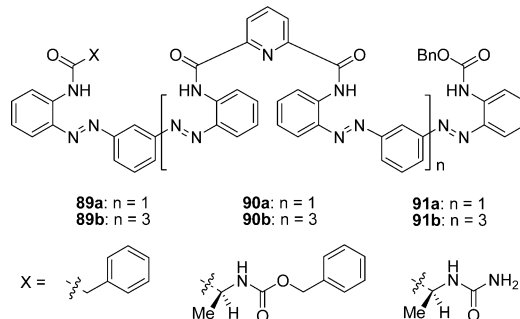
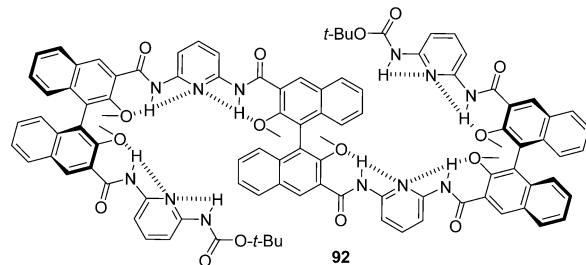


Figure 21. X-ray structure of **89a**: (A) side-on and (B) top-down views and (C) unit cell containing two right-handed and two left-handed molecules stacked in columns. Reproduced with permission from ref 146a. Copyright 2006 American Chemical Society.

decreased in efficacy for the longer helix. Appending an L-phenylalanine or L-alanine unit to the terminal produced a P helical bias for similar oligomers **90a,b** and **91a,b**.^{146b} This bias increased with oligomer length. Exposure to 350 nm light suppressed chiral induction within the helical structure by inducing isomerization of the terminal azo linkages, which caused the chiral terminal group to stay away from the helix.



Sanjayan and co-workers prepared oligomer **92** from iterative coupling of chiral BINOL diacid and 2,6-diaminopyridine.^{116b} This compound also gave rise to a chiral helical conformation, even though intramolecular stacking is relatively weak due to the herringbone conformation of the BINOL moiety. The three-centered hydrogen bonding was confirmed by ¹H NMR.



7.4. Oligomeric Amide–Sulfonamide Hybrids

The sulfonamide group adopts a tetrahedron configuration, and the S=O and N–H bonds of *N*-phenylbenzenesulfonamide are not coplanar with the benzene rings.¹⁴⁷ Hu and Chen found that, in the solid state, the amide hydrogen atoms of oligomer **93a** were both engaged in three-centered hydrogen bonding with the pyridine nitrogen and one of the sulfonamide oxygen atoms, which induced the backbone of the central trimer to form a V-shaped conformation (Figure 22).¹⁴⁸ The two

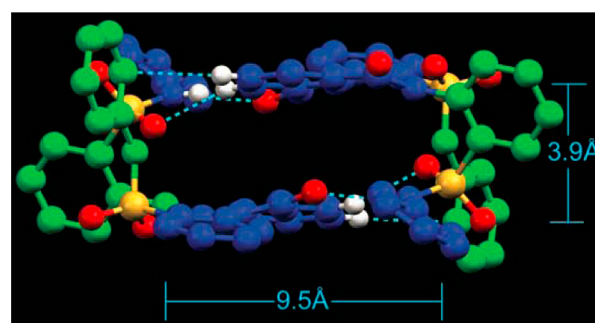
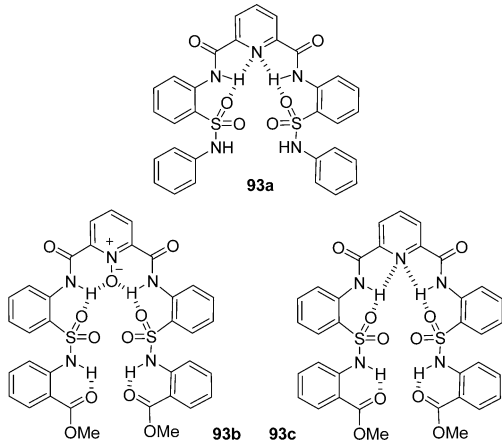


Figure 22. Rectangular dimeric structure of oligomer **93a** in the crystal structure. Dashed lines show the noncovalent interactions. Hydrogen atoms not involved in interactions are omitted for clarity. Reproduced with permission from ref 148. Copyright 2005 The Royal Society of Chemistry.

appended aniline units were twisted from the coplanar central trimer due to intermolecular N–H···O=S hydrogen bonding. Thus, two adjacent molecules formed a rectangular dimer. The crystal structures of oligomers **93b,c** were also reported,⁸¹ which revealed that the two amides also formed three-centered hydrogen bonding and the two appended aromatic units were engaged in six-membered N–H···O=C hydrogen bonding, while the whole backbones generate a twisted zigzag conformation.



7.5. Oligomeric Imides with Pyridine Spacers

Zhan, Yao, and co-workers synthesized imide oligomers **94a–c**.^{149a} Imides were incorporated into the backbones to form intramolecular N–H···N hydrogen bonding with connected pyridines. Crystal structures of **94b** and **94c** showed that the hydrogen bonds forced the oligomers to form helical conformations of large curvature, and about 2.5 pyridine units formed one turn (Figure 23). Longer oligomer **94d** was also reported. Its helical conformation was confirmed in solution by ¹H NMR.^{149b}

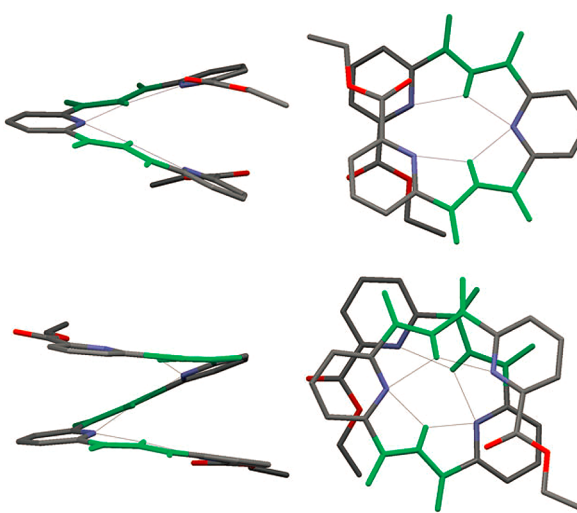
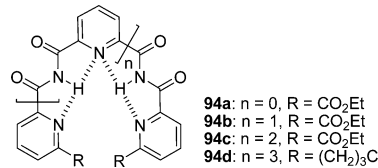
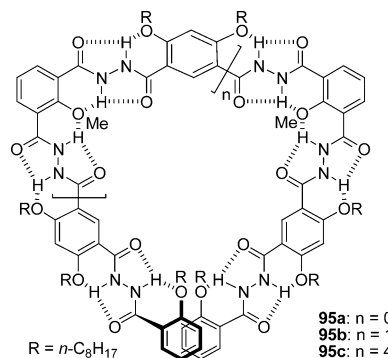


Figure 23. Crystal structures of **94b** (top) and **94c** (bottom): side view (left) and top view (right) with the imide units colored in green. The hydrogen atoms except for the imide protons are omitted for clarity. Reproduced with permission from ref 149a. Copyright 2008 The Royal Society of Chemistry.



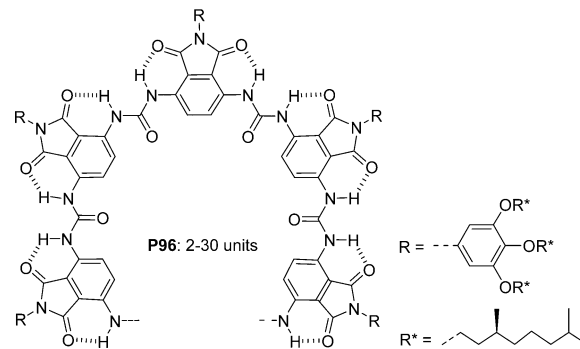
7.6. Oligomeric Hydrazides with Benzene Spacers

Oligomers **95a–c** are the first class of aromatic hydrazide-based foldamers.^{24a} The N–H···OR hydrogen-bonding motif for this kind of foldamer is similar to that used for amide-based foldamers. The planarity of the hydrazide moiety and the trans arrangement of the connecting amide units ensure a folded conformation for backbones. ¹H NMR experiments and molecular modeling confirmed that **95a** forms a folded conformation, whereas **95b** and **95c** produce helical conformations of one and two turns with a cavity of ~1.0 nm diameter.



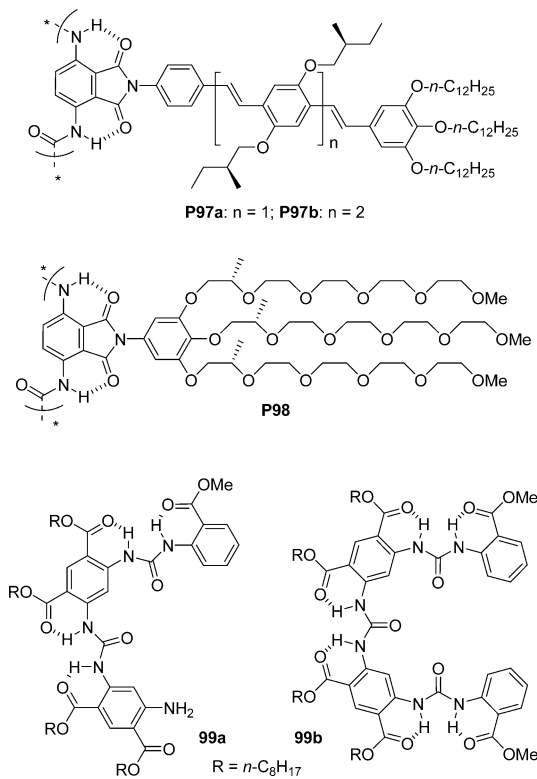
7.7. Poly- and Oligoureia Foldamers

Meijer and co-workers prepared polymers **P96** (~2–30 units) from the corresponding 1,4-diaminobenzene and 1,4-diisocyanatobenzene precursors.^{67a} The phthalimide spacer bears a chiral 3,4,5-tris[(S)-3,7-dimethyloctyloxy]phenyl group. ¹H NMR supported the formation of the intramolecular six-membered hydrogen bonding, which induced the backbone to form folded conformations. Shorter oligomers of up to 7 units showed no or only minor CD signals in tetrahydrofuran (THF), whereas the long polymer (~30 units) displayed a strong Cotton effect, indicating the formation of stable helical architectures in which chirality is transferred from the CD-silent peripheral side-chains to the accurately oriented, CD-active phthalimide chromophores. An improved methodology has been developed for the preparation of discrete 3,6-diaminophthalimide precursors.¹⁵⁰



To further investigate the stacking and helical bias of this kind of folded architecture, Meijer and co-workers prepared

polymers **P97a** and **P97b**, whose ureidophthalimide backbones were decorated with OPV chromophores.^{67b} The polymers were revealed to assume a random coil conformation in chloroform but a putative helical conformation in THF and heptane. Polymer **P98**, decorated with hydrophilic chains to ensure solubility in aqueous media, was also synthesized.^{67c} This helical polymer exhibited an almost temperature- and concentration-independent Cotton effect in water, indicating strong intramolecular organization. The bisignated Cotton effect in water was opposite in sign to that in THF, suggesting a solvent-dependent preference for one helical handedness. Compounds **99a** and **99b** represent another series of hydrogen-bonded urea foldamers that was developed by Gong and co-workers.¹⁵¹

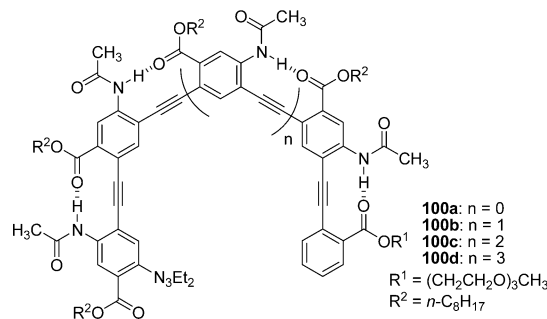


7.8. *m*-Phenylenethynylene Oligomers

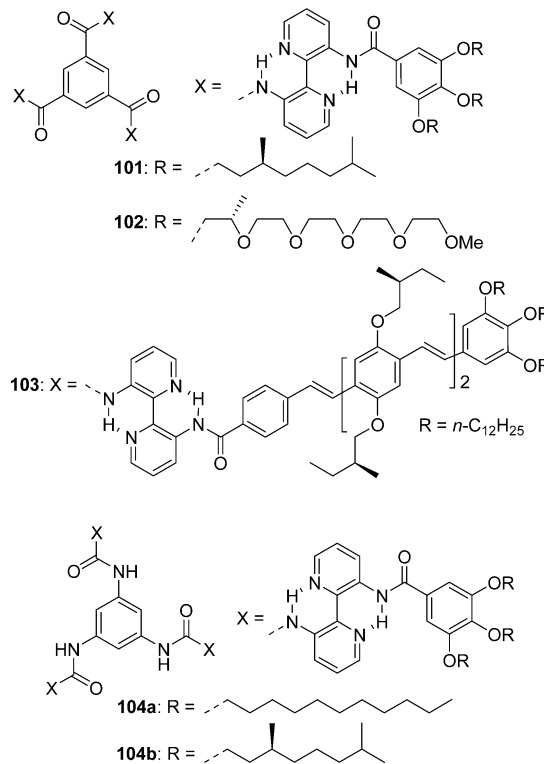
Gong and co-workers developed a general approach to achieving oligo(*m*-phenyleneethynylene) foldamers by utilizing the 10-membered hydrogen-bonding motif **HB-16** as the driving force.⁷⁸ The folded structures of corresponding oligomers **100a–d** were characterized using ¹H NMR and UV spectroscopy. Longer oligomers **100b–d** were revealed to adopt helical conformations in chloroform, a solvent in which *m*-(phenyleneethynylene) oligomers bearing hydrophilic oligo(ethylene glycol) chains are conformationally flexible.⁸

8. BRANCHED ARCHITECTURES

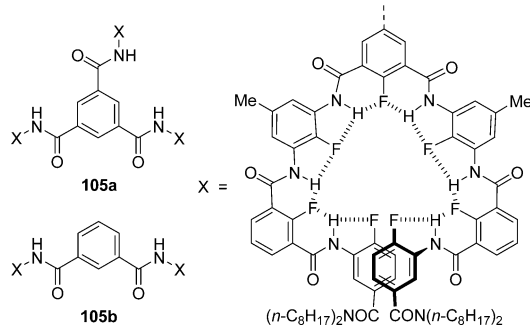
Disklike conjugated molecules may stack into columnar aggregates in unfavorable solvents. Hydrogen bonding can be used to promote their stacking via increasing their planarity. Meijer and co-workers systematically investigated the stacking property of C₃-symmetric molecules **101–104**.¹⁵² Their core segments are all rigidified with the **HB-46** hydrogen-bonding pattern. Compound **101** stacks into highly ordered chiral columns in dilute alkane solution, which cooperatively responds



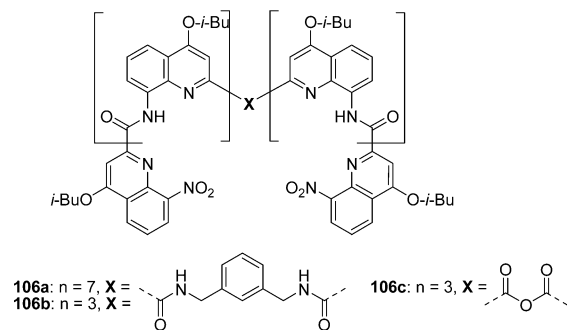
to chiral information,^{152a} whereas **102** stacks in a hierarchical fashion in polar protic media to afford thermotropic discotic liquid crystallines.^{69b} Compound **103** bears three chiral OPV chromophores appended with peripheral side-chains.^{152b} It also stacks strongly, but the strength and directionality of the stacking caused by the hydrogen-bonded bipyridyl segments and the OPVs are different and thus the aggregated objects are ill-defined. The stacking of hydrogen-bonded triurea derivatives **104a** and **104b** is different from that of **101–103**.^{152c} Their stacks are much more rigid, most likely due to the enhanced intermolecular hydrogen bonding formed by the urea units. It is also revealed that chiral **104b** first forms poorly defined stacks, which subsequently transform slowly into well-defined, chiral architectures.



Li et al. prepared disklike **105a**, which contains three F···H–N hydrogen-bonded folded segments attached to a 1,3,5-benzenetricarboxamide core.¹⁵³ The three folded units stacked strongly with fullerenes in chloroform, and the mixture formed honeycomb-styled nano networks on the surface due to cooperative foldamer–fullerene stacking. The folded segments of **105b** also stacked with fullerenes; the stacking was, however, relatively weak and only led to the formation of thin fibers on the surface.



Huc and co-workers prepared oligomers **106a–c**,^{154a} which contain two quinoline foldamer segments separated by a flexible *meta*-xylylene or carboxylic anhydride spacer, to investigate their conformational isomerization. Compounds **106b** and **106c** exist as one conformational species in solution, which was shown by X-ray crystal structure to be a racemic mixture of P/P and M/M helices. Longer oligomer **106a** forms P/P–M/M racemate and P/M meso conformers, which are in equal proportions in chloroform. The equilibria between these isomers are shifted in toluene, where one species largely prevails. X-ray crystallography revealed that the species is the P/P–M/M racemate.



Branched architectures **107a–c**, which comprise two pairs of foldamer oligomers connected via an ethylene glycol spacer, were also prepared.^{154b,c} The short spacer holds two helices in close proximity to enable interactions. Solution studies revealed that they were conformationally symmetrical, but intramolecular helix handedness communication occurred via side-by-side interactions. Crystal structures showed that they underwent conformational equilibria between P/M versus P/P–M/M conformers, parallel versus perpendicular relative orientation of the helical segments, and gauche versus anti conformation of the ethylene glycol spacer (Figure 24). In the solid state, the pyridine nitrogen atoms are hydrogen-bonded to adjacent amide hydrogen atoms. In terms of its dimension and structural complexity, compound **107c** (8.2 kDa) compares to a modest-sized protein tertiary fold.

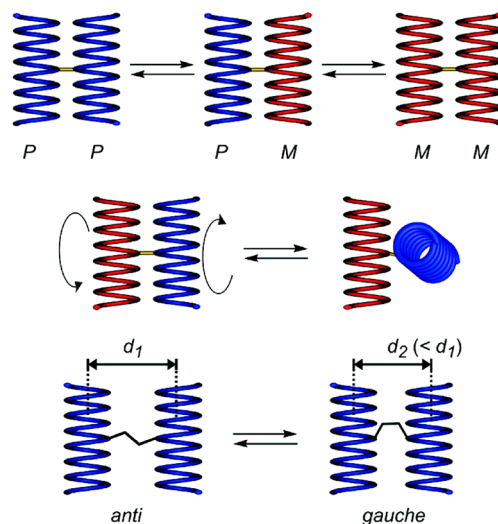
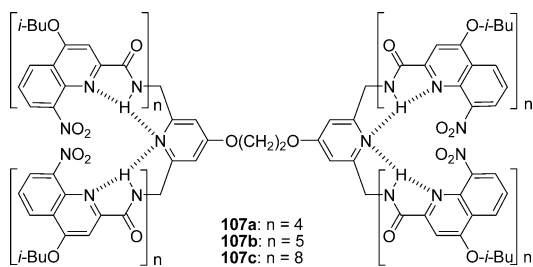
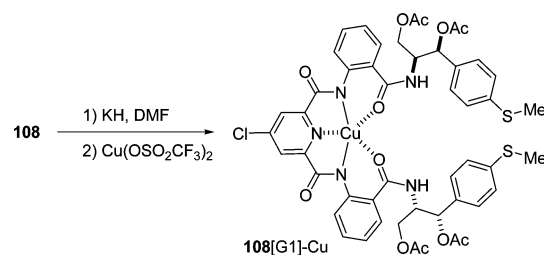


Figure 24. Conformation equilibria that **107a–c** may undergo: (top) helix handedness (P and M) inversion of helices; (middle) rotation about the ethylene glycol spacer between helices; (bottom) anti or gauche conformation of the spacer. Reproduced with permission from ref 154c. Copyright 2011 American Chemical Society.

9. FOLDED DENDRIMERS

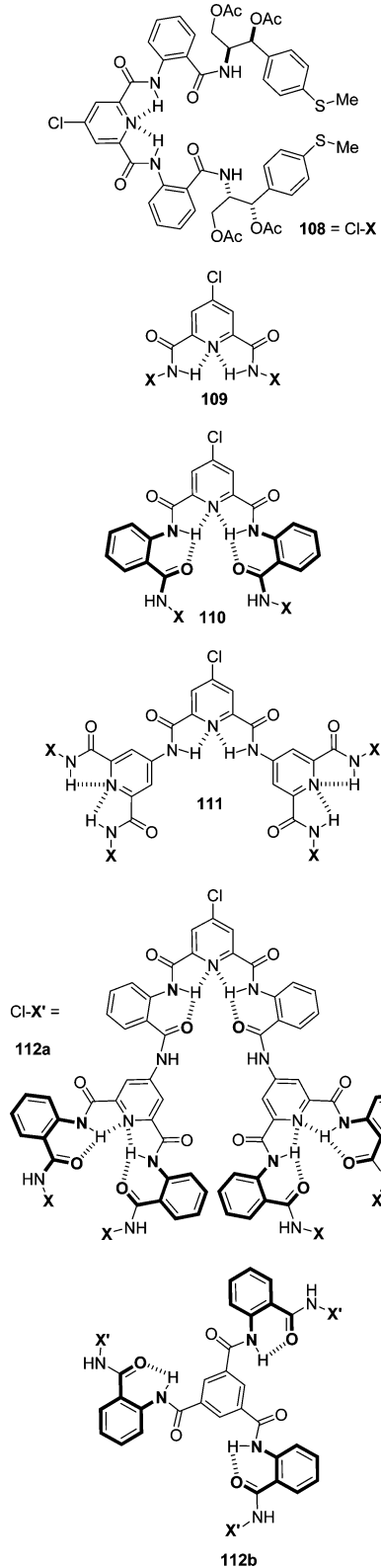
Parquette developed a general strategy for the construction of folded AB₂ dendrimers based on the hydrogen-bonded pyridine-2,6-dicarboxamide unit.¹⁵⁵ Compounds **108–110** were synthesized as the first, second, and third generations of dendrimers.^{156a} The hydrogen-bonded subunit bears two chiral groups derived from (1*S*,2*S*)-(+)-thiomalicamine. CD studies revealed that these dendrimers adopted two diastereomeric helical conformations (M and P helices) or secondary structures relating a pair of anthranilamide termini. The conformational interconversion is rapid for **108** and begins to bias the M-helicity for **109**. For **110**, this helical bias becomes very high, due to strong intramolecular packing of the terminal groups. Similar dendrimers bearing dodecyl peripheral chains were also reported.^{94a} X-ray analysis of the second-generation dendrimer showed that it formed a propeller-type secondary structure. The dynamically biased helical conformation of **108–110** can be locked in kinetically controlled conformations by coordination to Cu²⁺ ions (Scheme 3).^{156b} Binding to Cu²⁺

Scheme 3. Coordination of Cu²⁺ to Dendrons **108–110, with the Reaction of **108** As an Example**



ions forces them to exist in only the syn–syn conformation and dramatically rigidifies the dendrimer structure. To further investigate the effect of the internal anthranilamide turn unit on the structure and conformational stability of this kind of helically biased dendrimer, dendrons and dendrimers **111** and **112a,b** were also prepared.^{156c,d} CD studies suggested that

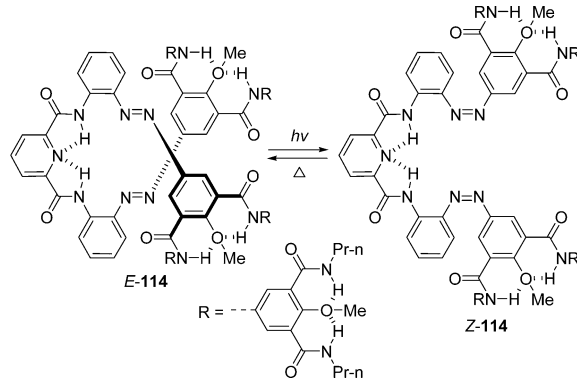
aromatic stacking played an important role in stabilizing the folded secondary structure in both the internal and peripheral regions, and it critically depended on the development of intramolecular packing interactions at higher dendrimer generation.



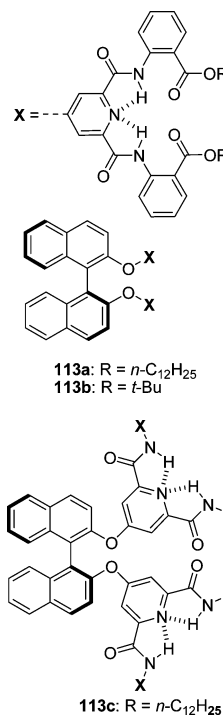
Parquette and co-workers further prepared dendrimers 113a–c by attaching hydrogen-bonded dendrons to S-

BINOL.^{156e} CD studies revealed that chirality transfer from the BINOL core to the periphery occurred in 113b, which bears sterically demanding terminal esters that cause packing interactions. Replacing the pyridine repeat unit with anisole produces dendrons with similar compact conformations.^{156f} Azobenzene-incorporated folded dendrimers were also constructed.^{156g} The largest one, 114, exhibited a compact helical conformation in the stable *E* form (Scheme 4). Upon exposure

Scheme 4. Photoswitchable Dendrimer 114:
Photoisomerization Induces a Reversible Disruption of the Helical Folded State



to light, the helical conformation expanded significantly due to the formation of the *Z*-form, which was dependent on the type of folding and increased with the dendrimer generation.



10. BINDING-INDUCED FOLDING

Driving forces for the folded or helical conformations of the above aromatic amide derivatives mainly come from intramolecular hydrogen bonding. Zhao, Li, and co-workers reported that alternating naphthalene and benzene-linked oligomers 115a–d were all conformationally flexible in

solution.^{157a} However, in the presence of benzene-1,3,5-tricarboxylate anion, the longer oligomers folded into helical conformation to strongly complex the trianion in polar DMSO driven by cooperative intermolecular N—H···O and C—H···O hydrogen bonds (Figure 25). Meta-substituted benzamide

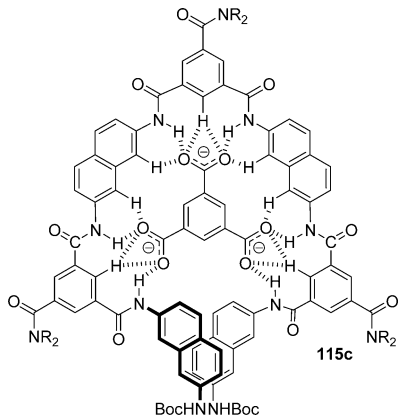
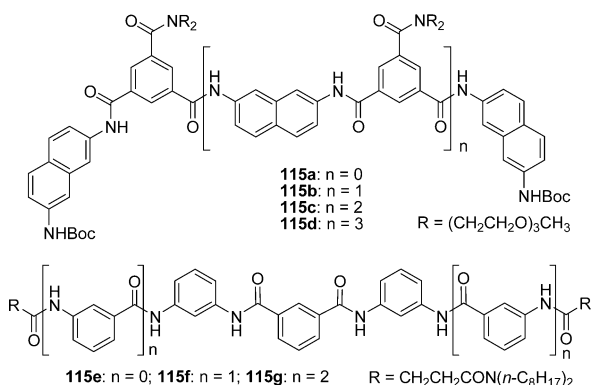


Figure 25. Structure of 1:1 complex between helical **115c** and benzene-1,3,5-tricarboxylate trianion, stabilized by cooperative intermolecular N—H···O and C—H···O hydrogen bonds.

oligomers **115e–g** are also conformationally flexible in solution.^{157b} Mono-, di-, and tricarboxylate anions can induce them to fold via forming 1:1 complexes. CD studies showed that chiral glutamic acid dianion induced the oligomers to produce chiral bias, leading to the formation of chiral supramolecular complexes.



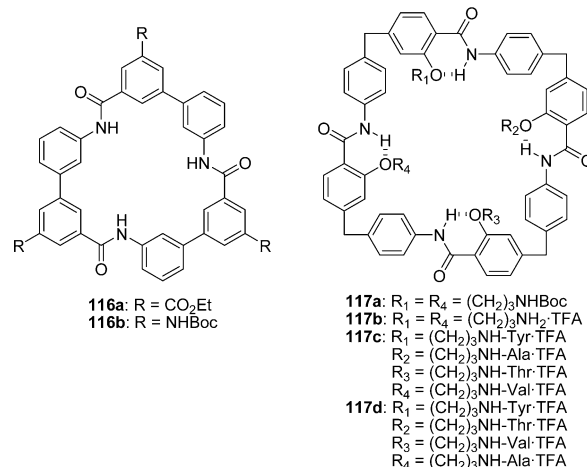
11. FOLDING-PROMOTED REACTIONS

11.1. Macrocyclization

The synthesis of macrocyclic molecules is usually of low efficiency due to competition of linear products and thus frequently needs high-dilution or template techniques.¹⁵⁸ Hydrogen-bonded aromatic amide oligomers adopt well-defined conformations. When the two ends of a folded backbone are appended with required reactive groups, the reaction of the groups for the formation of a macrocycle may be facilitated by the preorganization of the rigidified backbone. A variety of structurally complicated macrocycles have been constructed based on this strategy.

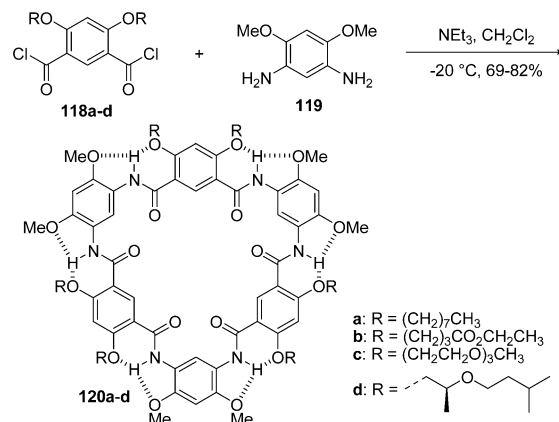
Kim et al. described that high-dilution reaction of isophthaloyl dichloride and benzene-1,3-diamine in toluene gave a mixture of cyclic hexamer, in 4–11% yield, and larger cyclic oligomers.¹⁵⁹ Choi and Hamilton reported the synthesis

of **116a** and **116b** by a step-by-step approach.¹⁶⁰ Using high-dilution technique, these macrocycles could be obtained in 40–60% yields. Nowick and co-workers developed a new kind of amino acid by modifying diphenylmethane.^{119b} Starting from these amino acid building blocks, they prepared water-soluble macrocycles **117a–d** by solid-phase synthesis of the protected linear tetrameric precursors, followed by macrocyclization and deprotection. The yield of cyclization is ~20%. These structurally rigid and planar macrocycles are useful receptors for discrete guests. However, macrocyclization is generally less efficient.

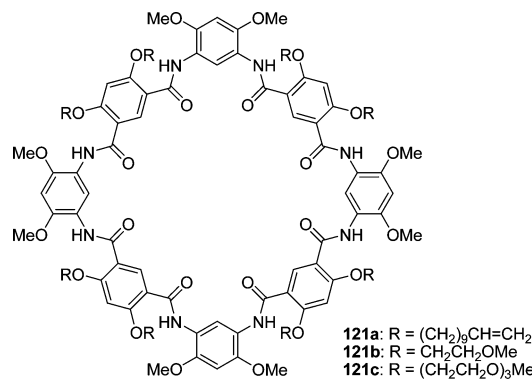


Gong and co-workers reported that cyclic hexamers **120a–d** could be prepared in high yields from one-pot reactions of simple precursors **118a–d** and **119** in dichloromethane at low temperature (Scheme 5).^{41a} The process involved the

Scheme 5. Synthesis of Macrocycles **120a–d**

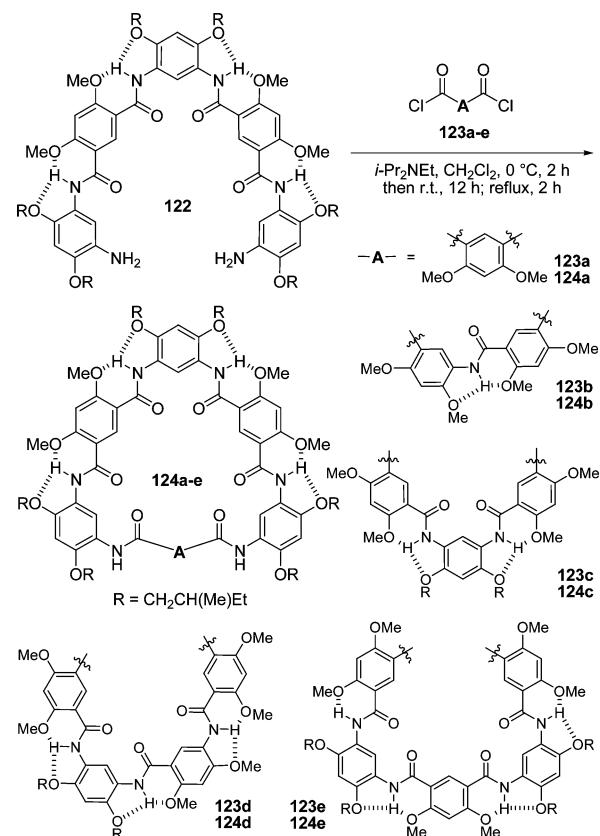


formation of six amide bonds, but the yields were still very high. MALDI-TOF MS of the untreated reaction mixtures showed the presence of only a trace amount of the eight-residue macrocycle. Clearly, hydrogen-bonding-driven folded preorganization of the last six-residue precursor played a crucial role, which forced the amino and acyl chloride at the ends to approach each other to maximize cyclization. By changing the reaction temperature and concentration, the eight-residue macrocycles **121a–c** can be obtained in up to 30% yield, but the six-residue macrocycles are still the major products.¹⁶¹ Using a step-by-step approach, **121c** can be produced in 40–75% yields from the 1 + 1 condensation of the corresponding oligomeric precursors.



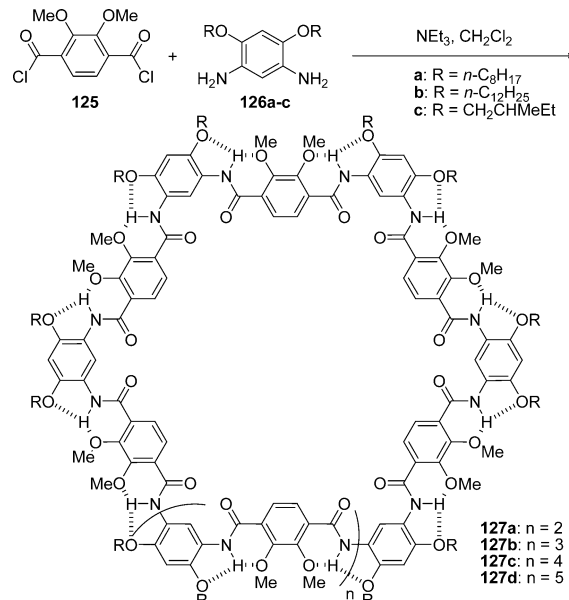
Yuan and co-workers further investigated the synthesis of macrocycles **124a–e** of varying sizes from the condensation of **122** and **123a–e** (Scheme 6).^{46a} Treating foldamer precursor

Scheme 6. Synthesis of Macrocycles **124a–e**



122 with **123a** and **123b** (1:1:1, 0.5 mM) in dichloromethane afforded 6-mer **124a** and 7-mer **124b** in 44% and 6% yields, respectively, indicating that the formation of the 6-mer macrocycle was overwhelmingly favored over other macrocycles. However, mixing **122** with **123b–e** (1:1) under identical reaction conditions could also afford macrocycles **124b–e** in 50%, 14%, 10%, and 6% yields, respectively. These results show that precursor preorganization also holds for the formation of larger macrocycles, even though the six-residue structures are most favored. When isophthaloyl dichloride was replaced with 2,3-dimethoxyterephthaloyl dichloride **125**, reactions with diamines **126a–c** afforded 16-mer macrocycles **127a–c** as major products (Scheme 7).^{46b} MALDI-TOF MS revealed that the reactions also afforded 14-, 18- and 20-mer

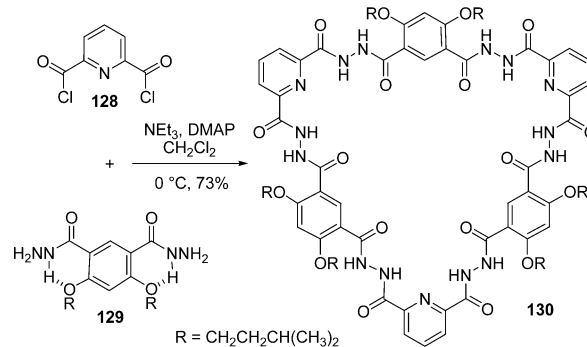
Scheme 7. Synthesis of Macrocycles **127a–d**



macrocycles with a total yield of 84%. Remarkably, the 16-mer macrocycles were obtained in ca. 81% yield after repeated recrystallization of the crude products from a mixture of methanol and dichloromethane and then DMF/acetone.

Gong and co-workers found that this strategy could be extended to aromatic hydrazide systems.¹⁶² For example, mixing **128** and **129** (1:1) in dichloromethane in the presence of DMAP afforded six-residue macrocycle **130** in 73% yield (Scheme 8). MALDI-TOF MS of the crude product revealed a

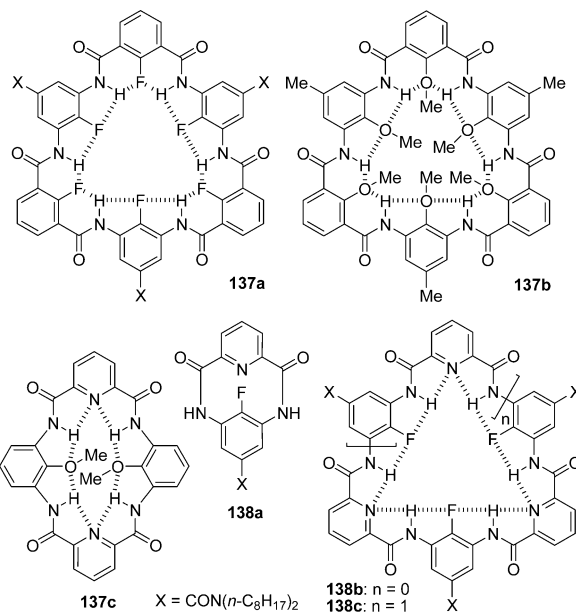
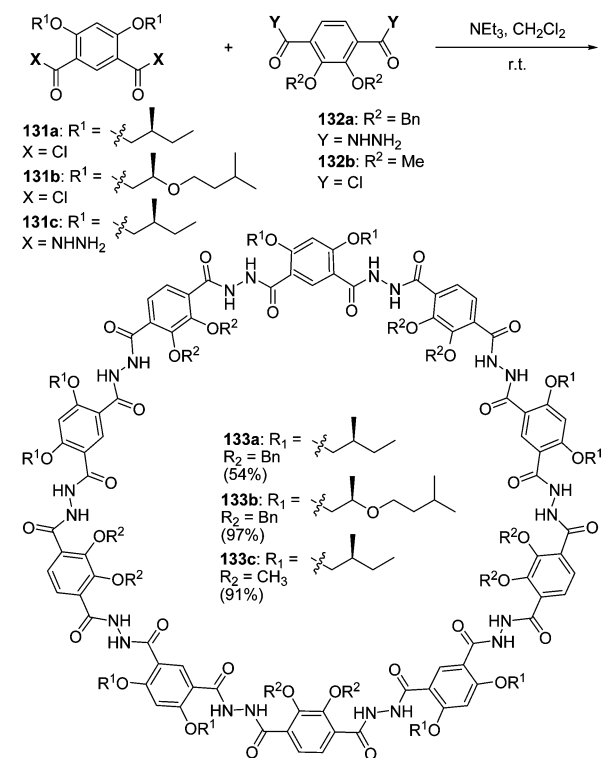
Scheme 8. Synthesis of Macrocycle **130**



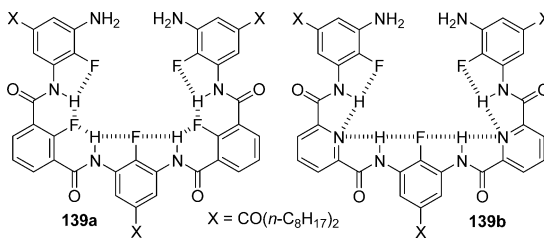
dominant peak corresponding to the $[\text{M} + \text{Na}]^+$ ion of **130**. When 2,3-dimethylterephthalohydrazide **132a** or 2,3-dialkoxycyano-terephthaloyl dichloride **132b** was used, one-pot reactions with isophthaloyl dichloride (**131a,b**) or isophthalohydrazide (**131c**) produced 10-residue macrocycles **133a–c** in 54–99% yields (Scheme 9). MALDI-TOF MS also exhibited the $[\text{M} + \text{Na}]^+$ signals of **133a–c** as the dominant peaks. These results indicated that the amide- and hydrazide-based preorganized segments have different geometric features. The latter series may be more rigid to facilitate the formation of 10-residue macrocycles.

Gong and co-workers also prepared nonaggregational macrocycles **136a** and **136b** from coupling of trimeric precursors **134** and **135** under dilution (Scheme 10).^{41b} The yields are significantly lower than those of macrocycles **120a–d**

Scheme 9. Synthesis of Macrocycles 133



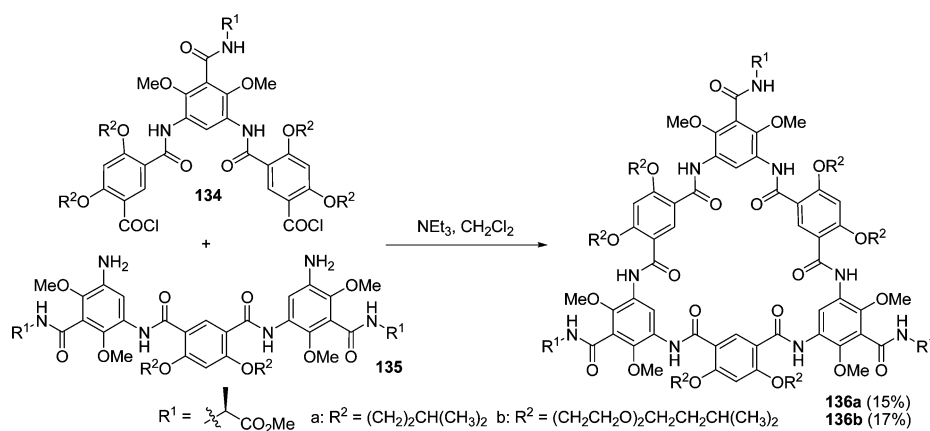
pentamers **139a** and **139b** with related diacid chlorides under the same reaction conditions gave rise to **137a** and **138c** in 55% and 54% yields, respectively. The crystal structure of **137b** showed that its backbone adopted a roughly planar conformation, but the six methyl groups in the cavity prevented column-styled stacking.

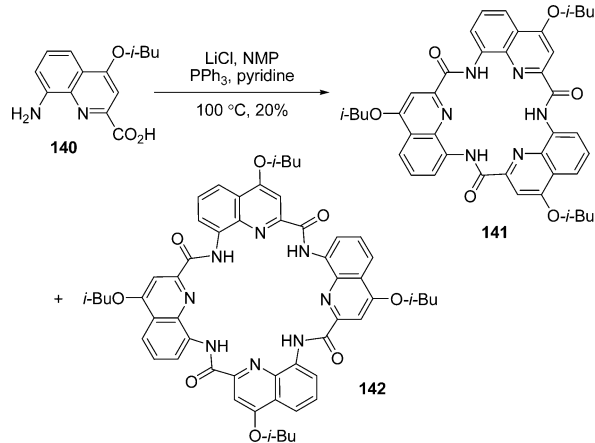


of the identical backbone. It has been proposed that weakened intermolecular stacking and intramolecular hydrogen bonding accounts for the low yield of **136**. Attempts to prepare **136** by one-pot coupling of the corresponding diacid chlorides and diamines failed, but afforded mixtures containing cyclic and noncyclic oligomers of 4–12 residues.

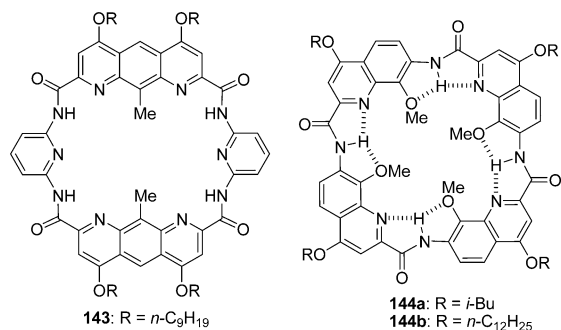
Li and co-workers found that one-pot reactions of the related diamine and diacid chloride precursors selectively afforded six-residue macrocycles **137a** and **137b** or four-residue macrocycles **137c** in total 40–45% yields, whereas a similar reaction produced two-, four-, and six-residue macrocycles **138a–c** in 80% total yield.⁴³ The yields of these six-residue macrocycles are considerably lower than those of macrocycles **120a–d**, which may be attributed to the fact that, for all these macrocycles, the hydrogen-bonding acceptors are located inwardly, which favors the formation of linear products. For comparison, the step-by-step approach was also used. Treating

Huc and co-workers reported that, in the presence of lithium chloride and triphenyl phosphorus, quinoline amino acid **140** underwent self-coupling in highly polar methylpyrrolidone/pyridine at 100 °C to afford three- and four-residue macrocycles **141** and **142** in 20% total yield (Scheme 11).^{40a} The formation of **142** was not expected, because a noncyclic helical tetramer was found to extend to over 1.5 turns in the crystal structure. The crystal structure of **142** showed that its

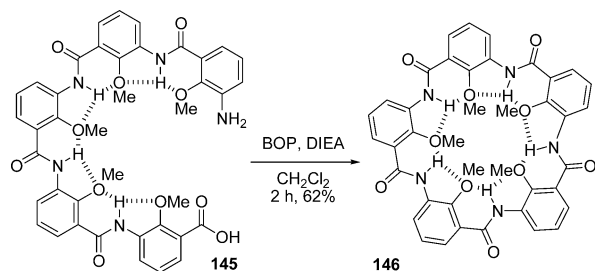
Scheme 10. Synthesis of Macrocycles **136a** and **136b**

Scheme 11. Synthesis of Macrocycles 141 and 142

backbone did strongly deviate from planarity to produce a saddle shape, indicating the existence of a large torsion. The harsh reaction conditions may favor its formation by weakening the intramolecular hydrogen bonding of the precursors. Huc's group also reported that macrocycle 143 could be obtained in 50% yield from the 2 + 2 reaction of the corresponding diacid chloride and 2,6-diaminopyridine in THF.^{40b} Jiang and co-workers described that treating the related quinoline amino acids with dichloro triphenylphosphorus in THF under reflux produced four-residue macrocycles 144a and 144b in 46% and 53% yields, respectively,⁴⁷ and no trimeric macrocycles were formed. The crystal structure of 144a showed that its backbone adopted a planar conformation.



Zeng and co-workers systematically investigated the synthesis of structurally unique pentagon macrocycles.^{45,83,163} Macrocycle 146, the first example of this family, was obtained in 62% yield from BOP-initiated intramolecular coupling of pentamer 145 in dichloromethane (Scheme 12).^{45a} The crystal structure revealed that it folded into an almost planar disk arrangement of nearly perfect C₅ symmetry. From the coupling of one-

Scheme 12. Synthesis of Pentagon 146

four-residue amino acid precursors, macrocycles that bear discrete exterior side-chains have been prepared in acetonitrile in the presence of phosphorus oxychloride and triethylamine.^{163a} The formation of these hybrid macrocycles involved a chain-growth mechanism, and successive addition of monomers onto higher oligomers was faster than reactions between two higher oligomers. The one-pot synthesis of 146 from 3-amino-2-methoxybenzoic acid has been optimized, and 46% yield can be reached in acetonitrile in the presence of phosphorus oxychloride and triethylamine.^{163b} Treating related fluorinated pentameric amino acid precursor with BOP in DIPEA and DMF could produce macrocycle 147 in 11% yield.^{45c} The crystal structure of 147 revealed a perfectly planar conformation of 5-fold symmetry and a densest striped crystalline lattice (2D packing density = 0.921) that could be achieved from pure pentagonal molecules by mathematically verified six-neighbor densest packing (Figure 26). Under the reaction

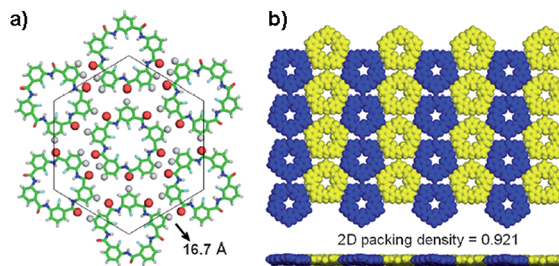
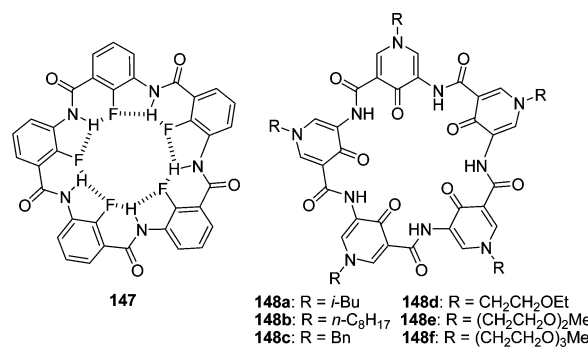


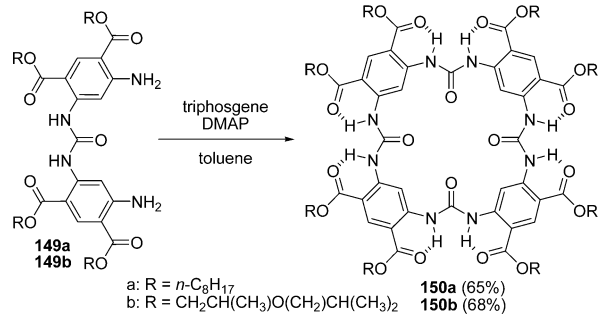
Figure 26. (a) Pseudohexagonal arrangement of pentagon 147. (b) Top and side views of alternating striped lattice packing, which reproduces the densest mathematical crystal formed by pentagons. Reproduced with permission from ref 45c. Copyright 2011 Wiley-VCH.

conditions for the preparation of 146, one-pot self-coupling reactions of 5-amino-1-alkyl-4-oxo-1,4-dihydropyridine-3-carboxylic acids could generate macrocycles 148a–f in 10–26% yields.⁸³ It is noteworthy that none of these reactions produced macrocycles of other sizes.



Gong and co-workers reported that treating urea precursors 149a and 149b with triphosgene in toluene produced 4-mer macrocycles 150a and 150b in 65% and 68% yields, respectively (Scheme 13).¹⁵¹ The high yield was also attributed to intramolecular hydrogen-bonding-induced preorganization of the noncyclic oligomer precursors. The macrocycles contain a small cavity of ~5 Å diameter.

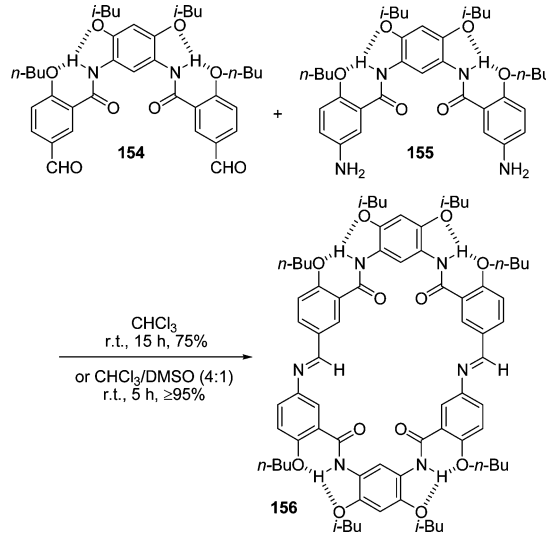
Li and co-workers also designed preorganized precursors by introducing ethynyl groups to the ends of oligomers 15a and 15b. Treating them with *trans*-Pt(PEt₃)₂Cl₂ in dichloromethane afforded metallomacrocycles 151a and 151b in 20% and 18% yields, respectively.³⁰ In a similar way, 151c was produced from

Scheme 13. Synthesis of Urea Macrocycles 150a and 150b

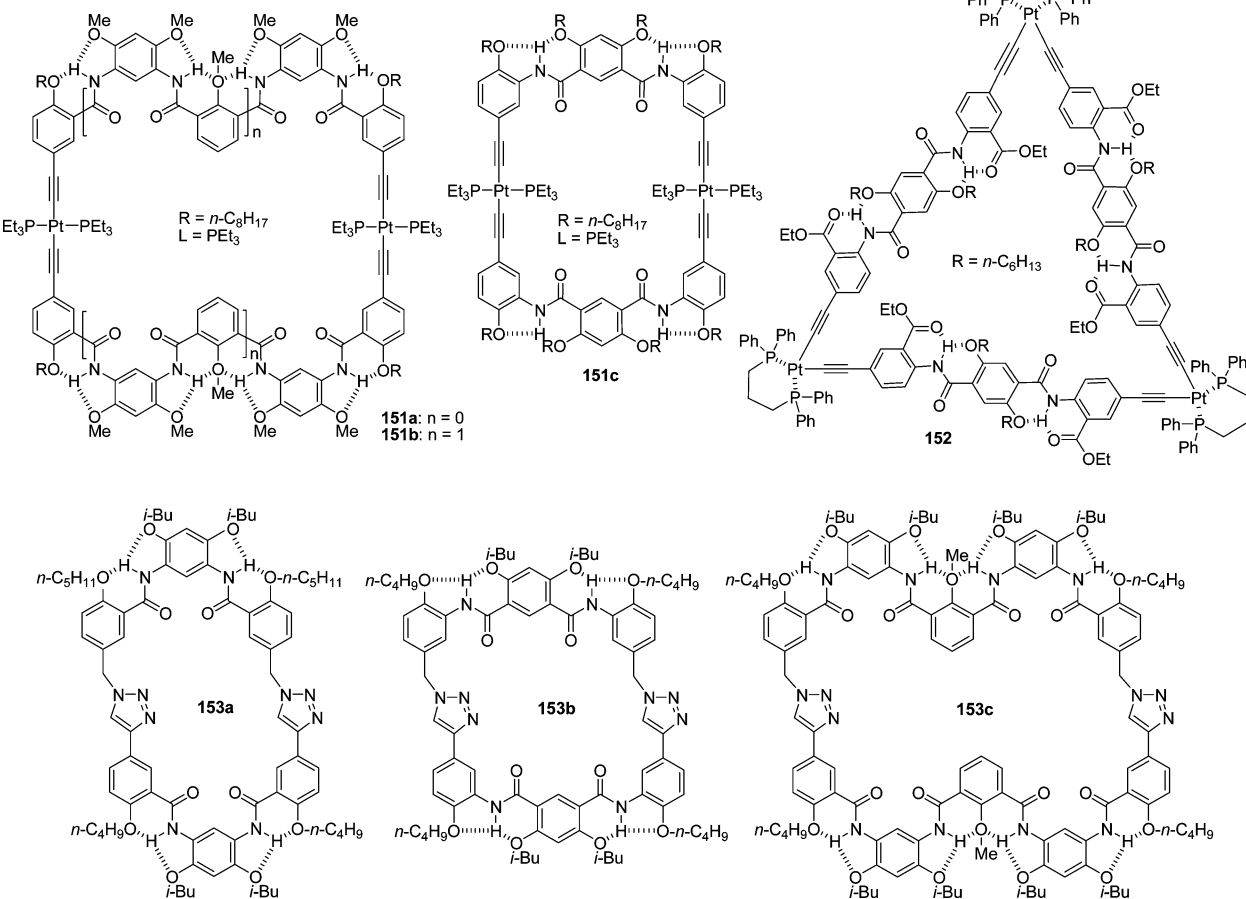
the reaction of another ethyne-bearing precursor.^{42a} From the reaction of the related ethyne-appending straight precursor with Pt(dppp)(OTf)₂, triangle macrocycle **152** was obtained in 15% yield,^{42b} whereas click reactions of the corresponding diacetylene and diazide precursors in chloroform in the presence of DIPEA and cupric iodide afforded macrocycles **153a–c** in 25–82% yields.¹⁶⁴

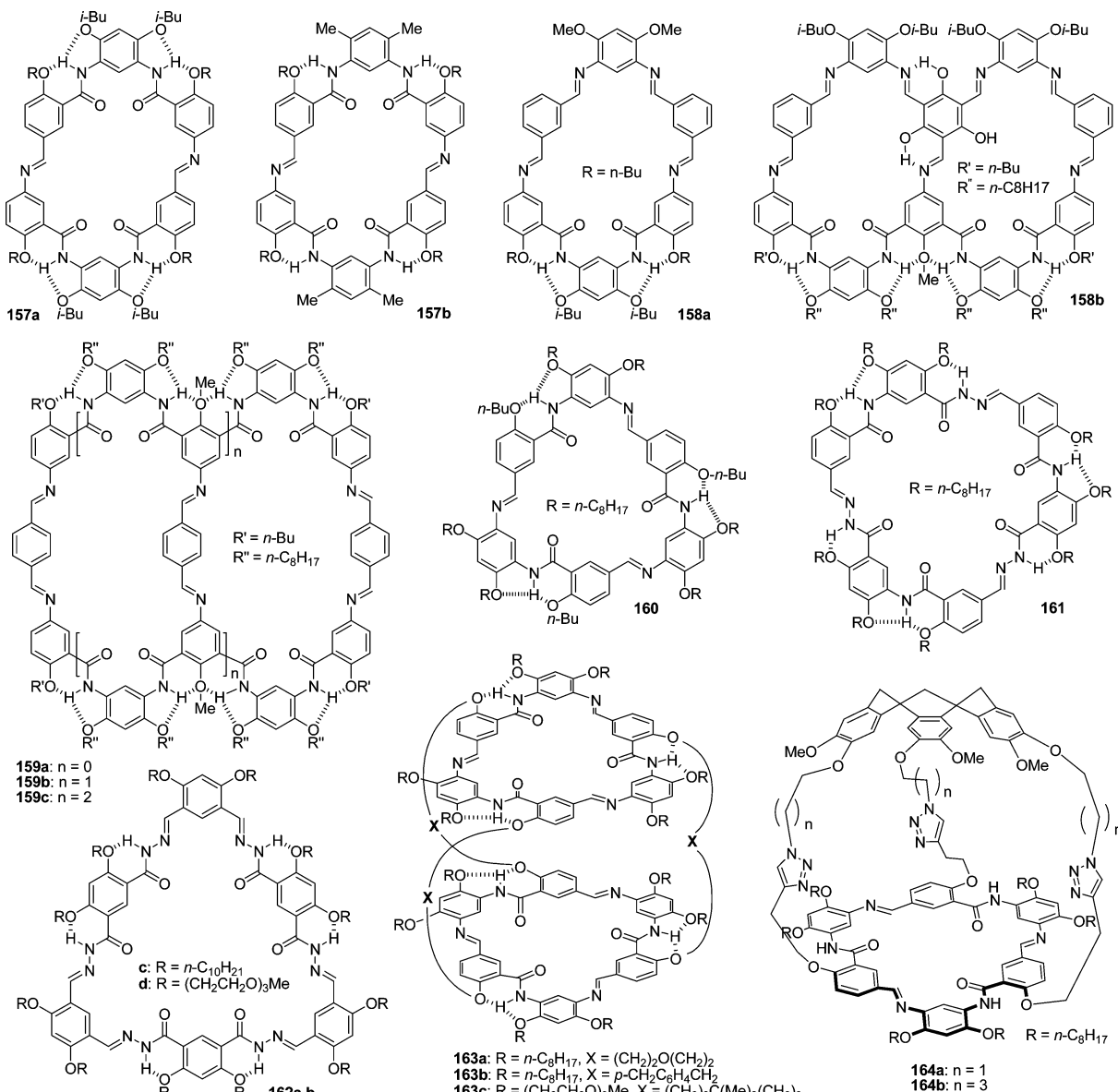
Many of the above hydrogen-bonding-assisted reactions afforded macrocyclic products in high yields. However, it is difficult to realize quantitative cyclization from these dynamically controlled reactions. Dynamic covalent chemistry (DCC) has been demonstrated as a robust approach to the construction of complicated macrocyclic architectures.¹⁶⁵ Li and co-workers reported that macrocycle **156** could be produced nearly quantitatively from the reaction of **154** and **155** (Scheme 14).⁴⁴ ¹H NMR showed that the reaction first

generated complicated products, which gradually evolved to the most stable **156** due to the reversible nature of the imine bond.

Scheme 14. Synthesis of Diimine Macrocycles 156

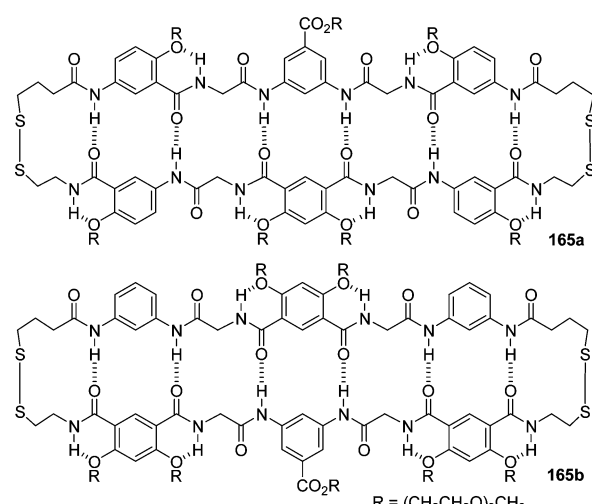
This DCC strategy has been extended to the construction of macrocyclic architectures **157–164**.^{44,166} Macrocycles **157a**, **158b**, **159a–c**, and **160** were all generated quantitatively from the related precursors through the formation of 2–8 imine bonds.^{44,166a} The precursor of **157b** formed only two intramolecular hydrogen bonds, and its yield decreased to





65%,⁴⁴ reflecting the importance of the three-centered hydrogen bonding in stabilizing the macrocyclic structures. Using fully hydrogen-bonded diamine **155** as template, **158a** was produced in 91% yield from its reaction with 4,6-dimethoxybenzene-1,3-diamine and isophthalaldehyde.⁴⁴ Macrocycles **160**, **161**, and **162a** and **162b** can also be formed selectively.^{166b,c} Hydrazone-based macrocycles are more stable than their imine analogues in solution. By modifying the precursor of **160**, dipodal or cyclotrimeratrylene-derived compounds have been designed for the preparation of capsular molecules **163a–c** and **164a** and **164b** in high yields.^{166b,d,e}

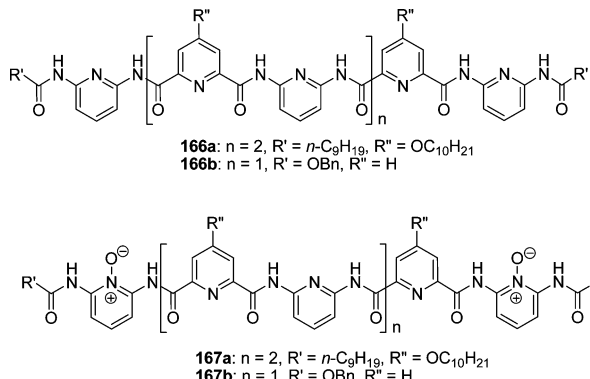
Hybrid aromatic/aliphatic amide oligomers developed by Gong and co-workers can form stable heterodimers by adopting extended conformations.¹²² When the two ends of the monomers are appended with tritylthio groups, the dimeric structures cause the two tritylthio groups of the same side to approach each other. Macro cyclic structures have been produced by oxidizing them to two disulfide bonds.¹⁶⁷ Macrocycles **165a** and **165b** are two examples generated using this strategy.



11.2. Pyridine Oxidation

Folding frequently results in steric hindrance for the preparation of long helical foldamers. However, several

reactions can be enhanced by folded structures, which was found by rational design or serendipity.^{168,169} Huc and co-workers reported that the ending pyridine units of **166a** and **166b** were selectively oxidized by *m*-CPBA to **167a** and **167b**, respectively.¹⁷⁰ The oxidation was remarkably faster than that of control compounds. In addition, oxidation occurred only for the ending pyridines. Because these oligomers form double-helical dimers,^{21,135} the selectivity has been ascribed to the large steric hindrance at the center position in the dimeric structures. The exact mechanism is still unclear. Dipolar interactions within the helical conformation and preassociation of the

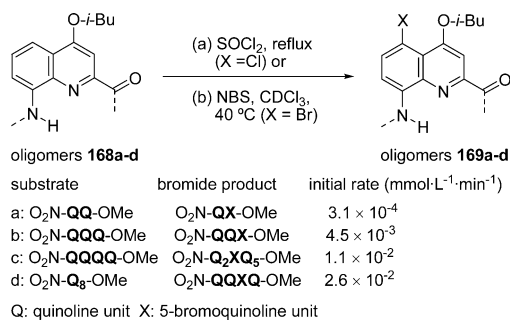


oxidative reagent in the polar cavity of the double helices have been proposed to rationalize the observation.

11.3. Quinoline Chlorination and Bromination

Ghosez, Huc, and co-workers reported that refluxing quinoline foldamers in thionyl chloride led to chlorination of one of the quinoline rings at the 5-position.¹⁷¹ Further investigation was carried out for the bromination of foldamers **168a–d** with

Scheme 15. Electrophilic Chlorination and Bromination of Quinoline-Derived Foldamers 168 and 169

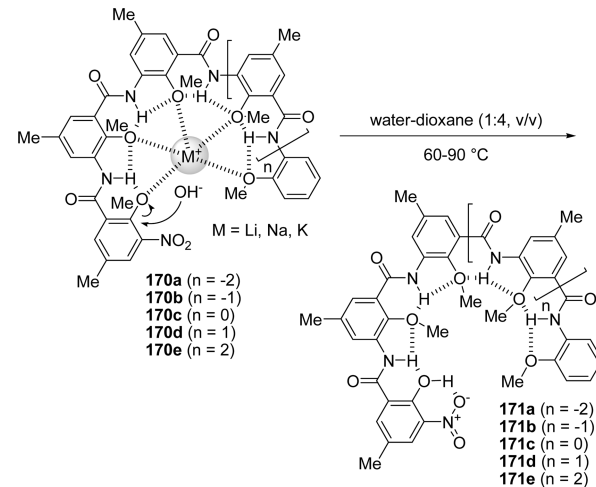


NBS, which selectively afforded monobrominated oligomers **169a–d** (Scheme 15). For all the substrates, quinoline ring one was not brominated due to the strong electron-withdrawing effect of the nitro group. However, for long oligomers **168b–d**, bromination always occurred on the third ring, even though the second ring was less hindered. The initial rate increased with the oligomer length (Scheme 15), which was ascribed to the ability of the helical conformation of long oligomers to produce large dispersive forces, as well as tight stacking-caused ring current effects. Local variation of steric hindrance associated with conformation dynamics, such as helix spring-like extension or helix handedness inversion, has been proposed for the regioselectivity.

11.4. Anisole Hydrolysis

Li and co-workers reported that the nitro-bearing anisole on the benzene ring of oligomers **170a–e** could be hydrolyzed to **171a–e** with alkali hydroxides in aqueous dioxane (Scheme 16).¹⁷² Kinetic experiments revealed that the hydrolysis rates

Scheme 16. Hydrolysis Reaction of Oligomers 170a–e to 171a–e



were notably higher (up to 4-fold) than those of shorter controls, and LiOH exhibited the highest reactivity. The acceleration was attributed to the complexation of alkali cations by the folded oligomers (Scheme 16), which activated both the hydroxide anion and the anisole ether bond and also helped the hydroxide anion to approach the activated ether bond. This result also indicates that, even in highly polar aqueous media, intramolecular N–H···O hydrogen bonding survives and enables the oligomers to keep their preorganized conformation.

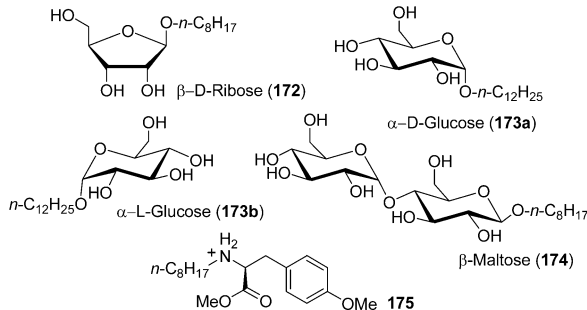
12. MOLECULAR RECOGNITION

The capacity of linear artificial receptors in binding nonlinear guests may be enhanced if they adopt compact conformations before binding. Foldamers are thus ideal receptors when there exists a driving force for binding.^{8,9,173} The length of aromatic amide foldamers can be readily regulated, and the backbones and side-chains can be easily modified with discrete functional groups. Therefore, this family of foldamers and their derivatives have been extensively exploited for molecular recognition.

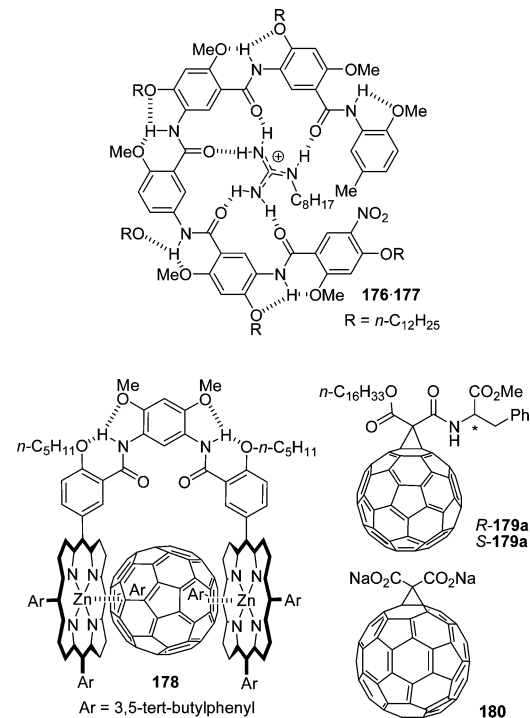
12.1. Amide Foldamer Receptors

Li and co-workers reported that **52a** and **52b** complexed saccharides **172–174** in chloroform driven by intermolecular C=O···HO hydrogen bonding.¹³⁴ The association constant (K_{assoc}) values were estimated to be 550–7800 M⁻¹. Molecular modeling showed that the cavity of the foldamers was smaller than the size of the saccharides. Thus, binding should occur on the surface of the folded frameworks or in an expanded cavity. Foldamers **46a–c** do not exhibit any binding ability to saccharides but bind diocetyl ammonium or decyl ammonium in chloroform,¹³² with K_{assoc} values being 17–360 M⁻¹. Intermolecular MeO···H–N hydrogen bonding and cation–π interaction have been proposed as driving forces. This binding is modest most likely due to the steric hindrance of the centrally located methoxyl groups. Foldamers **54a–c** form 1:1 complexes with diocetyl ammonium and **175** in chloroform, with $K_{\text{assoc}} = 8.1 \times 10^6$ and 7.3×10^5 M⁻¹, respectively.^{24b} Binding to

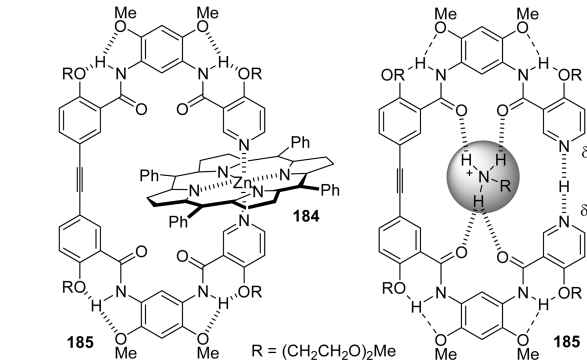
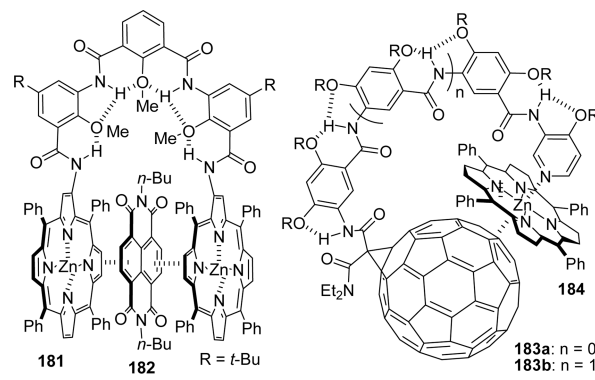
175 also causes the foldamers to generate helical bias, which is weakened by methanol, suggesting that the binding is driven by the intermolecular N–H···F hydrogen bonding.



Gong and co-workers described that hexamer **176** strongly complexed guanidinium tetraphenylborate **177**.¹⁷⁴ Multiple intermolecular NOEs were observed for their 1:1 mixture. By using the extraction method, the K_{assoc} values of the complexes of **176** with guanidinium and octylguanidinium in water-saturated chloroform were determined to be as high as 1.3×10^8 and $1.3 \times 10^7 \text{ M}^{-1}$, respectively.



Li and co-workers further utilized foldamer backbones to develop tweezer receptors.^{35,175} Foldamer-derived bisporphyrin **178** was found to complex C₆₀, C₇₀, and C₆₀ derivative R- or S-**179**.^{35a} The two porphyrin units are arranged roughly parallel to each other and thus exhibit high affinity to fullerenes. The K_{assoc} values of complexes **178**·C₆₀, **178**·C₇₀, and **178**·**179** in toluene were determined to be 1.0×10^5 , 1.1×10^6 , and $3.2 \times 10^3 \text{ M}^{-1}$, respectively. Binding for chiral **179** caused the bisporphyrin tweezers to generate supramolecular chirality. Replacing the six *meso*-3,5-di(*tert*-butyl)phenyl groups with six 3-N-methylpyridyl groups provides solubility in aqueous media.^{175a} The new tweezers do not encapsulate C₆₀ or C₇₀ but bind **180** in water, with $K_{\text{assoc}} = 1.1 \times 10^5 \text{ M}^{-1}$, driven by electrostatic interaction as well as porphyrin-C₆₀ stacking interaction.



Li and co-workers also prepared **181**,^{175b} whose folded conformation forced the two porphyrins to approach and stack each other. This receptor forms 1:1 complexes with planar electron-deficient molecules, such as **182**, in a sandwich-styled binding pattern. The K_{assoc} of complex **181**·**182** was determined as 850 M^{-1} in chloroform. Pyridine- and C₆₀- appended receptors **183a** and **183b**, which complex zinc porphyrins through coordination and stacking interactions, were also prepared.^{175c} As an extension of this “two-point” binding concept, Wang and co-workers prepared **185**, which comprises two foldamer moieties connected with an acetylene linker.^{175d} This compound forms a 1:2 complex with **184** at high concentrations ($\geq 5 \text{ mM}$) in chloroform. At low concentration ($< 4 \mu\text{M}$), the binding stoichiometry becomes 1:1, with $K_a = 5.3 \times 10^3 \text{ M}^{-1}$. The value is higher than that of a control molecule, supporting a “two-point” binding pattern. In the presence of 1 equiv of TFA, **185** also complexes alkylammonium to form a 1:1 complex mediated by an intramolecular N–H···N hydrogen bridge.^{175e}

By introducing six zinc porphyrin units to a 6-mer foldamer, Li and co-workers further synthesized **186**.^{35b} The foldamer segment induces the appended zinc porphyrins to have a roughly average spatial separation. Thus, it forms a 1:6 complex with structurally matching chiral C₆₀-ligand adduct **187** in a “domino” pattern (Figure 27). The apparent K_{assoc} of the complex between the zinc porphyrin units of **186** and **187** was determined to be $3.6 \times 10^4 \text{ M}^{-1}$, which is considerably larger than that of control system. CD studies revealed ICD signals stronger than those of shorter oligomeric analogues. Both results suggested that the binding is driven by intermolecular cooperative N–Zn(II) coordination and C₆₀-porphyrin stacking.

The amide and heterocyclic nitrogen atoms of heterocyclic amide foldamers are all located inwardly, which may produce polar cavities of varying size. If a folded cavity is large enough, it may host one or more guests of suitable size and/or binding

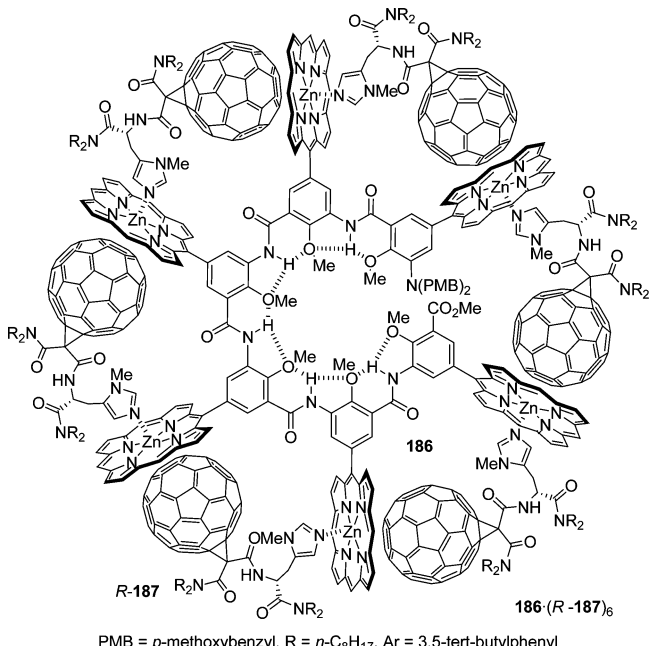
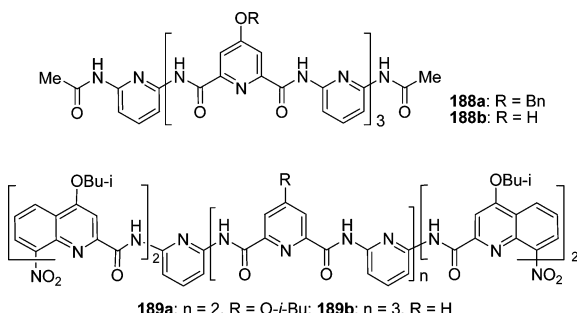


Figure 27. Propeller-styled structure of the 1:6 complex of **186** and **R-187**. The meso positions of the porphyrins are attached with 3,5-di-*tert*-butylphenyl groups, which are omitted for clarity.

sites. Huc et al. systematically investigated the binding behavior of this family of foldamers.^{65,84,142,176} 7-Mer foldamers **188a** and **188b** were found to entrap a water molecule in their cavity in the solid state, which was stabilized by intermolecular N···H–O(water) and (water)O···H–N hydrogen bonding.⁶⁵ This binding did not occur in solution. In chloroform, they dimerized to form double-helical structures with a K_{assoc} of ca. 50 M⁻¹.



Huc and co-workers found that quinoline–pyridine hybrid heptamer **80a** also encapsulated water in both solution and the solid state.¹⁴² Because the quinoline segments have no internal cavity, the foldamer formed a closed capsule with the shape of the skin of an apple peeled in a helical fashion, as proposed by the authors (Figure 28). ¹H NMR in dried and wet chloroform-*d* indicated that the capsule entrapped a water molecule, and its inside–outside exchange was slow at –50 °C on the ¹H NMR time scale, which led to the formation of two water peaks. A helix unwinding–rewinding mechanism was proposed for the binding and release process (Figure 28). The Huc group also prepared 9- and 11-mer expanded helical capsules **189a** and **189b**.^{176a} Although **189a** still encapsulated only one water molecule, **189b** hosted two water molecules in both the solid state and chloroform. The capsule could be empty, half-full, or full, which led to distinct signals in ¹H NMR at low

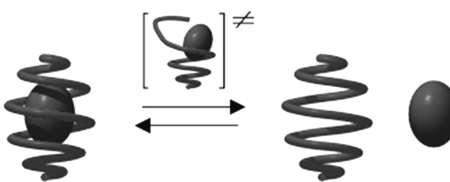
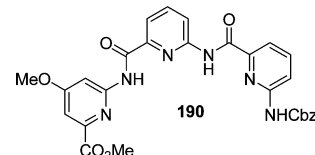


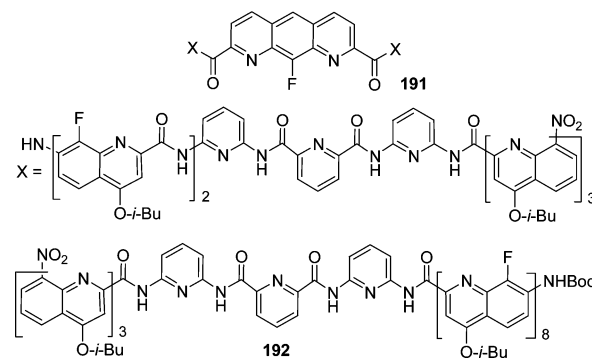
Figure 28. Encapsulation of an egg-shaped guest by partial unfolding of a helix possessing a reduced diameter at both ends. Foldamer **80a** exhibits this behavior by entrapping a water molecule. Reproduced with permission from ref 142. Copyright 2005 Wiley–VCH.

temperature. Other small polar molecules, such as hydrazine, hydrogen peroxide, or formic acid, could also be entrapped in the internal cavity, but water was the preferred choice.

Zeng and co-workers also reported that foldamers **49d** and **190** entrapped both conventional and unconventional dimeric water clusters in their small cavity (~2.5 Å radius).¹⁷⁷ In the so-called unconventional water dimer cluster, the two water molecules stayed in contact with an unusual short H–H distance (~2.25 Å), which might be caused by the shrinking space of the foldamers.

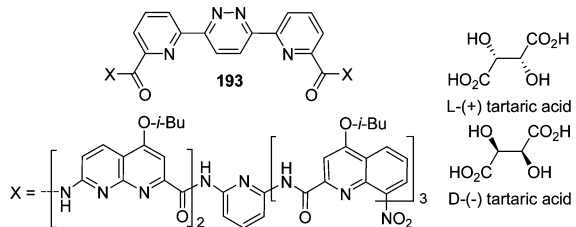


Huc and co-workers reported that 17-mer foldamer **191**, which contains a 1,8-diazaanthracene unit at the center, had a larger internal cavity that encapsulated linear dialkanediols, including ethylene glycol, 1,3-propanediol, 1,4-butanediol, *cis*-2-butene-1,4-diol, 4-amino-1-butanol, and 1,4-butanediamine, with K_{assoc} values being 500–5000 M⁻¹ in chloroform.⁸⁴ Crystal structures of the 1:1 complexes between **191** and 1,3-propanediol, 1,4-butanediol, and 1-amino-4-butanol revealed almost identical unit cells, suggesting that encapsulation did not cause important structural deformation of the helix capsule. 14-Mer oligomer **192** was found to form an even longer closed capsule through a double-helix structure,^{176b} which could isolate linear guests, such as 1,9-nanediol and 1,10-dicanediol, from the solvent molecules.

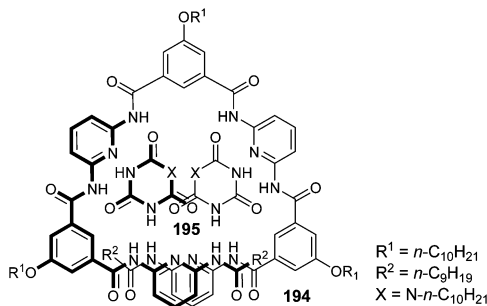


Foldamer **193** contains a linear pyridine–pyridazine–pyridine segment at the center,¹⁷⁸ which forces the two attached quinoline helix segments to orient on the same side and substantially enlarges the diameter of the cavity at the center.⁸⁶ This large helix entraps a L-(+)- or D-(–)-tartaric acid in CDCl₃ and DMSO-*d*₆ (9:1) with K_{assoc} being 5300 M⁻¹. Remarkably, both ¹H NMR and X-ray analysis showed that the

M and P helix selectively entrap L- and D-tartaric acid, respectively.

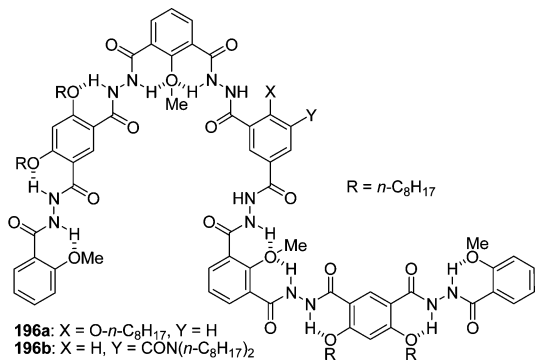


Conformationally flexible aromatic amide oligomers can also serve as receptors.¹⁵⁷ Lehn and co-workers reported that 7-mer oligomer 194 folded into a helical structure to complex cyanurate 195 in chloroform to form a 1:2 complex through six intermolecular DAD/ADA hydrogen bonds,¹⁷⁹ a binding motif developed by Hamilton and co-workers.¹⁸⁰ The 1:2 complex can also form other conformers, which depend on the rotation of the central aryl-CO bonds.



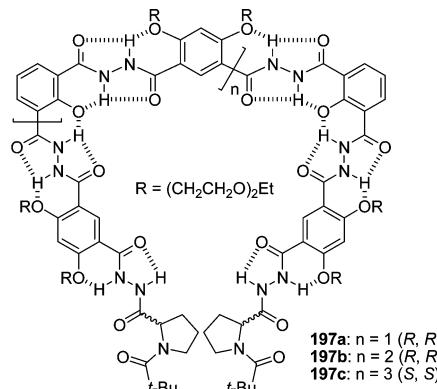
12.2. Hydrazide Foldamer Receptors

Li and co-workers reported that hydrazide foldamers 95a–c complexed saccharides 172–174 in chloroform by cooperative intermolecular C=O···H–O hydrogen bonding.^{24a} The diameter of these folded or helical backbones is ca. 1 nm, which is significantly larger than that of the aromatic amide series (45 and 52). The largest K_{assoc} of $6.9 \times 10^6 \text{ M}^{-1}$ was determined for complex 95c-174, which is substantially higher than that of complexes 95c-172 and 95c-173. To investigate the effect of the intramolecular hydrogen-bonding chain on binding, Li and co-workers also prepared 7-mer 196a and 196b, whose central benzene units form one or no hydrogen bond.¹⁸¹ As expected, their binding capacity for saccharides 172 and 173 is remarkably reduced.



Introducing two chiral proline units to the ends induced the helical backbones of foldamers 197a–c to produce helicity bias.^{32c} The new chiral receptors complexed enantiomers 173a and 173b in chloroform to form both diastereomeric and

enantiomeric complexes. The diastereomeric complexes exhibited varying binding stabilities, and the highest difference (144-fold) was observed between complexes 197b-173b and 197b-173a.



12.3. Macrocyclic Receptors

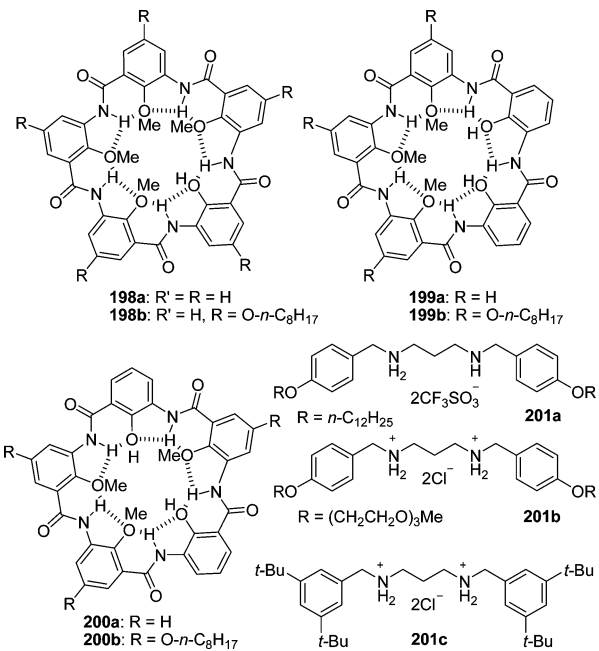
Aromatic amide-based macrocycles can bind guests, such as metal cations and chloride anions, via electrostatic interaction or hydrogen bonding.^{159,160} They can be further modified from inside or outside for achieving special binding, for example, for cholate anion.¹⁶¹ Hydrogen-bonded 6-mer macrocycles 120a–d have a well-defined internal cavity,⁴¹ which selectively complexes quanidinium ion in the presence of alkali cations or ammonium.^{182a} Macrocycle 120d can be inserted into lipid membranes to stack into tubular aggregates for transmembrane conductance.^{182b} Urea macrocycles 150a and 150b have been found to bind K⁺ more strongly than Na⁺ or Li⁺¹⁵¹ whereas quinoline macrocycle 142 is able to complex two *p*-toluenesulfonic acid molecules in chloroform, and the two binding events exhibit a positive allosteric effect.^{40a}

Zeng and co-workers prepared analogues of pentagon 146 by protecting the phenolic hydroxyl groups as benzyl ethers followed by a stepwise elongation. Subsequent debenzylation generated macrocycles 198–200 that bear one or two hydroxyl groups.^{45b} These macrocycles exhibit selective and differential binding affinity for alkali cations, and more ionizable hydroxyl groups enhance the binding. Separation of the two interior phenolic hydroxyl groups with one methoxyl group significantly alters the binding profile toward all five alkaline cations.

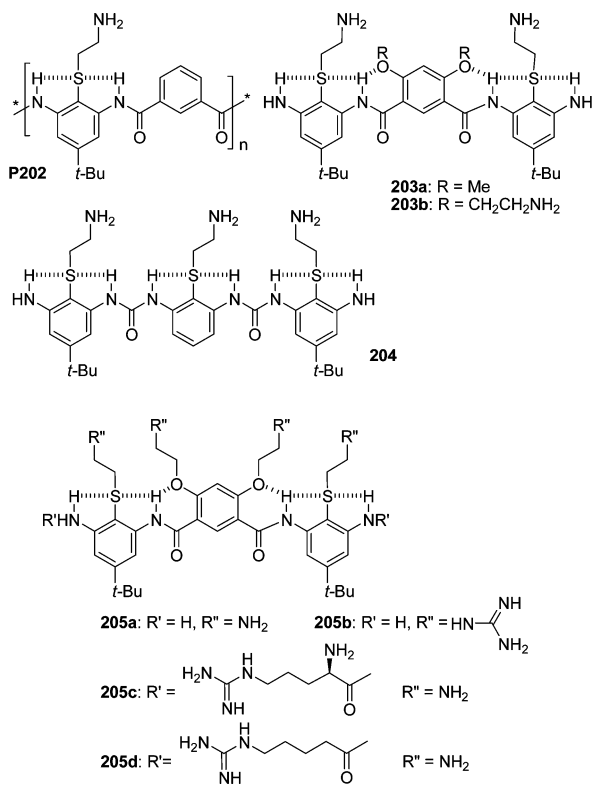
Li and co-workers reported that two-layered macrocycles 163a–c complexed both aliphatic ammoniums and diammoniums 201a–c in chloroform.^{166b} The linear diammoniums formed unique pseudo[3]rotaxane by threading through the two cyclophane units of the receptors. Li and co-workers also found that macrocycles 137a and 137b stacked with C₆₀ and C₇₀,⁴³ and K_{assoc} values of the corresponding 1:1 complexes 137a-C₆₀, 137a-C₇₀, 137b-C₆₀, and 137b-C₇₀ in chloroform were determined to be 5.9×10^4 , 9.1×10^4 , 2.5×10^4 , and $4.1 \times 10^4 \text{ M}^{-1}$, respectively.

12.4. Biological Functions

Hydrogen-bonded linear secondary structures based on aromatic amide and urea backbones have proven to be useful for the design of biologically active molecules.^{5,55,183–186} The general consideration is to utilize the well-defined backbones to produce special binding domains or to locate additional multiple-binding sites in a required space. DeGrado's group pioneered the application of aromatic amide foldamers as antimicrobial agents.⁵⁵ Facially amphiphilic AB polymer P202



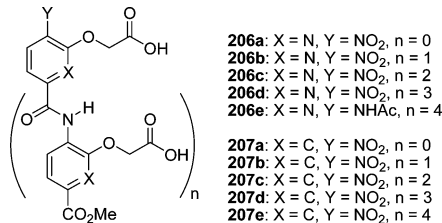
is the first example that was designed to mimic the structures and biological function of antimicrobial peptides magainins and cecropins.^{184a} This polymer and short three-ring analogues exhibit reasonable antimicrobial activity.^{184b,c} Trimmers **203a** and **203b** and **204** display improved antimicrobial potency presumably due to decreased flexibility of the backbones induced by the RO···H–N hydrogen bonding,^{34,184d–f} whereas **205a–d** inhibit the ability of low-molecular-weight heparins to activate antithrombin and, in this way, to affect the biological function of heparins.¹⁸⁵



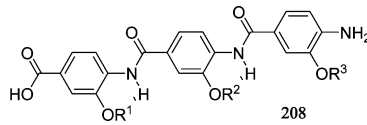
Hamilton and co-workers designed a variety of extended structures as α -helix mimetics for inhibiting protein–protein

interactions.¹⁸³ Compounds **19a–f** are the first examples of such artificial secondary structures, which were designed as antagonists of the Bak BH3/Bcl-x_L complex.²⁸ Compounds **19b**, **19d**, and **19e** have been found to have a low micromolar affinity for Bcl-x_L and thus to inhibit its interaction with Bak. The analogues of four pyridyl subunits exhibit a slightly lower affinity for Bcl-x_L. Benzoylurea oligomers **36a–d** were also developed as α -helix mimetics,¹²⁴ which could also disrupt the Bcl-x_L/Bak interaction.

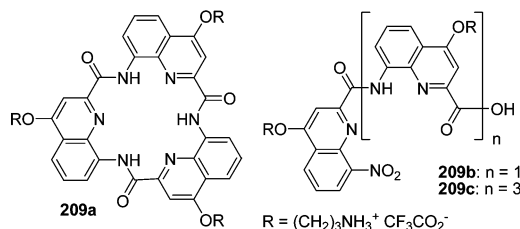
Hamilton and co-workers also prepared shorter dimers **206a–e** and **207a–e**.¹⁸⁷ The backbone of the **207** series, originally reported by Ahn, Wilson, and co-workers,¹²⁰ has a great conformational flexibility about the (aryl)C–C(=O) bond. Compounds **206a–e** can provide a complementary surface to interact with the α -helical domain on islet amyloid polypeptide and thus to accelerate its aggregation under lipid-free conditions. Under lipid-catalyzed conditions, they can retard the formation of amyloid deposits. Compounds **207a–e** follow the same general trend. However, **206a–e** shows a slight, but consistently higher effect, presumably due to a reduced entropic penalty upon binding as a result of the increased rigidity of the pyridylamide scaffold.



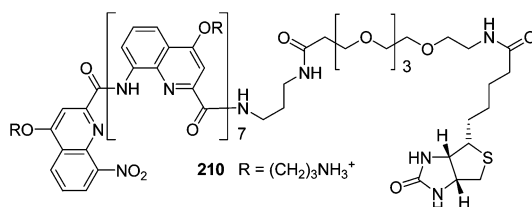
Boger and co-workers utilized the scaffold of trimers **19** to build a α -helix mimetic library of compounds **208** by attaching varying side-chains.¹⁸⁸ The library, comprising 400 mixtures of 20 compounds, was screened against the MDM2/p53 and HDM2/p53 protein–protein interaction, which resulted in a selection of a template that features a non-natural aryl monomer as the central unit and a natural amino acid at the two ends. Wilson and co-workers found that this type of trimer could also act as a potent inhibitor of the p53–hDM2 protein–protein interaction.¹⁸⁹ These results appear to show that this type of mimetic structure is generally effective against α -helix-mediated protein–protein interaction.¹⁸⁶



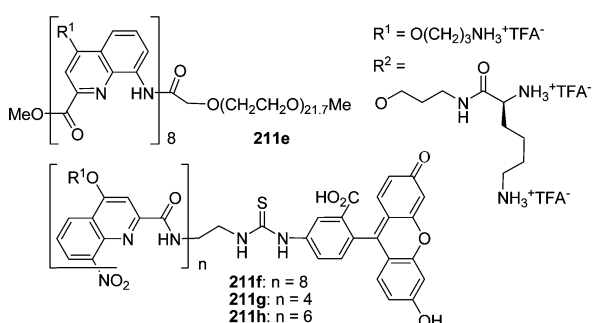
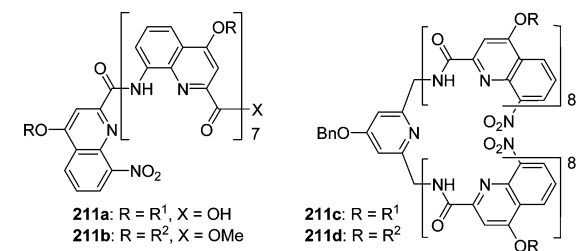
The development of ligands that bind to G-quadruplex sequences has received considerable interest due to their potential application as anticancer agents. Balasubramanian, Huc, and co-workers reported that cationic trimeric macrocycle **209a** and tetrameric helix **209c** recognized quadruplex DNA,¹⁹⁰ while acyclic dimer **209b** was a poor quadruplex ligand. They proposed that **209a** recognized G-quadruplex via hydrophobic interactions with the terminal G-tetrad, while **209c** might interact with loops rather than primarily via the G-tetrad due to its three-dimensional helical structure. Ha and co-workers further studied the effect of **209a** on the structural dynamics of human telomeric DNA.¹⁹¹ This macrocycle was found to bind extremely tightly to an unfolded telomeric strand and to promote G-quadruplex folding without preventing the intrinsic intramolecular dynamics of the telomeric DNA.



To investigate the interactions of longer foldamer sequences with DNA, Huc and co-workers further prepared compound **210** by attaching a biotin to an 8-mer cationic quinoline helix of over three turns.³³ By using SELEX method, they have identified DNA aptamers that have a strong affinity for **210** and established a specific interaction between multturn quinoline helices and G-quadruplex DNA. They also found that the interaction could be made diastereoselective, with one one-handed helix being bound to one quadruplex sequence selectively.



The biological activity of water-soluble 8-mer oligomers **211a–f** were also assessed.¹⁹² It was found that the toxicity of these oligomers is comparable to that of other polycations, such as polylysine, PEI, chitosan, and PAMAM dendrimers, which have been frequently used in applications such as DNA transfection, but they are all resistant to degradation by four proteases tested. Oligomer **211d** displayed a modest activity of transfection of HeLa cells, whereas **211f** showed an ability to cross HeLa cells. Cellular internalization of **211f–h** was also investigated, which revealed that they were all biocompatible, longer oligomers achieved greater cellular translocation, and **211f** was a remarkable vehicle for all three studied cell lines.¹⁹³



13. SELF-ASSEMBLY

13.1. Double, Triple, and Quadruple Helices

Aromatic foldamers tend to undergo nonspecific stacking due to their large size and coplanarity.¹⁹⁴ *N*-heterocyclic amide helices do not need additional substituents as intramolecular hydrogen-bonding donors. Their intermolecular stacking may thus be stronger than that of benzamide-derived foldamers. Lehn, Huc, and co-workers found that these type of helices may further intertwine to form double helices, which allow for more extensive cross-strand stacking. For example, 7-mer oligomer **65d** forms a double helix in the solid state when it recrystallizes from a less-polar mixture solvent (Figure 29).²¹ ¹H NMR of

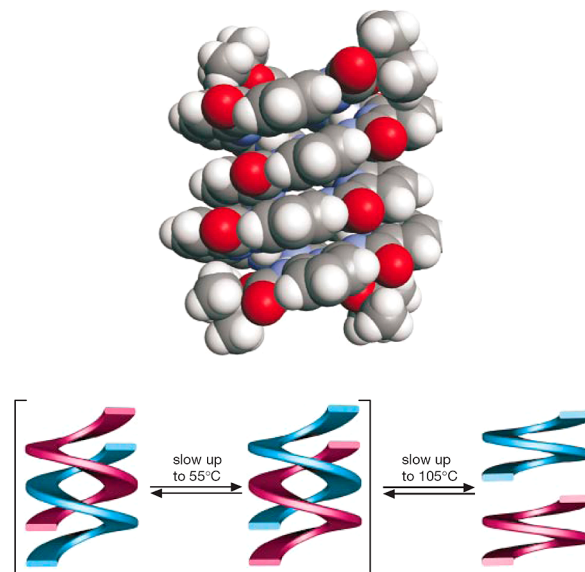
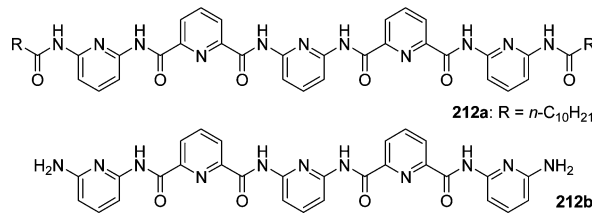


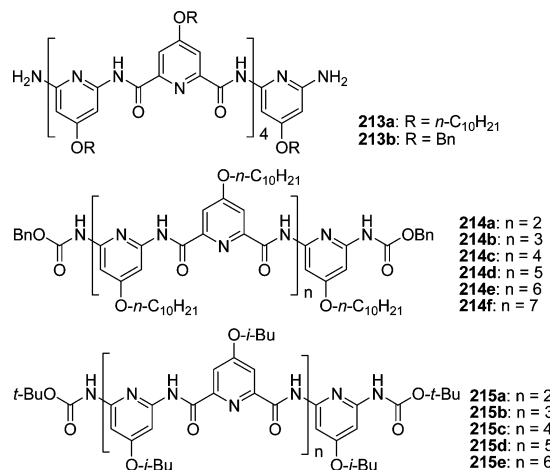
Figure 29. (Top) Double helix of **65d**. (Bottom) Schematic representation of the interconversion between two identical forms of dissymmetrical double helices of **65b** and their dissociation into two single helices. Reproduced with permission from ref 21. Copyright 2000 Nature Publishing Group.

65b in $\text{C}_2\text{D}_2\text{Cl}_4$ revealed that its P- and M-double helices exchange slowly below 55 °C and decompose to single helices above 105 °C (Figure 29). Shorter pentamer **212a** produces a less stable double helix in solution, with the $K_{\text{dim}} = 35 \text{ M}^{-1}$ at -72 °C in CD_2Cl_2 , whereas less-soluble **212b** gives rise to both P- and M-double helices in the solid state.^{97a} It was also found that electron donors at position-4 of the pyridine rings dramatically enhance dimerization, by up to 3 orders of magnitude.



The effect of discrete structural factors on the hybridization of this type of oligomer has been investigated.^{65,195,196} It was revealed that 7-mer oligomers **188a,b**, which bear hydroxyl or benzyloxy groups at position 4 of the pyridine rings of the 2,6-dicarboxamides, do not form double helices in the solid state,⁶⁵ whereas 9-mer oligomer **213a** exists as both single and double

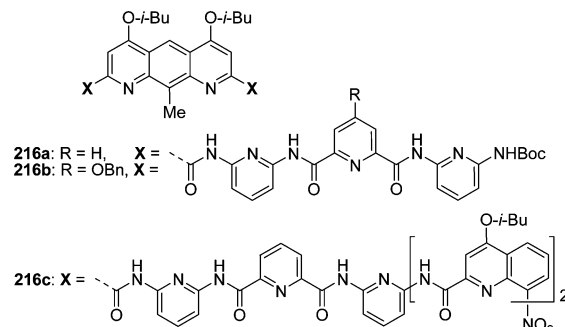
helix in chloroform. The two species exchange slowly on the ^1H NMR time scale, and the K_{dim} was determined to be $6 \times 10^4 \text{ M}^{-1}$.¹⁹⁵ It was also found that interactions between aliphatic chains enhance dimerization.^{196a} Oligomer **213b** exists only as double helix in both solution and the solid state. Its K_{dim} is at least 100 times higher than that of **213a** as a result of interstrand interactions between its phenyl rings in the side-chains.¹⁹⁵ ^1H NMR of oligomers **214a–f** in CDCl_3 showed that their dimerization increased with oligomer length up to a certain point, and then decreased down, to undetectable levels for the longest strand.^{196b} This result has been attributed to two competing factors: the enthalpic gain of dimerization decreases as strand length increases, while the entropic loss of hybridization decreases as strand length increases. In contrast, for oligomers **215a–e** that bear isobutoxyl groups on the pyridine rings, increasing strand length continually enhances their propensity of forming double-helical structures.^{196d} Compared to terminal flat Cbz groups, their bulky Boc terminal groups result in a 1–2 orders of magnitude enhancement of the K_{dim} as a result of facilitated spring-like extension of single helices.



Oligomer **166a** and its dioxide **167a** also form double helical dimers in chloroform with $K_{\text{dim}} = 30$ and 125 M^{-1} , respectively.^{97c} Their cross-hybrid, with K_{dim} of 1140 M^{-1} , is considerably more stable than either of them. The K_{dim} of shorter oligomers **166b** and **167b** is not available due to poor solubility. However, cocrystals of the two strands were obtained from their 1:1 mixture. The crystal structure also showed the formation of a heterodimeric helix. The increased stability of heterodimers presumably resulted from electrostatic interactions between amide, pyridine, and pyridine N-oxide moieties. This tendency of cross-hybridization is in contrast with other experiments where self-recognition prevails over heterologous recognition.¹⁹⁷ Oligomer **188a** has been deprotonated with sodium hydride in DMF. Treatment of the solution with $\text{Cu}(\text{OAc})_2$ afforded crystals of the corresponding Cu(II) complex.^{196e} X-ray analysis revealed that a neutral, C_2 symmetrical, head-to-tail heterotopic double helix (**188a**·Cu)₂ was formed. Shorter 5-mer analogues also formed similar double-helical structures. In these complexes, the geometrical requirement of the coordination of pyridine dicarboxamides dominates over that of bis(carbonylamino)pyridines.

By replacing the central pyridine ring with a 1,8-diazaanthracene ring within the pyridine strands, Huc and co-workers prepared 7-mer oligomers **216a** and **216b**, whose helical structures have a 4.7 Å enlargement parallel to the long

1,8-diazaanthracene axis.⁸⁵ This structural change results in a remarkable stabilization of the double-helical hybrids (factors of $>10^7$), because the augmented surface enhances intermolecular $\pi-\pi$ stacking and the enlarged diameter leads to a decrease of the tilt angle of the helical strand, which in turn results in smaller dihedral angles at the aryl–amide linkages. 11-Mer oligomer **216c** was originally designed to generate a helically folded conformation with an internal cavity larger than that of **189b**.^{97b} However, X-ray analysis revealed that it underwent hybridization to produce a unique helical duplex in which the two strands filled each other's internal cavity.



Jiang, Huc, and co-workers further synthesized 4- and 8-mer quinoline foldamers **217a** and **217b**.^{26a} Crystals of **217a** revealed an unprecedented quadruple helix, in which two molecules stacked in a head-to-tail dimer and two such dimers were further entwined with offset helical axes. The structure showed two pairs of grooves within and between the head-to-tail dimers, respectively (Figure 30). The K_{dim} of the dimer in

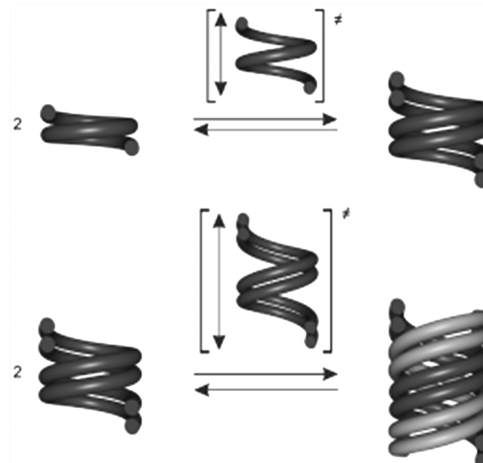
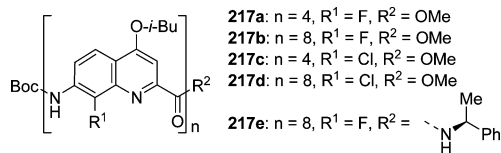


Figure 30. Schematic representation of the hybridization of the single helix of **217a** to a double helix (top) and of a double helix to a quadruple helix (bottom), both through springlike extension. Reproduced with permission from ref 26a. Copyright 2008 Wiley–VCH.

chloroform was determined to be 66 M^{-1} . Oligomer **217b** formed an antiparallel double helix in the solid state, and the K_{dim} 's in pyridine and chloroform were estimated to be 3.6×10^5 and $8.5 \times 10^5 \text{ M}^{-1}$, respectively. A molecular dynamics study revealed that these helices showed slippage of strands to some extent and the double-helical structure acted as a basic block for the formation of the quadruple helix.^{26b} 8-Chloroquinoline oligoamides **217c** and **217d** were also prepared.^{26c} The crystal structure of **217d** revealed an

antiparallel double helix, which was almost superimposable to that of **217b**. The double helix was too stable to be evaluated quantitatively by ^1H NMR. In chloroform, **217b** and **217d** formed cross-hybrids with a proportion of 70%, which was >50% of what was expected for a statistical distribution of the various duplexes. This result has been ascribed to the steric complementarity between fluorine and chlorine atoms in the internal cavity of the double helix. A CD study showed that the double helix formed by **217e** had a preferred handedness, which was tentatively assigned to P helicity.



Huc and co-workers also prepared 4-mer oligomers **218**, which formed three different structures, that is, single helix, parallel triple helix, and antiparallel triple helix, in the solid state (Figure 31). The parallel triplex had a perfect C_3 symmetry axis

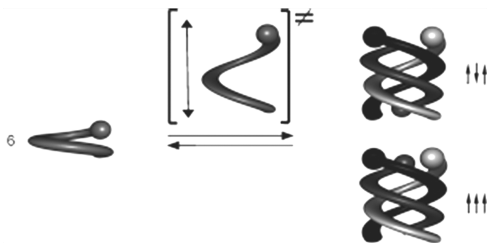
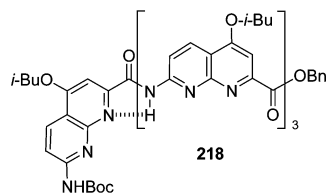
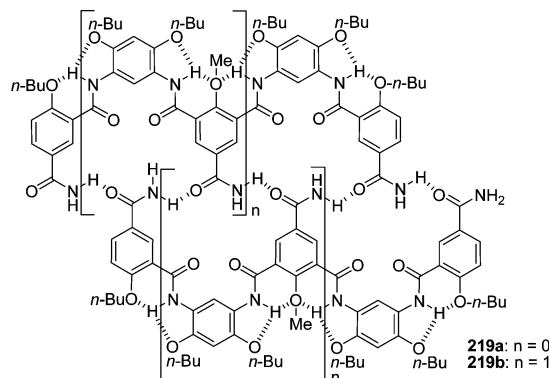


Figure 31. Hybridization of three single-helical strands of **218** into a triple helix through a springlike extension. Triple helices may adopt parallel (bottom right) or antiparallel (top right) configurations. The balls at the end of each strand discriminate the strand ends and symbolize the strand polarity. Reproduced with permission from ref 98. Copyright 2010 Wiley–VCH.

coinciding with the helix axis. In the second one, one strand was oriented antiparallel to the two others, and the helix had no symmetry element. The two triplex structures were almost superimposable except for the one strand that had inverted its orientation. In solution, **218** prevails as a mixture of different triplexes, but no duplex is formed. ^1H NMR diluting experiments provided a minimal estimate of the K_{trim} as $>10^8 \text{ M}^{-2}$ in CDCl_3 or CD_3CN .

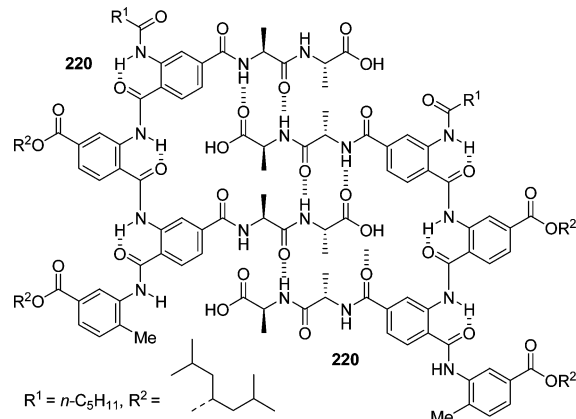


Li and co-workers introduced amide units to the para-position of the ether groups of the benzamide rings of oligomers **15a** and **15b** to generate **219a** and **219b**.⁹⁶ Crystal structures of model compounds revealed that this type of preorganized molecule formed planar homoduplexes stabilized by cooperative intermolecular hydrogen bonds. The K_{dim} 's of dimers **219a**–**219a** and **219b**–**219b** in chloroform were determined to be 3.0×10^3 and $2.3 \times 10^5 \text{ M}^{-1}$, respectively, indicating a positive cooperativity for the binding affair. Other amide units, such as (trifluoro)acetamido, formamido, and 3-



alkylureido, were also used as binding sites. The formamido and ureido groups were found to be more efficient than others in stabilizing the dimeric structures.¹⁹⁸

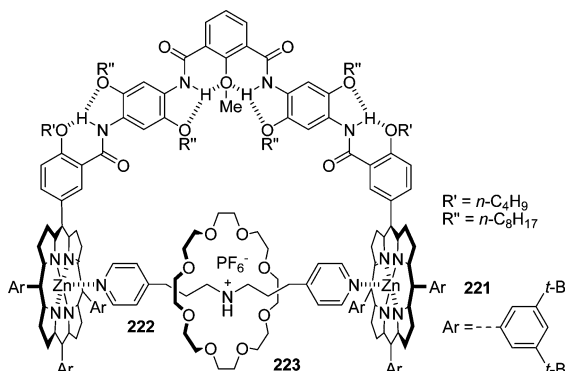
Hamuro and Hamilton functionalized the backbone of oligoanthranilamides **11** to afford **220**, which bears two parallel positioned dipeptide chains on one side of the backbone.¹⁹⁹ These parallel positioned peptide chains were found to dimerize through six intermolecular hydrogen bonds to form a sheetlike aggregate, with $K_{\text{dim}} = 10 \text{ M}^{-1}$ at 25°C and 330 M^{-1} at -20°C in chloroform. A similar molecule that bears two tripeptide chains did not dimerize, most likely due to intramolecular hydrogen bonding between the two peptide strands.



13.2. [2]Catenanes and [2]Rotaxanes

Li and co-workers reported that tweezer-styled compound **221** complexed bipyridine **222** with a high K_{assoc} of $5.7 \times 10^6 \text{ M}^{-1}$ in chloroform and acetonitrile (4:1, v/v).³¹ Because the ammonium unit in **222** can thread through the cavity of 24-crown-8 **223**, the 1:1:1 mixture of the three components (3 mM) in the same mixture solvent produced a dynamic [2]catenane in 55% yield. The exchange between the free and threaded crown ether was slow on the ^1H NMR time scale, which reflected the stability of the dynamic [2]catenane. When the temperature was reduced to -13°C and 2 equiv of **223** was present, the dynamic [2]catenane was formed quantitatively, which was evidenced by ^1H NMR.

Zhao and co-workers assembled bistable [2]rotaxanes **224a** and **224b**, whose threads contain an aromatic amide foldamer segment.³⁹ Model studies showed that the foldamer segments could provide an energy barrier for the tetracationic CBPQT^{4+} ring to thread over at a rate of 10^{-3} – 10^{-7} s^{-1} , depending on the polarity of media. They were thus designed to modulate the switching of CBPQT^{4+} between the TTF and 1,5-dioxynaph-



thalene (DNP) sites in the [2]rotaxanes. Because TTF is more electron-rich than DNP, in a two-state model, the equilibrium shifts toward CBPQT⁴⁺ encircling TTF to form ground-state co-conformation (GSCC) (A, Figure 32), rather than toward

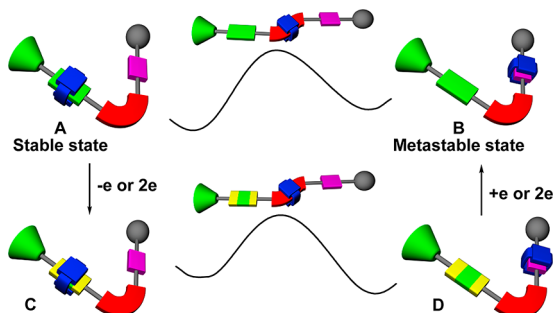
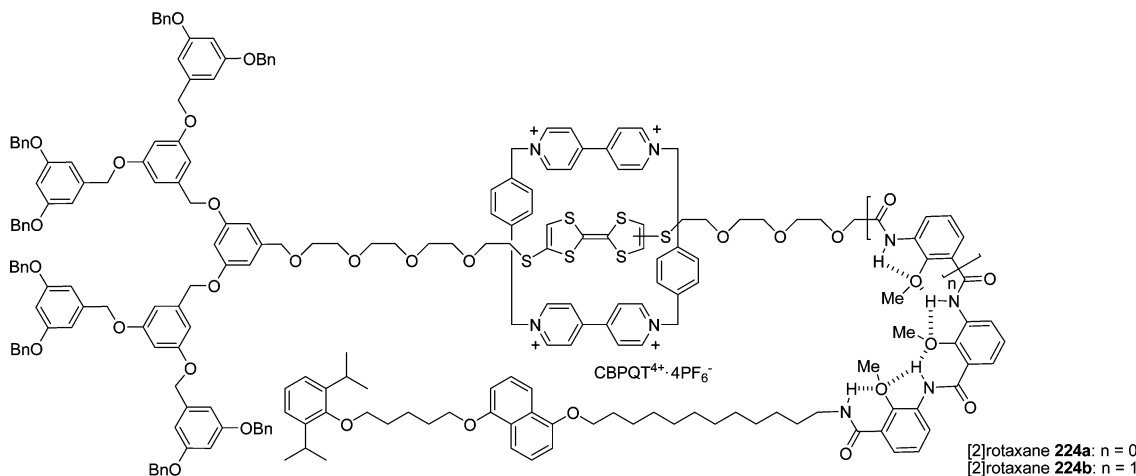


Figure 32. Schematic representation depicting the foldamer-tuned switching of CBPQT⁴⁺ between the TTF and DNP sites in bistable [2]rotaxanes 224a and 224b, with the TTF unit being neutral or oxidized to TTF⁺ or TTF²⁺.³⁹

CBPQT⁴⁺ encircling DNP to form the less stable metastable-state co-conformation (MSCC) (B, Figure 32). Oxidizing TTF to TTF⁺ or TTF²⁺ forces CBPQT⁴⁺ to shift to encircle DNP (A → B → D, Figure 32). Upon the TTF cations being reduced to the neutral one, CBPQT⁴⁺ shifts back to the TTF site again. The half-lives of the shuttling of CBPQT⁴⁺ of 224a and 224b from MSCC to GSCC (B → A, Figure 32) were determined to be 66 and 930 s in acetonitrile. In chloroform, this value was 19.5 h for 224a and much longer for 224, which exhibited no perceptible B → A shifting after 72 h.



Jiang, Huc, and co-workers reported the binding behavior of 9-, 11-, and 13-mer foldamers 225a–c toward linear molecules 226a and 226b.²⁰⁰ The foldamers themselves formed double helices. Upon adding a guest, the double helices decomposed into single helices to complex one guest molecule to generate a structurally new helix-derived [2]rotaxane. For the complex of 225a and 226a in chloroform, the threaded structure of which was confirmed by the X-ray analysis (Figure 33), the helix

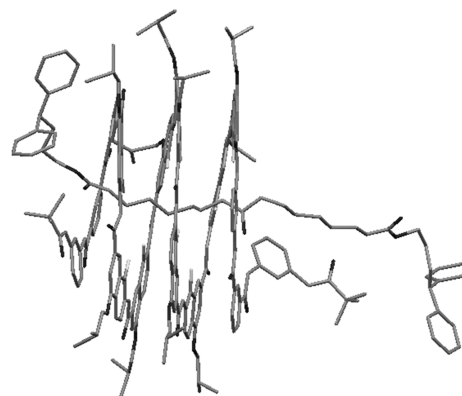


Figure 33. X-ray structure of the threaded complex between compounds 225c and 226a.²⁰⁰ The hydrogen atoms are omitted for clarity.

switched between the two stations of aliphatic chains. For 226b, its dialkylamino segment could serve as another station for the helix to encircle favorably over the station of the aliphatic chain. Protonation of the amino group caused the helix to shift to the aliphatic station. Generally, the rates of the shuttling processes were much faster than the disassembly of the helices.

Double helices can also be used to construct rotaxanes. For this purpose, Huc, Jiang, and co-workers prepared 7-mer oligomer 227,²⁰¹ which formed a stable double helix and complexed linear guests 228a and 228b to generate new rotaxanes. Interestingly, the double helix was found to slide along each other within the double-helical duplex and to shrink or expand so that the length of the duplex could match with the length of the guest (Figure 34).

13.3. Organogels, Vesicles, and Liquid Crystals

Discotic molecules represent a class of structurally unique gelators, which consist of a rigid aromatic core and suitably long

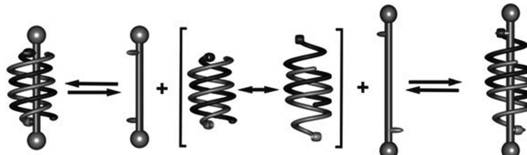
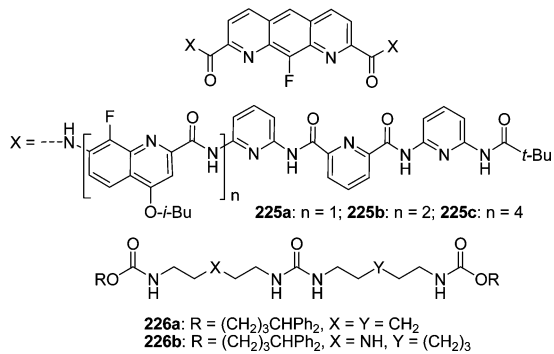
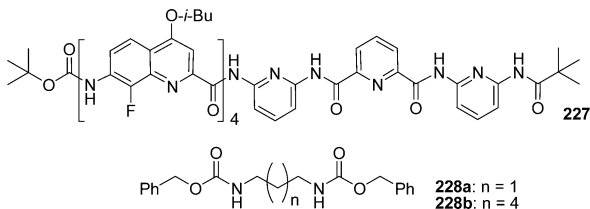
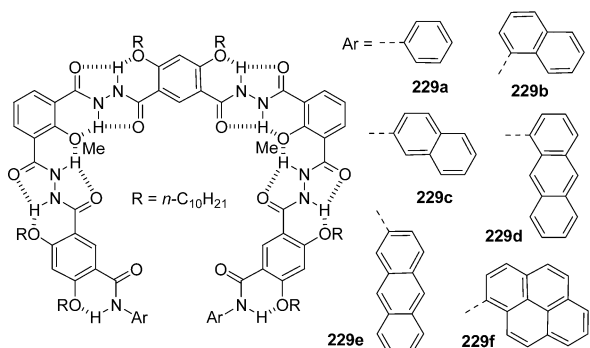


Figure 34. Screw motion of the two strands of the molecular duplex of 227 (middle) and the trapping of screwed (left) and unscrewed (right) double helices upon binding to short guest 228a and long rodlike guests 228b. Reproduced with permission from ref 201. Copyright 2011 Wiley–VCH.

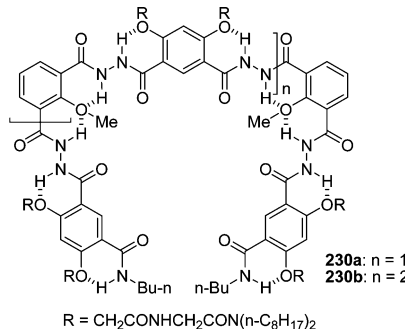


aliphatic chains.^{152b,202,203} Li and co-workers reported that hydrazide foldamers 229a–f gelated both apolar and polar solvents.^{35c} Gelation for apolar solvents was enhanced by addition of 173a or 173b, because they were entrapped in the cavity of the foldamers to promote their stacking.^{35a} CD studies showed that entrapment of the saccharides also caused dynamic helicity induction in organogels, which was time-dependent and exhibited a unique “sergeants and soldiers” effect.²⁰⁴

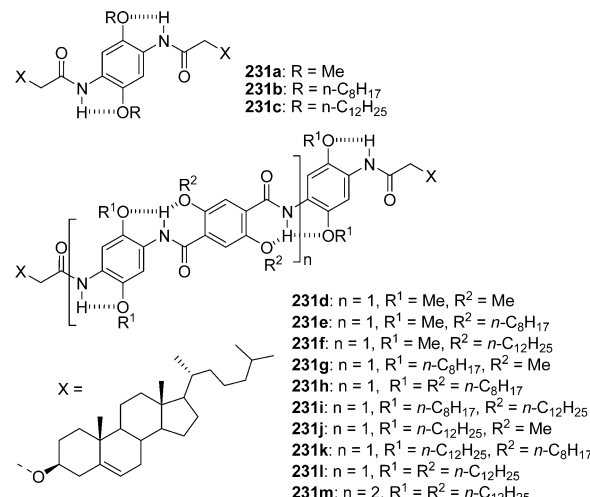


The backbone of hydrazide foldamers has been modified with amphiphilic amide chains.^{35d,205} The new folded molecules 230a and 230b gelated organic solvents, like hydrocarbons, and/or self-assembled into vesicles in methanol driven by π – π stacking of the backbones, intermolecular hydrogen bonding of the amide units in the side-chains, and van der Waals interactions of the aliphatic chains.^{35d} Notably, the amphiphilic side-chain and its analogues with different

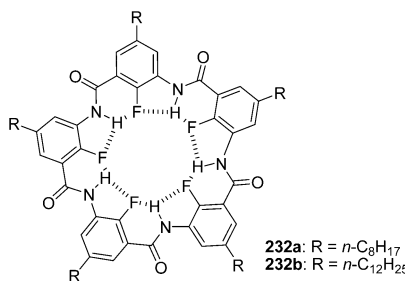
peripheral aliphatic groups were found to strongly promote aromatic backbones to form vesicles.^{38a,166c,206}



To develop new dimesogenic liquid crystals, Li and co-workers also prepared cholesterol-appended oligomers 231a–m.²⁰⁷ It was revealed that, at low temperature, the more and longer alkoxy chains facilitated the formation of the liquid crystal phases and 231j displayed a blue–red color change during both the heating and cooling cycles.



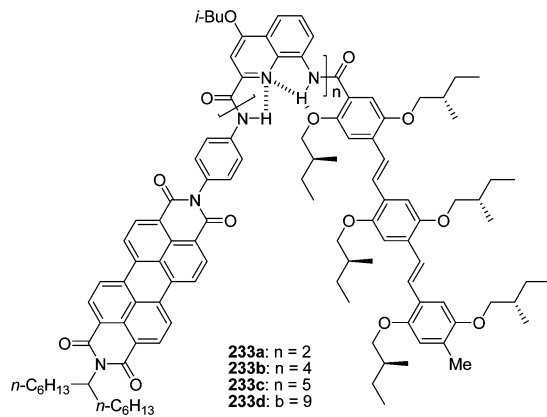
Zeng and co-workers reported that pentagons 232a and 232b gelated organic solvents like *n*-hexane, ether, ethyl acetate, and dioxane.²⁰⁸ TEM and XRD studies suggested that their gelling networks contained three-dimensional entangled nanofibers formed from intercolumnar association of one-dimensional aggregates, which were stabilized by interplanar hydrogen bonding and aromatic stacking.



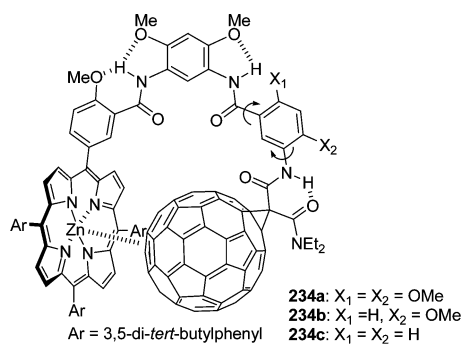
14. TUNING INTRAMOLECULAR DONOR–ACCEPTOR INTERACTIONS

The preorganized backbones of hydrogen-bonded aromatic amide foldamers can also be used to fix the distances and

orientations between the chromophores and hence to tune their interactions. Schenning, Huc, and co-workers demonstrated this potential by synthesizing oligomers 233a–d,³⁶ in which a quinoline foldamer segment was appended with an oligo(*p*-phenylene vinylene) (electron donor) unit and a perylene bisimide (electron acceptor) unit. Excitation of either of the chromophores resulted in nearly quantitative quenching of the fluorescence, indicating that fast charge separation occurred between them. The rate for this intramolecular charge separation was high for all the molecules, but the related attenuation factor was very low, for which a uniform description by the current theory did not hold. The result reflects the unique property of folded aromatic amide backbones in mediating the intramolecular charge separation.



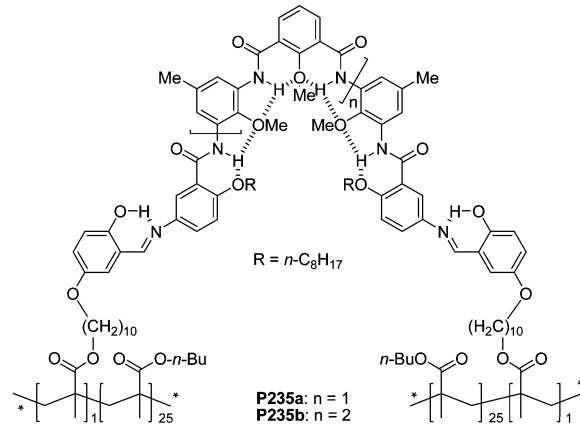
Li, Fu, and co-workers synthesized foldamer-bridged porphyrin-C₆₀ dyads 234a–c.³⁷ Molecular dynamic simulation indicated that the fully hydrogen-bonded foldamer bridge of 234a forced the appended porphyrin and C₆₀ units to contact in a face-to-face manner. ¹H NMR, UV-vis, and fluorescent studies in chloroform showed that such a structural matching remarkably facilitated the intramolecular energy and electron transfer and charge separation between the two chromophores and also retarded the recombination of their charge-separated state. Thus, compared to that of a porphyrin control, the molar absorption coefficient of the Soret band of the porphyrin unit of 234a in chloroform was decreased by 44%. In contrast, this value was only 16% for 234b and 2% for 234c.



15. TUNING DYNAMIC PROPERTY OF COPOLYMERS

Li, Guan, and co-workers synthesized methacrylate copolymers P235a and P235b by introducing a 3- or 5-mer foldamer segment as a cross-link.^{38b} Films of identical thickness and size were prepared from these copolymers. Their dynamic mechanical and creep/stress relaxation (recovery) properties

were tested and compared with those of control copolymers that contained intramolecular hydrogen-bonding-free cross-link of the same backbone. The results showed that the hydrogen-bonded foldamer cross-links could substantially improve the mechanical properties of the copolymers through reversible folding and unfolding as a result of dissipative cleavage and recovery of their intramolecular hydrogen bonding.



16. CONCLUSIONS AND PROSPECTS

This review has surveyed the study of aromatic amide-based foldamers that are stabilized by intramolecular hydrogen bonding. Since the first report of this family of foldamers in 1994, the major effort in this field has been devoted to the synthesis and structural characterization of new foldamers. Considerable structural complexity has been realized, which may compare with that of natural proteins. To date, only three aromatic rings, that is, benzene, pyridine, and quinoline, have been extensively utilized as linkers of the amide units to construct the backbones. Many other aromatic rings, mainly large conjugated heterocycles, have just received limited applications. Their potential should be exploited more vigorously in the future. Further design and synthesis of new versatile aromatic residues are also of importance, which will not only scale up the library of this family of foldamers but also provide a more solid and diverse structural base for achieving required properties or functions. In designing new sequences, a combination of different kinds of residual monomers is expected to receive more attention because this will help to construct compact backbones with a specific shape or conformation. In this context, sequences with alternating aromatic and aliphatic residues are particularly attractive because of their three-dimensional structural feature. Advance along this direction may lead to the creation of more complicated artificial supersecondary or even tertiary structures.

The past decade has already witnessed important advances in the study of the functions or applications of aromatic amide foldamers and their derivatives. In particular, they have been demonstrated to be robust in promoting the formation of macrocyclic architectures via preorganizing intermediates or precursors to favor cyclization. The macrocycles prepared in this way possess very rigid shape and planarity, and many of them have a cavity of defined size for hosting different guests. This capacity of molecular recognition may find further applications in transmembrane transport. Folded structures of similar backbones may also be envisioned for this potential. However, macrocyclic structures may be more attractive

because they are easier to access via the one-pot approach and also generally exhibit a relatively high stacking tendency.

It has been established that aromatic amide foldamers can form cavities with diameter ranging from several angstroms to 2–3 nm. However, for foldamers with large cavities, their limited length makes them impossible to produce a relatively deep tubular structure. One future challenge is the development of highly efficient synthetic methodology to prepare even longer oligomers or polymers that can fold into such tubular structures. Such single (macro)molecular aromatic amide tubes are structurally fascinating and may exhibit interesting properties such as molecular recognition, catalysis, and separation, as well as transport and delivery. Multiple folded and paired segments may also be introduced into polymeric structures to induce the backbones to fold into more complicated but defined superstructures, as proteins do, which may exhibit more complex properties than simple foldamers prepared to date.

The discrete functions exhibited by aromatic amide foldamers are, to a considerable extent, based on their rigidified, predictable conformations. The backbones themselves are rigid, stack strongly, and are insoluble in aqueous or organic media. Thus, their discrete functions are usually generated by further modification of the backbones. For example, their ability of targeting biomacromolecules has been realized by introducing multiple hydrophobic or ionic groups as side-chains or parts of them to achieve cooperativity of binding or interaction. This strategy should work for other research purposes, particularly in materials design.²⁰⁹ For instance, by iteratively introducing electron donors and acceptors, intra- or intermolecular charge transfer may be realized in a tunable way. Another interesting property of aromatic amide foldamers is that they may reversibly unfold and fold upon breaking and recovering their intramolecular hydrogen bonding. This process reversibly consumes and releases energy and thus may be a useful motif for designing stimuli-responsive materials. Therefore, the next decade will witness new important advances for their applications.

AUTHOR INFORMATION

Corresponding Author

*E-mail: ztli@fudan.edu.cn.

Notes

The authors declare no competing financial interest.

Biographies



Dan-Wei Zhang is currently Associate Professor in the Department of Chemistry at Fudan University. She became a faculty member in the Department after she received her Ph.D. in Organic Chemistry under

the direction of Professor Shi-Hui Wu from Fudan University in 2000. She joined Professor Dan Yang's group as a Research Associate at the University of Hong Kong in 2001. Her research focuses on the development of various artificial secondary structures.



Xin Zhao was born in 1972 in Yunnan, China. He received his B.S. in 1994 from Beijing Normal University and his Ph.D. in 2003 from Shanghai Institute of Organic Chemistry (SIOC) under the direction of Professors Zhan-Ting Li and Xi-Kui Jiang. After postdoctoral research with Professor William von E. Doering at Harvard University and Professor Luping Yu at The University of Chicago, he returned to SIOC as Associate Professor in 2008. His research interest mainly focuses on self-assembly of conjugated systems and fabrication of well-defined micro/nanoscaled structures via supramolecular strategies.



Jun-Li Hou was born in 1978 and studied chemistry at Hubei University (1997–2001). He earned his Ph.D. at SIOC under the supervision of Professor Zhan-Ting Li (2001–2006). After two years' postdoctoral research with Professor Julius Rebek, Jr., at The Scripps Research Institute, he joined Fudan University, where he is currently Associate Professor in the Department of Chemistry. His research focuses on supramolecular systems for their biomimicking applications as transmembrane channels and biosensors.



Zhan-Ting Li was born in 1966 in Henan, China. He received his B.S. from Zhengzhou University in 1985 and his Ph.D. in Organic Chemistry under the supervision of Professor Qing-Yun Chen at SIOC in 1992. He did postdoctoral research with Professor Jan Becher at the University of South Denmark (1994–1995) and was a visiting scholar with Professor Steven C. Zimmerman at the University of Illinois at Urbana—Champaign (2000–2001). He had been Associate Professor (1996–2002) and Professor (2003–2010) at SIOC and, since 2010, Professor at the Department of Chemistry, Fudan University. His research is mainly concerned with hydrogen bonding-mediated biomimetic structures, molecular recognition and self-assembly, and conjugated and porous supramolecular structures.

ACKNOWLEDGMENTS

The authors thank National Natural Science Foundation of China (Nos. 20974118 and 21172042), Ministry of Science and Technology of China, Ministry of Education of China (IRT1117), Chinese Academy of Sciences, and Technology Commission of Shanghai Municipality for financial support. Z.-T.L. also thanks his graduates and collaborators, whose names are cited in the references, for their contributions.

LIST OF ABBREVIATIONS

2D	two-dimensional
ADA	acceptor–donor–acceptor
Bak	Bcl-2 homologous antagonist killer
Bcl-x _L	B-cell lymphoma-extra large
BH3	Bcl-2 homology 3
BINOL	1,1'-bi-2-naphthol
BOP	benzotriazol-1-yl-oxytris-(dimethylamino)-phosphonium
CBPQT	cyclobis(paraquat- <i>p</i> -phenylene)
Cbz	carboxybenzyl
CD	circular dichroism
CPK	Corey–Pauling–Koltun
DAD	donor–acceptor–donor
DCC	dicyclohexyl carbodiimide
DIPEA	<i>N,N</i> -diisopropylethylamine
DMAP	4-dimethylaminopyridine
DMF	<i>N,N</i> -dimethylformamide
DFT	density functional theory
FMOC	fluorenylmethyloxycarbonyl
GLP-1	glucagon-like peptide-1
HDM2	human double minute 2
HMBC	heteronuclear multiple-bond correlation spectroscopy
HSQC	heteronuclear single-quantum correlation spectroscopy
ICD	induced circular dichroism
MALDI-TOF	matrix-assisted laser desorption/ionization, time-of-flight
<i>m</i> -CPBA	<i>meta</i> -chloroperoxybenzoic acid
MDM2	murine double minute
NBS	<i>N</i> -bromosuccinimide
OPV	oligo(<i>p</i> -phenylenevinylene)
p53	protein 53
PAMAM	polyamidoamine
PEI	polyethyleneimine
SELEX	systematic evolution of ligands by exponential enrichment
TEM	transmission electron microscopy
TFA	trifluoroacetic acid
TTF	tetrathiafulvalene
XRD	X-ray diffraction

REFERENCES

- (a) Seebach, D.; Matthews, J. L. *Chem. Commun.* **1997**, 2015.
- (b) Seebach, D.; Beck, A. K.; Bierbaum, D. J. *Chem. Biodiversity* **2004**, *1*, 1111. (c) Seebach, D.; Gardiner, J. *Acc. Chem. Res.* **2008**, *41*, 1366.
- (2) (a) Gellman, S. H. *Acc. Chem. Res.* **1998**, *31*, 173. (b) Horne, W. S.; Gellman, S. H. *Acc. Chem. Res.* **2008**, *41*, 1399.
- (3) Cheng, R. P.; Gellman, S. H.; DeGrado, W. F. *Chem. Rev.* **2001**, *101*, 3219.
- (4) (a) Li, X.; Yang, D. *Chem. Commun.* **2006**, 3367. (b) Li, X.; Wu, Y.-D.; Yang, D. *Acc. Chem. Res.* **2008**, *41*, 1428.
- (5) Goodman, C. M.; Choi, S.; Shandler, S.; DeGrado, W. F. *Nat. Chem. Biol.* **2007**, *3*, 252.
- (6) Wu, Y.-D.; Han, W.; Wang, D.-P.; Gao, Y.; Zhao, Y.-W. *Acc. Chem. Res.* **2008**, *41*, 1418.
- (7) Guichard, G.; Huc, I. *Chem. Commun.* **2011**, *47*, 5933.
- (8) (a) Zhao, D.; Moore, J. S. *Org. Biomol. Chem.* **2003**, *1*, 3471. (b) Stone, M. T.; Heemstra, J. M.; Moore, J. S. *Acc. Chem. Res.* **2006**, *39*, 11.
- (9) Juwarker, H.; Suk, J.-m.; Jeong, K.-S. *Chem. Soc. Rev.* **2009**, *38*, 3316.
- (10) Hou, J.-L.; Jia, M.-X.; Jiang, X.-K.; Li, Z.-T.; Chen, G.-J. *J. Org. Chem.* **2004**, *69*, 6228.
- (11) Zhao, Y. *Curr. Opin. Colloid Interface Sci.* **2007**, *12*, 92.
- (12) Cuccia, L. A.; Lehn, J.-M.; Homo, J.-C.; Schmutz, M. *Angew. Chem., Int. Ed.* **2000**, *39*, 233.
- (13) Lokey, R. S.; Iverson, B. L. *Nature* **1995**, *375*, 303.
- (14) Li, A. D. Q.; Wang, W.; Wang, L.-Q. *Chem.–Eur. J.* **2003**, *9*, 4594.
- (15) Zhan, C.; Li, A. D. Q. *Curr. Org. Chem.* **2011**, *15*, 1314.
- (16) Zhao, X.; Jia, M.-X.; Jiang, X.-K.; Wu, L.-Z.; Li, Z.-T.; Chen, G.-J. *J. Org. Chem.* **2004**, *69*, 270.
- (17) Hill, D. J.; Mio, M. J.; Prince, R. B.; Hughes, T. S.; Moore, J. S. *Chem. Rev.* **2001**, *101*, 3893.
- (18) Hecht, S.; Huc, I., Eds. *Foldamers: Structure, Properties and Applications*; Wiley–VCH: Weinheim, Germany, 2007; p 431.
- (19) Hamuro, Y.; Geib, S. J.; Hamilton, A. D. *Angew. Chem., Int. Ed. Engl.* **1994**, *33*, 446.
- (20) Hamuro, Y.; Geib, S. J.; Hamilton, A. D. *J. Am. Chem. Soc.* **1996**, *118*, 7529.
- (21) Berl, V.; Huc, I.; Khouri, R. G.; Krische, M. J.; Lehn, J.-M. *Nature* **2000**, *407*, 720.
- (22) (a) Jiang, H.; Léger, J.-M.; Huc, I. *J. Am. Chem. Soc.* **2003**, *125*, 3448. (b) Jiang, H.; Léger, J.-M.; Dolain, C.; Guionneau, P.; Huc, I. *Tetrahedron* **2003**, *59*, 8365.
- (23) (a) Zhu, J.; Parra, R. D.; Zeng, H.; Skrzypczak-Jankun, E.; Zeng, X. C.; Gong, B. *J. Am. Chem. Soc.* **2000**, *122*, 4219. (b) Gong, B.; Zeng, H.; Zhu, J.; Yua, L.; Han, Y.; Cheng, S.; Furukawa, M.; Parra, R. D.; Kovalevsky, A. Y.; Mills, J. L.; Skrzypczak-Jankun, E.; Martinovic, S.; Smith, R. D.; Zheng, C.; Szyperski, T.; Zeng, X. C. *Proc. Natl. Acad. Sci. U. S. A.* **2002**, *99*, 11583. (c) Yuan, L. H.; Zeng, H. Q.; Yamato, K;

- Sanford, A. R.; Feng, W.; Atreya, H. S.; Sukumaran, D. K.; Szyperski, T.; Gong, B. *J. Am. Chem. Soc.* **2004**, *126*, 16528. (d) Yuan, L.; Sanford, A. R.; Feng, W.; Zhang, A.; Zhu, J.; Zeng, H.; Yamato, K.; Li, M.; Ferguson, J. S.; Gong, B. *J. Org. Chem.* **2005**, *70*, 10660.
- (24) (a) Hou, J.-L.; Shao, X.-B.; Chen, G.-J.; Zhou, Y.-X.; Jiang, X.-K.; Li, Z.-T. *J. Am. Chem. Soc.* **2004**, *126*, 12386. (b) Li, C.; Ren, S.-F.; Hou, J.-L.; Yi, H.-P.; Zhu, S.-Z.; Jiang, X.-K.; Li, Z.-T. *Angew. Chem., Int. Ed.* **2005**, *44*, 5725.
- (25) Hu, Z.-Q.; Hu, H.-Y.; Chen, C.-F. *J. Org. Chem.* **2006**, *71*, 1131.
- (26) (a) Gan, Q.; Bao, C.; Kauffmann, B.; Grelard, A.; Xiang, J.; Liu, S.; Huc, I.; Jiang, H. *Angew. Chem., Int. Ed.* **2008**, *47*, 1715. (b) Zhang, B.; Yuan, T.; Jiang, H.; Lei, M. *J. Phys. Chem. B* **2009**, *113*, 10934. (c) Gan, Q.; Li, F.; Li, G.; Kauffmann, B.; Xiang, J.; Huc, I.; Jiang, H. *Chem. Commun.* **2010**, *46*, 297.
- (27) (a) Yan, Y.; Qin, B.; Ren, C.; Chen, X.; Yip, Y. K.; Ye, R.; Zhang, D.; Su, H.; Zeng, H. *J. Am. Chem. Soc.* **2010**, *132*, 5869. (b) Ong, W. Q.; Zhao, H.; Du, Z.; Yeh, J. Z. Y.; Ren, C.; Tan, L. Z. W.; Zhang, K.; Zeng, H. *Chem. Commun.* **2011**, *47*, 6416.
- (28) Ernst, J. T.; Becerril, J.; Park, H. S.; Yin, H.; Hamilton, A. D. *Angew. Chem., Int. Ed.* **2003**, *42*, 535.
- (29) Wu, Z.-Q.; Jiang, X.-K.; Zhu, S.-Z.; Li, Z.-T. *Org. Lett.* **2004**, *6*, 229.
- (30) Zhu, J.; Wang, X.-Z.; Chen, Y.-Q.; Jiang, X.-K.; Chen, X.-Z.; Li, Z.-T. *J. Org. Chem.* **2004**, *69*, 6221.
- (31) Wu, J.; Hou, J.-L.; Li, C.; Wu, Z.-Q.; Jiang, X.-K.; Li, Z.-T.; Yu, Y.-H. *J. Org. Chem.* **2007**, *72*, 2897.
- (32) (a) Dolain, C.; Jiang, H.; Léger, J.-M.; Guionneau, P.; Huc, I. *J. Am. Chem. Soc.* **2005**, *127*, 12943. (b) Ducasse, L.; Castet, F.; Fritsch, A.; Huc, I.; Buffeteau, T. *J. Phys. Chem. A* **2007**, *111*, 5092. (c) Li, C.; Wang, G.-T.; Yi, H.-P.; Jiang, Li, Z.-T.; Wang, R.-X. *Org. Lett.* **2007**, *9*, 1797. (d) Hu, H.-Y.; Xiang, J.-F.; Yang, Y.; Chen, C.-F. *Org. Lett.* **2008**, *10*, 1275.
- (33) Delaurié, L.; Dong, Z.; Laxmi-Reddy, K.; Godde, F.; Toulmé, J.-J.; Huc, I. *Angew. Chem., Int. Ed.* **2012**, *51*, 473.
- (34) Tang, H.; Doerksen, R. J.; Jones, T. V.; Klein, M. L.; Tew, G. N. *Chem. Biol.* **2006**, *13*, 427.
- (35) (a) Wu, Z.-Q.; Shao, X.-B.; Li, C.; Hou, J.-L.; Wang, K.; Jiang, X.-K.; Li, Z.-T. *J. Am. Chem. Soc.* **2005**, *127*, 17460. (b) Hou, L.-L.; Yi, H.-P.; Shao, X.-B.; Li, C.; Wu, Z.-Q.; Jiang, X.-K.; Wu, L.-Z.; Tung, C.-H.; Li, Z.-T. *Angew. Chem., Int. Ed.* **2006**, *45*, 796. (c) Cai, W.; Wang, G.-T.; Du, P.; Wang, R.-X.; Jiang, X.-K.; Li, Z.-T. *J. Am. Chem. Soc.* **2008**, *130*, 13450. (d) Cai, W.; Wang, G.-T.; Xu, Y.-X.; Jiang, X.-K.; Li, Z.-T. *J. Am. Chem. Soc.* **2008**, *130*, 6936.
- (36) Wolffs, M.; Delsuc, N.; Veldman, D.; Nguyen, V. A.; Williams, R. M.; Meskers, S. C. J.; Janssen, R. A. J.; Huc, I.; Schenning, A. P. H. J. *J. Am. Chem. Soc.* **2009**, *131*, 4819.
- (37) Wang, K.; Wu, Y.-S.; Wang, G.-T.; Wang, R.-X.; Jiang, X.-K.; Fu, H.-B.; Li, Z.-T. *Tetrahedron* **2009**, *65*, 7718.
- (38) (a) Zhou, C.; Cai, W.; Wang, G.-T.; Zhao, X.; Li, Z.-T. *Macromol. Chem. Phys.* **2010**, *211*, 2090. (b) Shi, Z.-M.; Huang, J.; Ma, Z.; Zhao, X.; Guan, Z.; Li, Z.-T. *Macromolecules* **2010**, *43*, 6185.
- (39) Zhang, K.-D.; Zhao, X.; Wang, G.-T.; Liu, Y.; Zhang, Y.; Lu, H.-J.; Jiang, X.-K.; Li, Z.-T. *Angew. Chem., Int. Ed.* **2011**, *50*, 9866.
- (40) (a) Jiang, H.; Léger, J.-M.; Guionneau, P.; Huc, I. *Org. Lett.* **2004**, *6*, 2985. (b) Berni, E.; Dolain, C.; Kauffmann, B.; Léger, J.-M.; Zhan, C.; Huc, I. *J. Org. Chem.* **2008**, *73*, 2687.
- (41) (a) Yuan, L.; Feng, W.; Yamato, K.; Sanford, A. R.; Xu, D.; Guo, H.; Gong, B. *J. Am. Chem. Soc.* **2004**, *126*, 11120. (b) Wu, X.; Liang, G.; Ji, G.; Fun, H.-K.; He, L.; Gong, B. *Chem. Commun.* **2012**, *48*, 2228.
- (42) (a) Chen, Y.-Q.; Wang, X.-Z.; Shao, X.-B.; Hou, J.-L.; Chen, X.-Z.; Jiang, X.-K.; Li, Z.-T. *Tetrahedron* **2004**, *60*, 10253. (b) Wu, Z.-Q.; Jiang, X.-K.; Li, Z.-T. *Tetrahedron Lett.* **2005**, *46*, 8067.
- (43) Zhu, Y.-Y.; Li, C.; Li, G.-Y.; Jiang, X.-K.; Li, Z.-T. *J. Org. Chem.* **2008**, *73*, 1745.
- (44) Lin, J.-B.; Xu, X.-N.; Jiang, X.-K.; Li, Z.-T. *J. Org. Chem.* **2008**, *73*, 9403.
- (45) (a) Qin, B.; Chen, X.; Fang, X.; Shu, Y.; Yip, Y. K.; Yan, Y.; Pan, S.; Ong, W. Q.; Ren, C.; Su, H.; Zeng, H. *Org. Lett.* **2008**, *10*, 5127.
- (b) Qin, B.; Ren, C.; Ye, R.; Sun, C.; Chiad, K.; Chen, X.; Li, Z.; Xue, F.; Su, H.; Chass, G. A.; Zeng, H. *J. Am. Chem. Soc.* **2010**, *132*, 9564.
- (c) Ren, C.; Zhou, F.; Qin, B.; Ye, R.; Shen, S.; Su, H.; Zeng, H. *Angew. Chem., Int. Ed.* **2011**, *50*, 10612.
- (46) (a) Yang, L.; Zhong, L.; Yamato, K.; Zhang, X.; Feng, W.; Deng, P.; Yuan, L.; Zeng, X. C.; Gong, B. *New J. Chem.* **2009**, *33*, 729. (b) Feng, W.; Yamato, K.; Yang, L.; Ferguson, J. S.; Zhong, L.; Zou, S.; Yuan, L.; Zeng, X. C.; Gong, B. *J. Am. Chem. Soc.* **2009**, *131*, 2629.
- (47) Li, F.; Gan, Q.; Xue, L.; Wang, Z.-m.; Jiang, H. *Tetrahedron Lett.* **2009**, *50*, 2367.
- (48) (a) Gong, B. *Chem.—Eur. J.* **2001**, *7*, 4336. (b) Sanford, A. R.; Gong, B. *Curr. Org. Chem.* **2003**, *7*, 1649.
- (49) Huc, I. *Eur. J. Org. Chem.* **2004**, 17.
- (50) (a) Li, Z.-T.; Hou, J.-L.; Li, C.; Yi, H.-P. *Chem.—Asian J.* **2006**, *1*, 766. (b) Zhao, X.; Li, Z.-T. *Chem. Commun.* **2010**, *46*, 1601.
- (51) Saraogi, I.; Hamilton, A. D. *Chem. Soc. Rev.* **2009**, *38*, 1726.
- (52) Gan, Q.; Wang, Y.; Jiang, H. *Curr. Org. Chem.* **2011**, *15*, 1293.
- (53) Gong, B. *Acc. Chem. Res.* **2008**, *41*, 1376.
- (54) Li, Z.-T.; Hou, J.-L.; Li, C. *Acc. Chem. Res.* **2008**, *41*, 1343.
- (55) Tew, G. N.; Scott, R. W.; Klein, M. L.; DeGrado, W. F. *Acc. Chem. Res.* **2010**, *43*, 30.
- (56) (a) Fischer, L.; Guichard, G. *Org. Biomol. Chem.* **2010**, *8*, 3101. (b) Roy, A.; Prabhakaran, P.; Baruah, P. K.; Sanjayan, G. J. *Chem. Commun.* **2011**, *47*, 11593.
- (57) (a) Nowick, J. S. *Acc. Chem. Res.* **1999**, *32*, 287. (b) Nowick, J. S. *Org. Biomol. Chem.* **2006**, *4*, 3869. (c) Nowick, J. S. *Acc. Chem. Res.* **2008**, *41*, 1319.
- (58) Sewald, N.; Jakubke, H.-D., Eds. *Peptides: Chemistry and Biology*; Wiley—VCH: Weinheim, Germany, 2009; p 6.
- (59) Arunan, E.; Desiraju, G. R.; Klein, R. A.; Sadlej, J.; Scheiner, S.; Alkorta, I.; Clary, D. C.; Crabtree, R. H.; Dannenberg, J. J.; Hobza, P.; Kjaergaard, H. G.; Legon, A. C.; Mennucci, B.; Nesbitt, D. *J. Pure Appl. Chem.* **2011**, *83*, 1637.
- (60) Pauling, L. *The Nature of the Chemical Bond*, 3rd ed.; Cornell University Press: Ithaca, NY, 1960.
- (61) Desiraju, G. R., Steiner, T., Eds. *The Weak Hydrogen Bond in Structural Chemistry and Biology*; Oxford University Press: Oxford, 1999.
- (62) (a) Dunitz, J. D.; Taylor, R. *Chem.—Eur. J.* **1997**, *3*, 89. (b) Dunitz, J. D. *ChemBioChem* **2004**, *5*, 614.
- (63) (a) Zhu, Y.-Y.; Wu, J.; Li, C.; Zhu, J.; Hou, J.-L.; Li, C.-Z.; Jiang, X.-K.; Li, Z.-T. *Cryst. Growth Des.* **2007**, *7*, 1490. (b) Zhu, Y.-Y.; Yi, H.-P.; Li, C.; Jiang, X.-K.; Li, Z.-T. *Cryst. Growth Des.* **2008**, *8*, 1294. (c) Du, P.; Jiang, X.-K.; Li, Z.-T. *Tetrahedron Lett.* **2009**, *50*, 320.
- (64) Mazik, M.; Bläser, D.; Boese, R. *Tetrahedron* **1999**, *55*, 12771.
- (65) Huc, I.; Maurizot, V.; Gornitzka, H.; Léger, J.-M. *Chem. Commun.* **2002**, 578.
- (66) Dolain, C.; Maurizot, V.; Huc, I. *Angew. Chem., Int. Ed.* **2003**, *42*, 2738.
- (67) (a) van Gorp, J. J.; Vekemans, J. A. J. M.; Meijer, E. W. *Chem. Commun.* **2004**, *60*. (b) Sinkeldam, R. W.; Hoeben, F. J. M.; Pouderoijen, M. J.; De Cat, I.; Zhang, J.; Furukawa, S.; De Feyter, S.; Vekemans, J. A. J. M.; Meijer, E. W. *J. Am. Chem. Soc.* **2006**, *128*, 16113. (c) Sinkeldam, R. W.; van Houtem, M. H. C. J.; Pieterse, K.; Vekemans, J. A. J. M.; Meijer, E. W. *Chem.—Eur. J.* **2006**, *12*, 6129.
- (68) Maurizot, V.; Dolain, C.; Leydet, Y.; Léger, J.-M.; Guionneau, P.; Huc, I. *J. Am. Chem. Soc.* **2004**, *126*, 10049.
- (69) (a) Delnoye, D. A. P.; Sijbesma, R. P.; Vekemans, J. A. J. M.; Meijer, E. W. *J. Am. Chem. Soc.* **1996**, *118*, 8717. (b) Brunsved, L.; Zhang, H.; Glasbeek, M.; Vekemans, J. A. J. M.; Meijer, E. W. *J. Am. Chem. Soc.* **2000**, *122*, 6175.
- (70) Corbin, P. S.; Zimmerman, S. C.; Thiessen, P. A.; Hawryluk, N. A.; Murray, T. J. *J. Am. Chem. Soc.* **2001**, *123*, 10475.
- (71) Zimmerman, S. C.; Corbin, P. S. *Struct. Bonding (Berlin)* **2000**, *96*, 63.
- (72) Sánchez-García, D.; Kauffmann, B.; Kawanami, T.; Ihara, H.; Takafuji, M.; Delville, M.-H.; Huc, I. *J. Am. Chem. Soc.* **2009**, *131*, 8642.
- (73) Du, P.; Jiang, X.-K.; Li, Z.-T. *Tetrahedron Lett.* **2009**, *50*, 316.

- (74) (a) Smith, G.; Kennard, C. H. L.; Katekar, G. F. *Aust. J. Chem.* **1983**, *36*, 2455. (b) Shivanyuk, A.; Rissanen, K.; Korner, S. K.; Rudkevich, D. M.; Rebek, J., Jr. *Helv. Chim. Acta* **2000**, *83*, 1778.
- (75) Gellman, S. H.; Dado, G. P.; Liang, G.-B.; Adams, B. R. *J. Am. Chem. Soc.* **1991**, *113*, 1164.
- (76) Kemp, D. S.; Li, Z. Q. *Tetrahedron Lett.* **1995**, *36*, 4175.
- (77) Cary, J. M.; Moore, J. S. *Org. Lett.* **2002**, *4*, 4663.
- (78) (a) Yang, X.; Brown, A. L.; Furukawa, M.; Li, S.; Gardinier, W. E.; Bukowski, E. J.; Bright, F. V.; Zheng, C.; Zeng, X. C.; Gong, B. *Chem. Commun.* **2003**, *56*. (b) Yang, X.; Yuan, L.; Yamato, K.; Brown, A. L.; Feng, W.; Furukawa, M.; Zeng, X. C.; Gong, B. *J. Am. Chem. Soc.* **2004**, *126*, 3148.
- (79) Hu, W.; Zhu, N.; Tang, W.; Zhao, D. *Org. Lett.* **2008**, *10*, 2669.
- (80) Kanamori, D.; Okamura, T.-a.; Yamamoto, H.; Ueyama, N. *Angew. Chem., Int. Ed.* **2005**, *44*, 969.
- (81) Hu, Z.-Q.; Chen, C.-F. *Tetrahedron* **2006**, *62*, 3446.
- (82) Rozas, I.; Alkorta, I.; Elguero, J. *J. Phys. Chem. A* **1998**, *102*, 9925.
- (83) Du, Z.; Ren, C.; Ye, R.; Shen, J.; Maurizot, V.; Lu, Y.; Wang, J.; Zeng, H. *Chem. Commun.* **2011**, *47*, 12488.
- (84) Bao, C.; Kauffmann, B.; Gan, Q.; Srinivas, K.; Jiang, H.; Huc, I. *Angew. Chem., Int. Ed.* **2008**, *47*, 4153.
- (85) Berni, E.; Kauffmann, B.; Bao, C.; Lefevre, J.; Bassani, D. M.; Huc, I. *Chem.—Eur. J.* **2007**, *13*, 8463.
- (86) Ferrand, Y.; Kendhale, A. M.; Kauffmann, B.; Grélard, A.; Marie, C.; Blot, V.; Pipelier, M.; Dubreuil, D.; Huc, I. *J. Am. Chem. Soc.* **2010**, *132*, 7858.
- (87) (a) Albrecht, G.; Corey, R. B. *J. Am. Chem. Soc.* **1939**, *61*, 1087. (b) Marsh, R. E. *Acta Crystallogr.* **1958**, *11*, 654. (c) Parthasarathy, R. *Acta Crystallogr.* **1969**, *B25*, 509. (d) Jönsson, P. G.; Kvick, A. *Acta Crystallogr.* **1972**, *B28*, 1827.
- (88) (a) Donohue, J. *Structural Chemistry and Molecular Biology*; Freeman: San Francisco, 1968. (b) Desiraju, G. R. *Crystal Engineering. The Design of Organic Solids*; Elsevier: Amsterdam/New York, 1989. (c) Jeffrey, G. A.; Saenger, W. *Hydrogen Bonding in Biological Structures*; Springer-Verlag: Berlin/Heidelberg, 1991. (d) Jeffrey, G. A. *An Introduction to Hydrogen Bonding*; Oxford University Press: New York, 1997.
- (89) (a) Feibush, B.; Figueiroa, A.; Charles, R.; Onan, K. D.; Feibush, P.; Karger, B. L. *J. Am. Chem. Soc.* **1986**, *108*, 3310. (b) Mocilac, P.; Tallon, M.; Lough, A. J.; Gallagher, J. F. *CrystEngComm* **2010**, *12*, 3080. (c) Tosi, G.; Bruni, P.; Cardellini, L.; Stipa, P.; Bocelli, G.; Rizzoli, C. *Gazz. Chim. Ital.* **1989**, *119*, 399. (d) Kim, T. H.; Seo, J.; Lee, S. J.; Lee, S. S.; Kim, J.; Jung, J. H. *Chem. Mater.* **2007**, *19*, 5815.
- (90) Malone, J. F.; Murray, C. M.; Dolan, G. M. *Chem. Mater.* **1997**, *9*, 2983.
- (91) (a) Hanan, G. S.; Lehn, J.-M.; Kyritsakas, N.; Fischer, J. *J. Chem. Soc., Chem. Commun.* **1995**, 765. (b) Bassani, D. M.; Lehn, J.-M.; Baum, G.; Fenske, D. *Angew. Chem., Int. Ed. Engl.* **1997**, *36*, 1845. (c) Ohkita, M.; Lehn, J.-M.; Baum, G.; Fenske, D. *Chem.—Eur. J.* **1999**, *5*, 3471. (d) Petitjean, A.; Cuccia, L. A.; Lehn, J.-M.; Nierengarten, H.; Schmutz, M. *Angew. Chem., Int. Ed.* **2002**, *41*, 1195.
- (92) (a) Hunter, C. A.; Purvis, D. H. *Angew. Chem., Int. Ed. Engl.* **1992**, *31*, 792. (b) Popovits, V.; Vemparala, S.; Ivanov, I.; Liu, Z.; Klein, M. L.; DeGrado, W. F. *J. Phys. Chem. B* **2006**, *110*, 3517. (c) Liu, Z.; Remsing, R. C.; Liu, D.; Moyna, G.; Popovits, V. *J. Phys. Chem. B* **2009**, *113*, 7041. (d) Galan, J. F.; Brown, J.; Wildin, J. L.; Liu, Z.; Liu, D.; Moyna, G.; Popovits, V. *J. Phys. Chem. B* **2009**, *113*, 12809. (e) Liu, Z.; Teslja, A.; Popovits, V. *J. Comput. Chem.* **2011**, *32*, 1846.
- (93) Etter, M. C. *J. Phys. Chem.* **1991**, *95*, 4601.
- (94) (a) Huang, B.; Parquette, J. R. *Org. Lett.* **2000**, *2*, 239. (b) Parra, R. D.; Zeng, H. Q.; Zhu, J.; Zheng, C.; Zeng, X. C.; Gong, B. *Chem.—Eur. J.* **2001**, *7*, 4352. (c) Parra, R. D.; Furukawa, M.; Gong, B.; Zeng, X. C. *J. Chem. Phys.* **2001**, *115*, 6030.
- (95) (a) Yang, H. H. *Aromatic High-Strength Fibers*; John Wiley & Sons: New York, 1989. (b) Tanner, D.; Fitzgerald, J. A.; Phillips, B. R. *Angew. Chem., Int. Ed.* **1989**, *28*, 649.
- (96) Zhu, J.; Lin, J.-B.; Xu, Y.-X.; Shao, X.-B.; Jiang, X.-K.; Li, Z.-T. *J. Am. Chem. Soc.* **2006**, *128*, 12307.
- (97) (a) Berl, V.; Huc, I.; Khouri, R. G.; Lehn, J.-M. *Chem.—Eur. J.* **2001**, *7*, 2810. (b) Berni, E.; Garric, J.; Lamit, C.; Kauffmann, B.; Léger, J.-M.; Huc, I. *Chem. Commun.* **2008**, 1968. (c) Zhan, C.; Léger, J.-M.; Huc, I. *Angew. Chem., Int. Ed.* **2006**, *45*, 4625.
- (98) Ferrand, Y.; Kendhale, A. M.; Garric, J.; Kauffmann, B.; Huc, I. *Angew. Chem., Int. Ed.* **2010**, *49*, 1778.
- (99) Zhang, D.-W.; Li, Z.-T. In *Current Trends in X-Ray Crystallography*; Chandrasekaran, A., Ed.; Intech: Rejeka, Croatia, 2011; pp 95–112.
- (100) (a) Kampf, M.; Richter, R.; Hennig, L.; Eidner, A.; Baldamus, J.; Kirmse, R. *Z. Anorg. Allg. Chem.* **2004**, *630*, 2677. (b) Lewis, R. J.; Camilleri, P.; Kirby, A. J.; Marby, C. A.; Slawin, A. A.; Williams, D. J. *J. Chem. Soc., Perkin Trans. 2* **1991**, 1625. (c) Guo, D.; Nichol, G. S.; Cain, J. P.; Yalkowsky, S. H. *Acta Crystallogr., Sect. E* **2009**, *65*, o2644. (d) Zhu, S.; Nieger, M.; Daniels, J.; Felder, T.; Kossev, I.; Schmidt, T.; Sokolowski, M.; Vögtle, F.; Schalley, C. A. *Chem.—Eur. J.* **2009**, *15*, 5040.
- (101) (a) Ostaszewski, R.; Urbanczyk-Lipkowska, Z. *J. Mol. Struct.* **1999**, *474*, 197. (b) Geib, S. J.; Hirst, S. C.; Vicent, C.; Hamilton, A. D. *J. Chem. Soc., Chem. Commun.* **1991**, 1283. (c) Dixon, R. P.; Geib, S. J.; Hamilton, A. D. *J. Am. Chem. Soc.* **1992**, *114*, 365.
- (102) Dolain, C.; Maurizot, V.; Huc, I. *Angew. Chem., Int. Ed.* **2003**, *42*, 2737.
- (103) Howl, J., Ed. *Peptide Synthesis and Applications*; Humana Press: Totowa, NJ, 2005.
- (104) (a) Montalbetti, C. A. G. N.; Falque, V. *Tetrahedron* **2005**, *61*, 10827. (b) Joullié, M. M.; Lassen, K. M. *ARKIVOC* **2010**, 189.
- (105) (a) König, H. M.; Abbel, R.; Schollmeyer, D.; Kilbinger, A. F. *M. Org. Lett.* **2006**, *8*, 1819. (b) Baptiste, B.; Douat-Casassus, C.; Laxmi-Reddy, K.; Godde, F.; Huc, I. *J. Org. Chem.* **2010**, *75*, 7175. (c) Lee, T.-K.; Ahn, J.-M. *ACS Comb. Sci.* **2011**, *13*, 107.
- (106) (a) Hoofar, A.; Ollis, W. D.; Stoddart, J. F. *Tetrahedron Lett.* **1980**, *4211*. (b) Hoofar, A.; Ollis, W. D.; Price, J. A.; Stephanatou, J. S.; Stoddart, J. F. *J. Chem. Soc., Perkin Trans. 1* **1982**, *8*, 1649. (c) Feigel, M.; Lugert, G.; Manero, J.; Bremer, M. *Liebig Ann. Chem.* **1989**, 1089.
- (107) Ghosez, L.; Haveaux, B.; Viehe, H. G. *Angew. Chem., Int. Ed. Engl.* **1969**, *8*, 454.
- (108) Gillies, E. R.; Dolain, C.; Léger, J.-M.; Huc, I. *J. Org. Chem.* **2006**, *71*, 7931.
- (109) Creighton, C. J.; Reitz, A. B. *Org. Lett.* **2001**, *3*, 893.
- (110) Zhang, A. M.; Ferguson, J. S.; Yamato, K.; Zheng, C.; Gong, B. *Org. Lett.* **2006**, *8*, 5117.
- (111) (a) Dolain, C.; Grélard, A.; Laguerre, M.; Jiang, H.; Maurizot, V.; Huc, I. *Chem.—Eur. J.* **2005**, *11*, 6135. (b) Perrin, C. L.; Dwyer, T. J.; Rebek, J.; Duff, R. J. *J. Am. Chem. Soc.* **1990**, *112*, 3122. (c) Steffel, L. R.; Cashman, T. J.; Reutershan, M. H.; Linton, B. P. *J. Am. Chem. Soc.* **2007**, *129*, 12956.
- (112) (a) Legon, A. C. *Chem. Soc. Rev.* **1990**, *19*, 197. (b) Nowick, J. S.; Powell, N. A.; Martinez, E. J.; Smith, E. M.; Noronha, G. J. *Org. Chem.* **1992**, *57*, 3763. (c) Dado, G. P.; Gellman, S. H. *J. Am. Chem. Soc.* **1994**, *116*, 1054.
- (113) Hoofar, A.; Ollis, W. D.; Stoddart, J. F. *J. Chem. Soc., Perkin Trans. 1* **1982**, 1721.
- (114) Choi, S.; Isaacs, A.; Clements, D.; Liu, D.; Kim, H.; Scott, R. W.; Winkler, J. D.; DeGrado, W. F. *Proc. Natl. Acad. Sci. U.S.A.* **2009**, *106*, 6968.
- (115) Liu, S.-G.; Li, Y.-Z.; Zuo, J.-L.; You, X.-Z. *Acta Crystallogr., Sect. E* **2004**, *60*, o1527.
- (116) (a) Kendhale, A. M.; Gonnade, R.; Rajamohan, P. R.; Hofmann, H.-J.; Sanjayan, G. J. *Chem. Commun.* **2008**, 2541. (b) Baruah, P. K.; Gonnade, R.; Rajamohan, P. R.; Hofmann, H.-J.; Sanjayan, G. J. *J. Org. Chem.* **2007**, *72*, 5077. (c) Prabhakaran, P.; Puranik, V. G.; Chandran, J. N.; Rajamohan, P. R.; Hofmann, H.-J.; Sanjayan, G. J. *Chem. Commun.* **2009**, 3446.
- (117) Marimganti, S.; Cheemala, M. N.; Ahn, J.-M. *Org. Lett.* **2009**, *11*, 4418.

- (118) Runge, S.; Thøgersen, H.; Madsen, K.; Lau, J.; Rudolph, R. *J. Biol. Chem.* **2008**, *283*, 11340.
- (119) (a) Gothard, C. M.; Rao, N. A.; Nowick, J. S. *J. Am. Chem. Soc.* **2007**, *129*, 7272. (b) Kang, S. W.; Gothard, C. M.; Maitra, S.; Atiatul, W.; Nowick, J. S. *J. Am. Chem. Soc.* **2007**, *129*, 1486.
- (120) (a) Ahn, J.-M.; Han, S.-Y. *Tetrahedron Lett.* **2007**, *48*, 3543. (b) Plante, J.; Campbell, F.; Malkova, B.; Kilner, C.; Warriner, S. L.; Wilson, A. *J. Org. Biomol. Chem.* **2008**, *6*, 138. (c) Kulikov, O. V.; Hamilton, A. D. *RSC Adv.* **2012**, *2*, 2454.
- (121) Seyler, H.; Kilbinger, A. F. M. *Macromolecules* **2010**, *43*, 5659.
- (122) (a) Gong, B. *Synlett* **2001**, 582. (b) Gong, B. *Polym. Int.* **2007**, *56*, 436. (c) Yuan, L.; Zhang, P.; Feng, W.; Gong, B. *Curr. Org. Chem.* **2011**, *15*, 1250. (d) Gong, B.; Yan, Y.; Zeng, H.; Skrzypczak-Jankunn, E.; Kim, Y. W.; Zhu, J.; Ickes, H. *J. Am. Chem. Soc.* **1999**, *121*, 5607. (e) Zeng, H.; Yang, X.; Brown, A. L.; Martinovic, S.; Smith, R. D.; Gong, B. *Chem. Commun.* **2003**, 1556. (f) Zhang, P.; Chu, H.; Li, X.; Feng, W.; Deng, P.; Yuan, L.; Gong, B. *Org. Lett.* **2011**, *13*, 54. (g) Yang, X.; Gong, B. *Angew. Chem., Int. Ed.* **2005**, *45*, 1352.
- (123) (a) Baruah, P. K.; Sreedevi, N. K.; Gonnade, R.; Ravindranathan, S.; Damodaran, K.; Hofmann, H.-J.; Sanjayan, G. J. *J. Org. Chem.* **2007**, *72*, 636. (b) Baruah, P. K.; Sreedevi, N. K.; Majumdar, B.; Pasricha, R.; Poddar, P.; Gonnade, R.; Ravindranathan, S.; Sanjayan, G. *J. Chem. Commun.* **2008**, 712. (c) Srinivas, D.; Gonnade, R.; Ravindranathan, S.; Sanjayan, G. *J. J. Org. Chem.* **2007**, *72*, 7022. (d) Prabhakaran, P.; Kale, S. S.; Puranik, V. G.; Rajamohan, P. R.; Chetina, O.; Howard, J. A. K.; Hofmann, H.-J.; Sanjayan, G. *J. J. Am. Chem. Soc.* **2008**, *130*, 17743.
- (124) Rodriguez, J. M.; Hamilton, A. D. *Angew. Chem., Int. Ed.* **2007**, *46*, 8614.
- (125) Branden, C.; Tooze, J. *Introduction to Protein Secondary Structure*; Garland Publishing: New York, 1991.
- (126) (a) Rodriguez, J. M.; Hamilton, A. D. *Tetrahedron Lett.* **2006**, *47*, 7443. (b) Adler, M. J.; Hamilton, A. D. *J. Org. Chem.* **2011**, *76*, 7040.
- (127) Zhao, X.; Wang, X.-Z.; Jiang, X.-K.; Chen, Y.-Q.; Li, Z.-T.; Chen, G.-J. *J. Am. Chem. Soc.* **2003**, *125*, 15128.
- (128) (a) Yang, Y.; Chu, W.-J.; Liu, J.-W.; Chen, C.-F. *Curr. Org. Chem.* **2011**, *15*, 1302. (b) Yang, Y.; Zhang, Y.-Z.; Tang, Y.-L.; Chen, C.-F. *New J. Chem.* **2006**, *30*, 140. (c) Yang, Y.; Yan, H.-J.; Chen, C.-F.; Wan, L.-J. *Org. Lett.* **2007**, *9*, 4991. (d) Yang, Y.; Xiang, J.-F.; Xue, M.; Hu, H.-Y.; Chen, C.-F. *J. Org. Chem.* **2008**, *73*, 6369. (e) Yang, Y.; Chen, T.; Xiang, J.-F.; Yan, H.-Y.; Chen, C.-F.; Wan, L.-J. *Chem.—Eur. J.* **2008**, *14*, 5742.
- (129) (a) Palmans, A. R. A.; Vekemans, J. A. J. M.; Meijer, E. W. *Recl. Trav. Chim. Pays-Bas* **1995**, *114*, 277. (b) Pieterse, K.; Vekemans, J. A. J. M.; Kooijman, H.; Spek, A. L.; Meijer, E. W. *Chem.—Eur. J.* **2000**, *6*, 4597.
- (130) Wyrembak, P. N.; Hamilton, A. D. *J. Am. Chem. Soc.* **2009**, *131*, 4566.
- (131) Loughlin, W. A.; Tyndall, J. D. A.; Glenn, M. P.; Fairlie, D. P. *Chem. Rev.* **2004**, *104*, 6085.
- (132) Yi, H.-P.; Li, C.; Hou, J.-L.; Jiang, X.-K.; Li, Z.-T. *Tetrahedron* **2005**, *61*, 7974.
- (133) Yan, Y.; Qin, B.; Shu, Y.; Chen, X.; Yip, Y. K.; Zhang, D.; Su, H.; Zeng, H. *Org. Lett.* **2009**, *11*, 1201.
- (134) Yi, H.-P.; Shao, X.-B.; Hou, J.-L.; Li, C.; Jiang, X.-K.; Li, Z.-T. *New J. Chem.* **2005**, *29*, 1213.
- (135) Berl, V.; Huc, I.; Khoury, R. G.; Lehn, J.-M. *Chem.—Eur. J.* **2001**, *7*, 2798.
- (136) Maurizot, V.; Dolain, C.; Huc, I. *Eur. J. Org. Chem.* **2005**, 1293.
- (137) Delsuc, N.; Kawanami, T.; Lefevre, J.; Shundo, A.; Ihara, H.; Takafuji, M.; Huc, I. *ChemPhysChem* **2008**, *9*, 1882.
- (138) Jiang, H.; Dolain, C.; Léger, J.-M.; Gornitzka, H.; Huc, I. *J. Am. Chem. Soc.* **2004**, *126*, 1034.
- (139) Kendhale, A. M.; Poniman, L.; Dong, Z.; Laxmi-Reddy, K.; Kauffmann, B.; Ferrand, Y.; Huc, I. *J. Org. Chem.* **2011**, *76*, 195.
- (140) Buffeteau, T.; Ducasse, L.; Poniman, L.; Delsuc, N.; Huc, I. *Chem. Commun.* **2006**, 2714.
- (141) Hamuro, Y.; Geib, S. J.; D. Hamilton, A. D. *J. Am. Chem. Soc.* **1997**, *119*, 10587.
- (142) Garric, J.; Léger, J.-M.; Huc, I. *Angew. Chem., Int. Ed.* **2005**, *44*, 1954.
- (143) Delsuc, N.; Godde, F.; Kauffmann, B.; Léger, J.-M.; Huc, I. *J. Am. Chem. Soc.* **2007**, *129*, 11348.
- (144) (a) Hu, H.-Y.; Xiang, J.-F.; Cao, J.; Chen, C.-F. *Org. Lett.* **2008**, *10*, 5035. (b) Hu, H.-Y.; Xiang, J.-F.; Chen, C.-F. *Org. Biomol. Chem.* **2009**, *7*, 2534.
- (145) (a) Hu, H.-Y.; Xiang, J.-F.; Yang, Y.; Chen, C.-F. *Org. Lett.* **2008**, *10*, 69. (b) Hu, H.-Y.; Xue, W.; Hu, Z.-Q.; Xiang, J.-F.; Chen, C.-F.; He, S.-G. *J. Org. Chem.* **2009**, *74*, 4949.
- (146) (a) Tie, C.; Gallucci, J. C.; Parquette, J. R. *J. Am. Chem. Soc.* **2006**, *128*, 1162. (b) King, E. D.; Tao, P.; Sanan, T. T.; Hadad, C. M.; Parquette, J. R. *Org. Lett.* **2008**, *10*, 1671.
- (147) Perlovich, G. L.; Ryzhakov, A. M.; Tkachev, V. V.; Hansen, L. K. *Cryst. Growth Des.* **2011**, *11*, 1067.
- (148) Hu, Z.-Q.; Chen, C.-F. *Chem. Commun.* **2005**, 2445.
- (149) (a) Li, X.; Zhan, C.; Wang, Y.; Yao, J. *Chem. Commun.* **2008**, 2444. (b) Zhu, H.; He, W.; Zhan, C.; Li, X.; Guan, Z.; Guo, F.; Yao, J. *Tetrahedron* **2011**, *67*, 8458.
- (150) (a) Sinkeldam, R. W.; van Houtem, M. H. C. J.; Koeckelberghs, G.; Vekemans, J. A. J. M.; Meijer, E. W. *Org. Lett.* **2006**, *8*, 383. (b) Katayama, H.; de Greef, T. F. A.; Kooijman, H.; Spek, A. L.; Vekemans, J. A. J. M.; Meijer, E. W. *Tetrahedron* **2007**, *63*, 6642.
- (151) Zhang, A. M.; Han, Y. H.; Yamato, K.; Zeng, X. C.; Gong, B. *Org. Lett.* **2006**, *8*, 803.
- (152) (a) Palmans, A. R. A.; Vekemans, J. A. J. M.; Havinga, E. E.; Meijer, E. W. *Angew. Chem., Int. Ed. Engl.* **1997**, *36*, 2648. (b) van Gorp, J. J.; Vekemans, J. A. J. M.; Meijer, E. W. *J. Am. Chem. Soc.* **2002**, *124*, 14759. (c) van Herrikhuyzen, J.; Jonkheijm, P.; Schenning, A. P. H. J.; Meijer, E. W. *Org. Biomol. Chem.* **2006**, *4*, 1539.
- (153) Li, C.; Zhu, Y.-Y.; Yi, H.-P.; Li, C.-Z.; Jiang, X.-K.; Li, Z.-T. *Chem.—Eur. J.* **2007**, *13*, 9990.
- (154) (a) Dolain, C.; Léger, J.-M.; Delsuc, N.; Gornitzka, H.; Huc, I. *Proc. Natl. Acad. Sci. U.S.A.* **2005**, *102*, 16146. (b) Delsuc, N.; Léger, J.-M.; Massip, S.; Huc, I. *Angew. Chem., Int. Ed.* **2007**, *46*, 214. (c) Delsuc, N.; Massip, S.; Léger, J.-M.; Kauffmann, B.; Huc, I. *J. Am. Chem. Soc.* **2011**, *133*, 3165.
- (155) Lockman, J. W.; Paul, N. M.; Parquette, J. R. *Prog. Polym. Sci.* **2005**, *30*, 423.
- (156) (a) Recker, J.; Tomcik, D. J.; Parquette, J. R. *J. Am. Chem. Soc.* **2000**, *122*, 10298. (b) Rauckhorst, M. R.; Wilson, P. J.; Hatcher, S. A.; Hadad, C. M.; Parquette, J. R. *Tetrahedron* **2003**, *59*, 3917. (c) Huang, B.; Parquette, J. R. *J. Am. Chem. Soc.* **2001**, *123*, 2689. (d) Huang, B.; Prantil, M. A.; Gustafson, T. L.; Parquette, J. R. *J. Am. Chem. Soc.* **2003**, *125*, 14518. (e) Gandhi, P.; Huang, B.; Gallucci, J. C.; Parquette, J. R. *Org. Lett.* **2001**, *3*, 3129. (f) Gabriel, C. J.; DeMatteo, M. P.; Paul, N. M.; Takaya, T.; Gustafson, T. L.; Hadad, C. M.; Parquette, J. R. *J. Org. Chem.* **2006**, *71*, 9035. (g) Gabriel, C. J.; Parquette, J. R. *J. Am. Chem. Soc.* **2006**, *128*, 13708.
- (157) (a) Xu, Y.-X.; Zhao, X.; Jiang, X.-K.; Li, Z.-T. *J. Org. Chem.* **2009**, *74*, 7267. (b) Shi, Z.-M.; Chen, S.-G.; Zhao, X.; Jiang, X.-K.; Li, Z.-T. *Org. Biomol. Chem.* **2011**, *9*, 8122.
- (158) Gibson, S. E.; Lecci, C. *Angew. Chem., Int. Ed.* **2006**, *45*, 1364.
- (159) Kim, Y. H.; Calabrese, J.; McEwen, C. *J. Am. Chem. Soc.* **1996**, *118*, 1545.
- (160) Choi, K.; Hamilton, A. D. *J. Am. Chem. Soc.* **2003**, *125*, 10241.
- (161) Zou, S.; He, Y.; Yang, Y.; Zhao, Y.; Yuan, L.; Feng, W.; Yamato, K.; Gong, B. *Synlett* **2009**, 1437.
- (162) Ferguson, J. S.; Yamato, K.; Liu, R.; He, L.; Zeng, X. C.; Gong, B. *Angew. Chem., Int. Ed.* **2009**, *48*, 3150.
- (163) (a) Qin, B.; Sun, C.; Liu, Y.; Shen, J.; Ye, R.; Zhu, J.; Duan, X.-F.; Zeng, H. *Org. Lett.* **2011**, *13*, 2270. (b) Qin, B.; Ong, W. Q.; Ye, R.; Du, Z.; Chen, X.; Yan, Y.; Zhang, K.; Su, H.; Zeng, H. *Chem. Commun.* **2011**, *47*, 5419.
- (164) Zhu, Y.-Y.; Wang, G.-T.; Li, Z.-T. *Org. Biomol. Chem.* **2009**, *7*, 3243.

- (165) (a) Rowan, S. J.; Cantrill, S. J.; Cousins, G. R. L.; Sanders, J. K. M.; Stoddart, J. F. *Angew. Chem., Int. Ed.* **2001**, *41*, 898. (b) Corbett, P. T.; Leclaire, J.; Vial, L.; West, K. R.; Wietor, J.-L.; Sanders, J. K. M.; Otto, S. *Chem. Rev.* **2006**, *106*, 3652.
- (166) (a) Lin, J.; Wu, J.; Jiang, X.; Li, Z. *Chin. J. Chem.* **2009**, *27*, 117. (b) Xu, X.-N.; Wang, L.; Lin, J.-B.; Wang, G.-T.; Jiang, X.-K.; Li, Z.-T. *Chem.—Eur. J.* **2009**, *15*, 5763. (c) Lu, B.-Y.; Lin, J.-B.; Jiang, X.-K.; Li, Z.-T. *Tetrahedron Lett.* **2010**, *51*, 3830. (d) Xu, X.-N.; Wang, L.; Zhao, X.; Li, Z.-T. *Gaodeng Xuexiao Huaxue Xuebao* **2011**, *32*, 2162. (e) Wang, L.; Wang, G.-T.; Zhao, X.; Jiang, X.-K.; Li, Z.-T. *J. Org. Chem.* **2011**, *76*, 3531.
- (167) Li, M.; Yamato, K.; Ferguson, J. S.; Singarapu, K. K.; Szyperski, T.; Gong, B. *J. Am. Chem. Soc.* **2008**, *130*, 491.
- (168) Smaldone, R. A.; Moore, J. S. *Chem.—Eur. J.* **2008**, *14*, 2650.
- (169) (a) Oh, K.; Jeong, K.-S.; Moore, J. S. *Nature* **2001**, *414*, 889. (b) Licini, G.; Prins, L. J.; Scrimin, P. *Eur. J. Org. Chem.* **2005**, 969. (c) Dong, Z.; Yap, G. P. A.; Fox, J. M. *J. Am. Chem. Soc.* **2007**, *129*, 11850. (d) Muller, M. M.; Windsor, M. A.; Pomerantz, W. C.; Gellman, S. H.; Hilvert, D. *Angew. Chem., Int. Ed.* **2009**, *48*, 922. (e) Cho, H.; Zhong, Z.; Zhao, Y. *Tetrahedron* **2009**, *65*, 7311. (f) Maayan, G.; Ward, M. D.; Kirshenbaum, K. *Proc. Natl. Acad. Sci. U. S. A.* **2009**, *106*, 13679.
- (170) Dolain, C.; Zhan, C.; Léger, J.-M.; Daniels, L.; Huc, I. *J. Am. Chem. Soc.* **2005**, *127*, 2400.
- (171) Srinivas, K.; Kauffmann, B.; Dolain, C.; Léger, J.-M.; Ghosez, L.; Huc, I. *J. Am. Chem. Soc.* **2008**, *130*, 13210.
- (172) Yi, H.-P.; Wu, J.; Ding, K.-L.; Jiang, X.-K.; Li, Z.-T. *J. Org. Chem.* **2007**, *72*, 870.
- (173) (a) Zhu, Y.-Y.; Wang, G.-T.; Li, Z.-T. *Curr. Org. Chem.* **2011**, *15*, 1266. (b) Li, Z.-T. *Huaxue Jinzhan* **2011**, *23*, 1.
- (174) Yamato, K.; Yuan, L.; Feng, W.; Helsel, A. J.; Sanford, A. R.; Zhu, J.; Deng, J.; Zeng, X. C.; Gong, B. *Org. Biomol. Chem.* **2009**, *7*, 3643.
- (175) (a) Liu, H.; Wu, J.; Jiang, X.-K.; Li, Z.-T. *Tetrahedron Lett.* **2007**, *48*, 7327. (b) Feng, D.-J.; Wang, G.-T.; Wu, J.; Wang, R.-X.; Li, Z.-T. *Tetrahedron Lett.* **2007**, *48*, 6181. (c) Wu, Z.-Q.; Li, C.-Z.; Feng, D.-J.; Jiang, X.-K.; Li, Z.-T. *Tetrahedron* **2006**, *62*, 11054. (d) Li, C.-Z.; Zhu, J.; Wu, Z.-Q.; Hou, J.-L.; Li, C.; Shao, X.-B.; Jiang, X.-K.; Li, Z.-T.; Gao, X.; Wang, Q.-R. *Tetrahedron* **2006**, *62*, 6973. (e) Li, C.-Z.; Li, Z.-T.; Gao, X.; Wang, Q.-R. *Chin. J. Chem.* **2007**, *25*, 1417. (f) Xiao, Z.-Y.; Hou, J.-L.; Jiang, X.-K.; Li, Z.-T.; Ma, Z. *Tetrahedron* **2009**, *65*, 10182.
- (176) (a) Garric, J.; Léger, J.-M.; Huc, I. *Chem.—Eur. J.* **2007**, *13*, 8454. (b) Bao, C.; Gan, Q.; Kauffmann, B.; Jiang, H.; Huc, I. *Chem.—Eur. J.* **2009**, *15*, 11530.
- (177) Ong, W. Q.; Zhao, H.; Fang, X.; Woen, S.; Zhou, F.; Yap, W.; Su, H.; Li, S. F. Y.; Zeng, H. *Org. Lett.* **2011**, *13*, 3194.
- (178) Bakkali, H.; Marie, C.; Ly, A.; Thobie-Gautier, C.; Graton, J.; Pipelier, M.; Sengmany, S.; Léonel, E.; Nédélec, J.-Y.; Evain, M.; Dubreuil, D. *Eur. J. Org. Chem.* **2008**, 2156.
- (179) Berl, V.; Krische, M. J.; Huc, I.; Lehn, J.-M.; Schmutz, M. *Chem.—Eur. J.* **2000**, *6*, 1938.
- (180) Chang, S.-K.; Van Engen, D.; Fan, E.; Hamilton, A. D. *J. Am. Chem. Soc.* **1991**, *113*, 7640.
- (181) Du, P.; Xu, Y.-X.; Jiang, X.-K.; Li, Z.-T. *Sci. China, Ser. B: Chem.* **2009**, *52*, 489.
- (182) (a) Sanford, A. R.; Yuan, L.; Feng, W.; Yamato, K.; Flowers, R. A.; Gong, B. *Chem. Commun.* **2005**, 4720. (b) Helsel, A. J.; Brown, A. L.; Yamato, K.; Feng, W.; Yuan, L.; Clements, A. J.; Harding, S. V.; Szabo, G.; Shao, Z.; Gong, G. *J. Am. Chem. Soc.* **2008**, *130*, 15784.
- (183) (a) Yin, H.; Hamilton, A. D. *Angew. Chem., Int. Ed.* **2005**, *44*, 4130. (b) Fletcher, S.; Hamilton, A. D. *Curr. Opin. Chem. Biol.* **2005**, *9*, 632. (c) Cummings, C. G.; Hamilton, A. D. *Curr. Opin. Chem. Biol.* **2010**, *14*, 341. (d) Adler, M. J.; Jamieson, A. G.; Hamilton, A. D. *Curr. Top. Microbiol. Immunol.* **2011**, *348*, 1. (e) Yin, H.; Lee, G.-i.; Sedey, K. A.; Rodriguez, J. M.; Wang, G.-G.; Sebti, S. M.; Hamilton, A. D. *J. Am. Chem. Soc.* **2005**, *127*, 5463.
- (184) (a) Tew, G. N.; Liu, D.; Chen, B.; Doerksen, R. J.; Kaplan, J.; Carroll, P. J.; Klein, M. L.; DeGrado, W. F. *Proc. Natl. Acad. Sci. U.S.A.* **2002**, *99*, 5110. (b) Liu, D.; Choi, S.; Chen, B.; Doerksen, R. J.; Clements, D. J.; Winkler, J. D.; Klein, M. L.; DeGrado, W. F. *Angew. Chem., Int. Ed.* **2004**, *43*, 1158. (c) Yin, H.; Frederick, K. K.; Liu, D.; Wand, A. J.; DeGrado, W. F. *Org. Lett.* **2006**, *8*, 223. (d) Doerksen, R. J.; Chen, B.; Liu, D.; Tew, G. N.; Degrado, W. F.; Klein, M. L. *Chem.—Eur. J.* **2004**, *10*, 5008. (e) Tang, H.; Doerksen, R. J.; Tew, G. N. *Chem. Commun.* **2005**, *12*, 1537. (f) Lopez, C.; Nielsen, S.; Srinivas, G.; DeGrado, W. F.; Klein, M. L. *J. Chem. Theor. Comput.* **2006**, *2*, 649.
- (185) Choi, S.; Clements, D. J.; Pophristic, V.; Ivanov, I.; Vempalala, S.; Bennett, J. S.; Klein, M. L.; Winkler, J. D.; DeGrado, W. F. *Angew. Chem., Int. Ed.* **2005**, *44*, 6685.
- (186) Edwards, T. A.; Wilson, A. J. *Amino Acids* **2011**, *41*, 743.
- (187) (a) Saraogi, I.; Incarvito, C. D.; Hamilton, A. D. *Angew. Chem., Int. Ed.* **2008**, *47*, 9691. (b) Saraogi, I.; Hebda, J. A.; Becerril, J.; Estroff, L. A.; Miranker, A. D.; Hamilton, A. D. *Angew. Chem., Int. Ed.* **2010**, *49*, 736. (c) Hebda, J. A.; Saraogi, I.; Magzoub, M.; Hamilton, A. D.; Miranker, A. D. *Chem. Biol.* **2009**, *16*, 943.
- (188) Shaginian, A.; Whitby, L. R.; Hong, S.; Hwang, I.; Farooqi, B.; Searcey, M.; Chen, J.; Vogt, P. K.; Boger, D. L. *J. Am. Chem. Soc.* **2009**, *131*, 5564.
- (189) Plante, J. P.; Burnley, T.; Malkova, B.; Webb, M. E.; Warriner, S. L.; Edwards, T. A.; Wilson, A. J. *Chem. Commun.* **2009**, 5091.
- (190) Shirude, P. S.; Gillies, E. R.; Ladame, S.; Godde, F.; Shin-ya, K.; Huc, I.; Balasubramanian, S. *J. Am. Chem. Soc.* **2007**, *129*, 11890.
- (191) Jena, P. V.; Shirude, P. S.; Okumus, B.; Laxmi-Reddy, K.; Godde, F.; Huc, I.; Balasubramanian, S.; Ha, T. *J. Am. Chem. Soc.* **2009**, *131*, 12522.
- (192) Gillies, E. R.; Deiss, F.; Staedel, C.; Schmitter, J.-M.; Huc, I. *Angew. Chem., Int. Ed.* **2007**, *46*, 4081.
- (193) Iriondo-Alberdi, J.; Laxmi-Reddy, K.; Bouquerne, B.; Staedel, C.; Huc, I. *ChemBioChem* **2010**, *11*, 1679.
- (194) Zang, L.; Che, Y.; Moore, J. S. *Acc. Chem. Res.* **2008**, *41*, 1596.
- (195) Haldar, D.; Jiang, H.; Léger, J.-M.; Huc, I. *Angew. Chem., Int. Ed.* **2006**, *45*, 5483.
- (196) (a) Haldar, D.; Jiang, H.; Léger, J.-M.; Huc, I. *Tetrahedron* **2007**, *63*, 6322. (b) Jiang, H.; Maurizot, V.; Huc, I. *Tetrahedron* **2004**, *60*, 10029. (c) Maurizot, V.; Léger, J.-M.; Guionneau, P.; Huc, I. *Russ. Chem. Bull. Int. Ed.* **2004**, *53*, 1572. (d) Baptiste, B.; Zhu, J.; Haldar, D.; Kauffmann, B.; Léger, J.-M.; Huc, I. *Chem.—Asian J.* **2010**, *5*, 1364. (e) Maurizot, V.; Linti, G.; Huc, I. *Chem. Commun.* **2004**, 924.
- (197) (a) Wu, A.; Isaacs, L. *J. Am. Chem. Soc.* **2003**, *125*, 4831. (b) Bilgiçer, D.; Xing, X.; Kumar, K. *J. Am. Chem. Soc.* **2001**, *123*, 11815.
- (198) Zhu, J.; Lin, J.-B.; Xu, Y.-X.; Jiang, X.-K.; Li, Z.-T. *Tetrahedron* **2006**, *62*, 11933.
- (199) Hamuro, Y.; Hamilton, A. D. *Bioorg. Med. Chem.* **2001**, *9*, 2355.
- (200) Gan, Q.; Ferrand, Y.; Bao, C.; Kauffmann, B.; Grélard, A.; Jiang, H.; Huc, I. *Science* **2011**, *331*, 1172.
- (201) Ferrand, Y.; Gan, Q.; Kauffmann, B.; Jiang, H.; Huc, I. *Angew. Chem., Int. Ed.* **2011**, *50*, 7572.
- (202) Snijder, C. S.; de Jong, J. C.; Meetsma, A.; van Bolhuis, F.; Feringa, B. L. *Chem.—Eur. J.* **1995**, *1*, 594.
- (203) Ikeda, M.; Takeuchi, M.; Shinkai, S. *Chem. Commun.* **2003**, 1354.
- (204) Green, M. M.; Cheon, K.-S.; Yang, S.-Y.; Park, J.-W.; Swansburg, S.; Liu, W. *Acc. Chem. Res.* **2001**, *34*, 672.
- (205) (a) Wang, L.; Xiao, Z.-Y.; Hou, J.-L.; Wang, G.-T.; Jiang, X.-K.; Li, Z.-T. *Tetrahedron* **2009**, *65*, 10544. (b) You, L.-Y.; Jiang, X.-K.; Li, Z.-T. *Tetrahedron* **2009**, *65*, 9494. (c) Xu, X.-N.; Wang, L.; Li, Z.-T. *Chem. Commun.* **2009**, 6634.
- (206) (a) You, L.-Y.; Li, Z.-T. *Chin. J. Chem.* **2010**, *28*, 1547. (b) Zhang, K.-D.; Wang, G.-T.; Zhao, X.; Jiang, X.-K.; Li, Z.-T. *Langmuir* **2010**, *26*, 6878.
- (207) Wang, G.-T.; Zhao, X.; Li, Z.-T. *Tetrahedron* **2011**, *67*, 48.
- (208) Ren, C.; Xu, S.; Xu, J.; Chen, H.; Zeng, H. *Org. Lett.* **2011**, *13*, 3840.
- (209) Prabhakaran, P.; Priya, G.; Sanjayan, G. J. *Angew. Chem., Int. Ed.* **2012**, *51*, 4006.